Tidal control in the Lower Ems

An indicative study into the effects of controlled barrier operation on the tidal asymmetry in the Lower Ems river

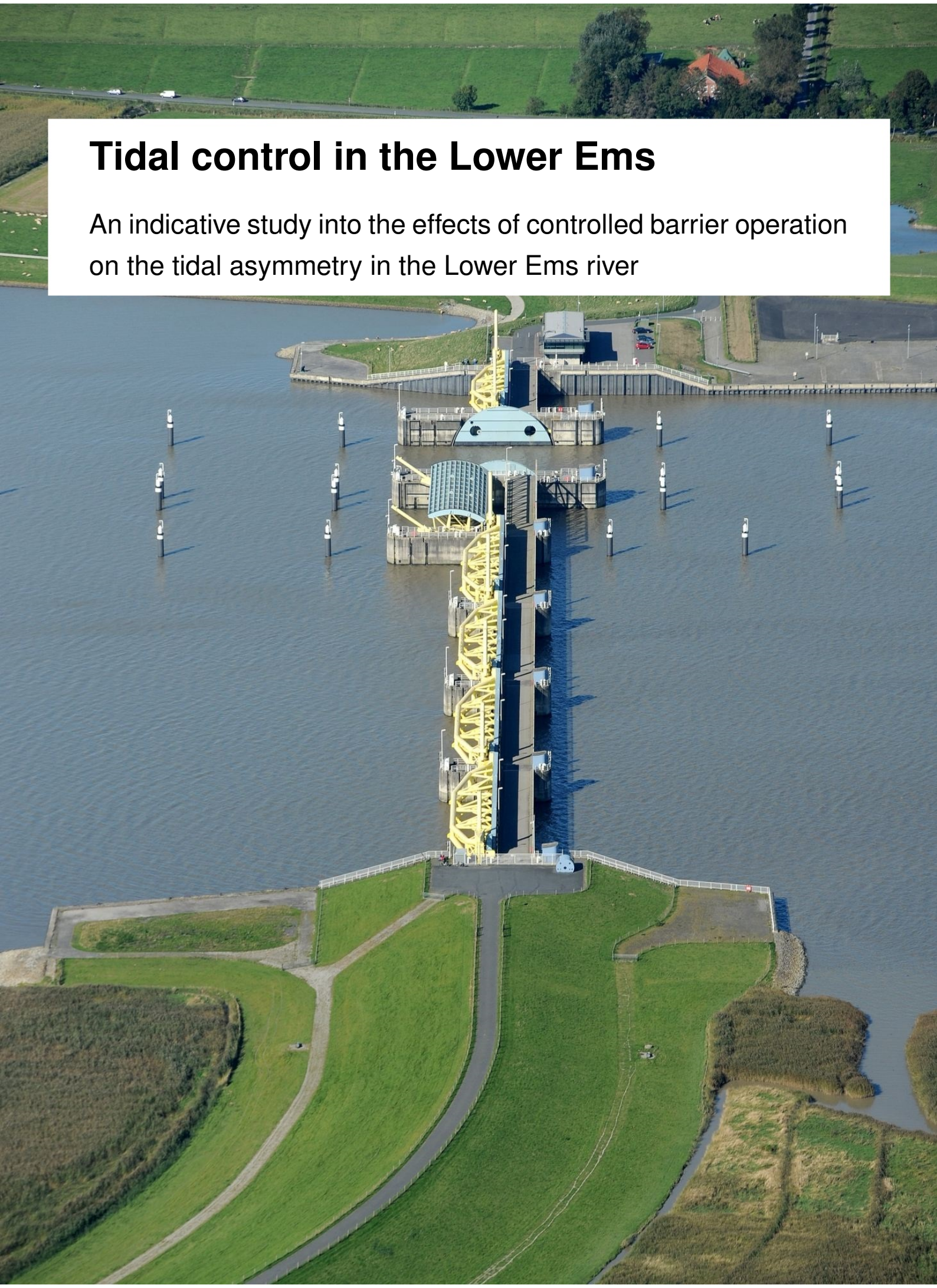

Tidal control in the Lower Ems

An indicative study into the effects of controlled barrier operation on the tidal asymmetry in the Lower Ems river

T.A. Vos

in partial fulfilment of the requirements for the degree of

Master of Science
in Civil Engineering

at the Delft University of Technology
Faculty of Civil Engineering and Geosciences

Date:	19/04/2021	
Student number:	4163419	
Graduation committee:	Prof.dr.ir. S.G.J. Aarninkhof	Professor of Coastal Engineering, TU Delft
	Ir. T.J. Zitman	Assistant Professor of Coastal Engineering, TU Delft
	Dr. ir. B. van Maren	Senior Researcher, Deltares

Preface

The subject of this thesis attracted my attention because it involved a ingenious method of using existing infrastructure to solve problems that have been a century in the making. It also illustrated how sediment and water influence many things far beyond the boundaries of the channel banks or levies.

The subject of the thesis is the operation of a tidal barrier in the Lower Ems region. It contributes to answering the question: how can a tidal barrier be used to remove sediment from a highly-turbid tidal river in order to improve the water quality and flood safety.

This thesis is part of the master 'Coastal Engineering' at the faculty of Civil Engineering and Geosciences at the Delft University of Technology. I would like to thank all the members of my graduation committee, the people from the NLWKN who provided me with feedback, valuable inputs and data, as well my close family and friends for their support.

Abstract

The lower Ems river suffers from hyper-turbid conditions. These conditions are caused by channel deepening over the last 50 years, resulting in an asymmetrical tidal wave. This asymmetry has resulted in an increased import of sediment into the Ems river. Recently some effort has gone into determining whether or not the local tidal barrier (Emssperrwerk) can be used to alter the asymmetry of the tidal waves propagating through the Ems estuary. Previous modelling studies, using state-of-the-art models, have been able to reproduce prototype tests involving the same tidal barrier but very little effort has thus far gone into determining what the optimal barrier control regime is and what the restriction imposed on the barrier operation mean for the overall effectiveness of the barrier.

The operation of the tidal barrier was schematised and described using two factors: closure percentage and closure duration. The effectiveness of a broad spectrum of combinations determining the tidal barrier operation is modelled using a simple one-dimensional model which takes only into account the (simplified) hydrodynamics in the lower Ems river.

The results of the model indicate that only in part of the Lower Ems the tide can be adjusted to become symmetrical or slightly ebb-dominant. This requires a closure duration longer than approximately 240 minutes. The length of this stretch of river is increase further by increasing the closure percentage. Similarly, increasing the closure percentage also leads to a decrease in the tidal volume and the amplitude of the M4 component. For this reason, the closure percentage should be kept as low as possible, as long as the barrier operation is able to reduce the sediment import into the Lower Ems. The required length of the stretch of the Lower Ems with a symmetric tide is estimated to be around 12 km. Applying restrictions to the barrier operations showed that shorter barrier operations should be preferred, since short operations allow a larger number of tidal waves to be altered, increasing the effectiveness in a realistic setting. Based on these considerations an optimal barrier operation consists of a closure duration of approximately 300 minutes and a closure percentage of approximately 60%.

The results showed that the method used for evaluating the barrier operation is unable to distinguish between water levels signals consisting of altered and unaltered waves. The effectiveness of the barrier operation is still estimated by considering the whole water level signal. The impact of the barrier operation in the model interfered with the seaward model boundary. This error increases in magnitude with increasing closure percentages. Making the results for those combinations unreliable. In order to make more reliable conclusions about the effect of the tidal barrier operation, subsequent models should encompass a larger domain and include a more detailed schematisation of the channel geometry, river discharge and the tidal barrier itself.

Contents

Chapter 1

Introduction

Estuaries and tidal rivers are regions near the mouth of large rivers, which are influenced by the tide. In estuaries the salinity of the water is comparable to salt water in seas in oceans, which is not the case for tidal rivers. Human activity near estuaries and tidal rives is common, because these regions are often highly populated and provide easy and useful ways of transporting goods.

The tidal amplitudes in many estuaries and tidal rivers across the world have increased significantly over the last 50 years. Although this phenomenon is most common in European rivers, it also occurs in rivers in Asia and America. At the same time the suspended sediment concentrations in most of these rivers have increased significantly as well (Winterwerp and Wang 2013).

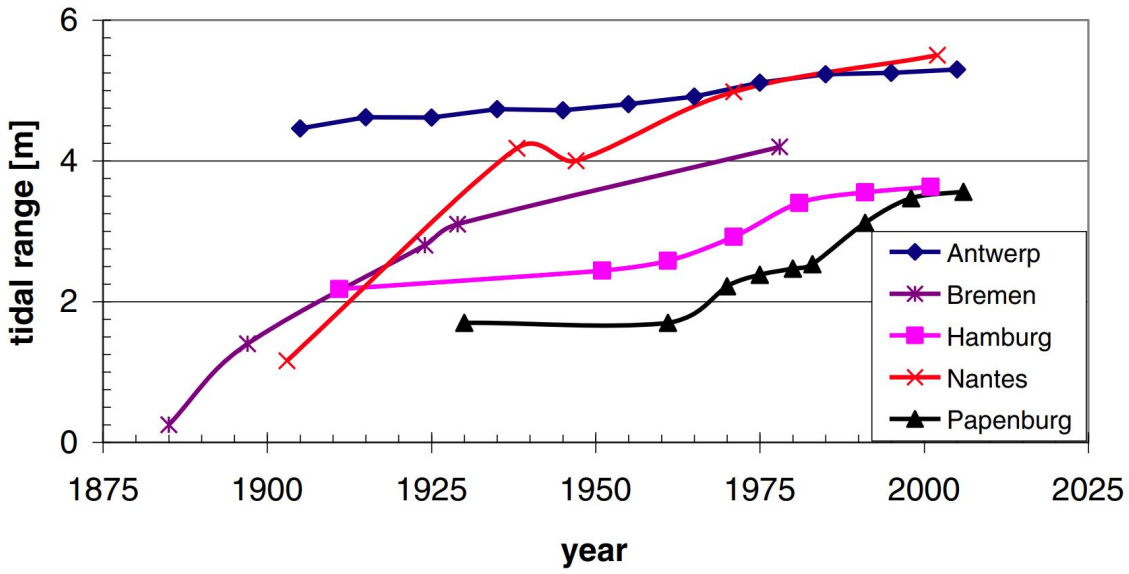

Figure 1.1: Tidal evolution in five European ports, from Winterwerp and Wang (2013)

The increase in suspended sediment concentrations and the increased tidal ranges cause a number of different issues. Increasing tidal ranges result in lower minimum water levels, which in turn affect groundwater levels in the surrounding land. The maximum water levels are increased as well, which leads to increased flood risks.

The increased suspended sediment concentrations have led to more frequent occurrences of hypoxic or anoxic conditions. These conditions negatively affect the water quality and local fauna through a wide range of mechanisms (Pena et al. 2010, Lin et al. 2006). One of the regions in Europe where the severity of these changes is abundantly clear is the Ems estuary.

1.1 The Ems estuary

The Ems estuary is located in the north-western part of Germany, on the border with The Netherlands. The estuary region consists of three distinct parts. The outer estuary is a common funnel shaped estuary that flows into the North Sea after crossing the Waddensea. The Dollard is located near the landward end of the Ems estuary. It is a bay-like feature that consist mostly of tidal flats. The extend of the Dollard has been gradually reduced over the last five centuries as a result of land reclamation (Krebs and Weilbeer 2008, Van Maren et al. 2016).

The mouth of the part of the Ems river that is influenced by the tide, also called the Lower Ems, is located on the north-eastern side of the Dollard region, although it is separated from the Dollard by a training wall. A navigation channel is maintained on the northern side of this training wall, which is used to access the Emden port and the Lower Ems from the outer estuary.

The Lower Ems is influenced by the tide until Herbrum, where a tidal weir is located. This approximately 60 km long stretch of river features a greatly amplified tide. Near Papenburg the tidal range is approximately 3.6m, which is a roughly 50% increase of the tidal range in the outer estuary. A tidal barrier has been constructed near Gandersum between 1998 and 2002, to increase the flood safety of the hinterlands. An overview of the region is presented in figure 1.2.

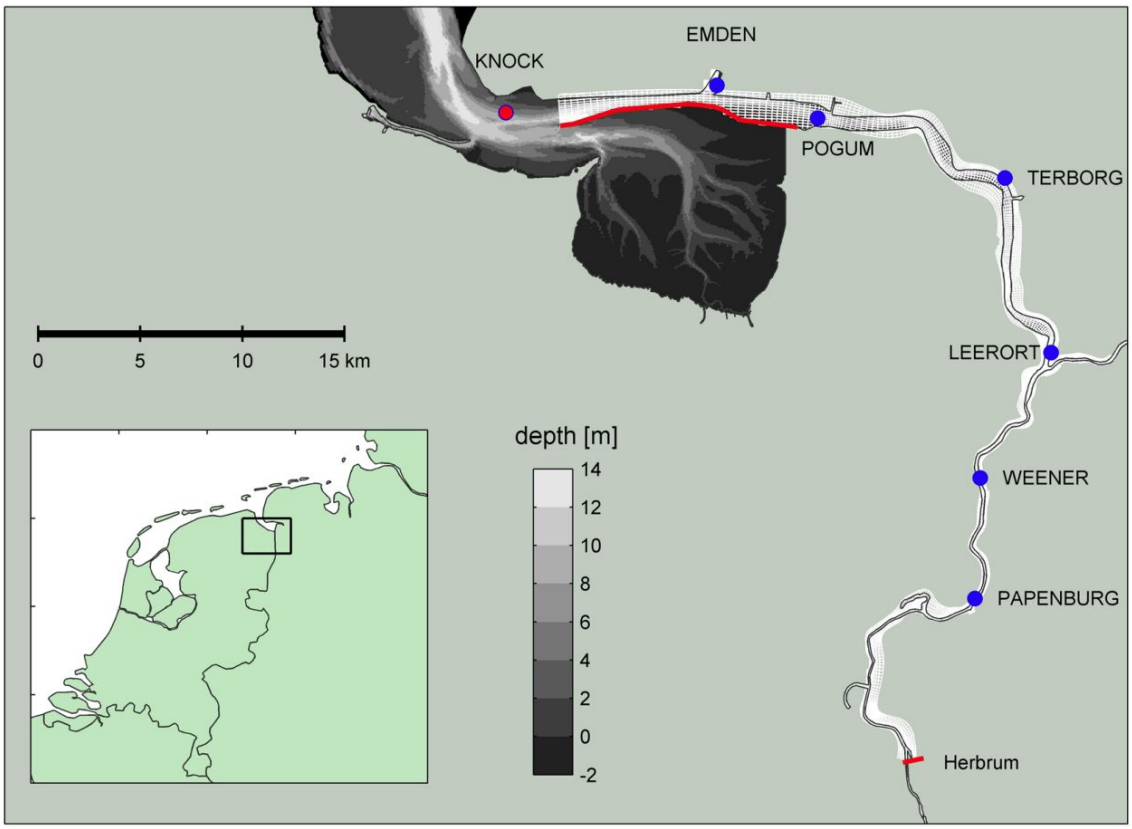

Figure 1.2: Map of the lower Ems river and part of the Ems estuary. The blue dots denote the denote water level observation stations. The red line in the Dollard represents the dam separating the navigation channel near Emden from the Ems estuary. The red line near Herbrum denotes the location of the tidal weir, which is the upstream model boundary. The red dot near Knock denotes the location of a water level measurement station. The measurements of that station are used to define the seaward boundary condition. From Maren, Winterwerp, and Vroom 2015

Although tourism is becoming an increasingly important economic activity in the region, the primary economic activity in the region remains shipping (Winterwerp and Wang 2013). The Emshaven is located in the outer Ems estuary, the port of Emden is located near the mouth of the Lower Ems and a shipyard is located near Papenburg in the upstream reaches of the Lower Ems (Winterwerp and Wang 2013).

In order to facilitate the ever-increasing size of cargo vessels, a number of changes have been made to the Ems estuary and Lower Ems. In the end of the 19th and 20th centuries, the Lower Ems was straightened and groynes were constructed along most of its length. Other changes made to the estuary up until 1983 were mostly related to maintaining the navigation channel to the Emdem port. From 1983 onward the depth of the Lower Ems was steadily increased as well (Krebs and Weilbeer 2008). An summary of the changes made to the region is presented in figure 1.3.

Year	Intervention	Historic scenario			
		1945	1965	1985	2005
Before 1939	Emden fairway below −6 m CD				
1932–1939	Pogum-Leerort 5.5 m below MHW, Leerort-Papenburg 4.2 m below MHW				
1939–1942	Emden fairway at −7 m CD				
1942–1948	No maintenance dredging: Emden fairway at −5.8 m CD				
1957	Emden fairway at −8 m CD				
1961–1962	Leerort-Papenburg 5 m below MHW.				
1965	Emden fairway at −8.5 m CD				
1983–1986	Emden-Papenburg 5.7 m below MHW				
1984–1985	Straightening of bends, reducing the river length with 1 km.				
1991–1994	Emden-Papenburg 7.3 m below MHW				
2001–2002	Construction of storm surge barrier (near Pogum)				

MHW mean high water, *CD* chart datum

Figure 1.3: Overview of the interventions in the lower Ems River over the last century, from Maren, Winterwerp, and Vroom 2015

Coinciding with the changes made to the region, a shift in the consistency and volume of dredged material has been observed. In the period between 1965 and 1980, the material dredged from the Lower Ems consisted of approximately 80% sand. Since 1995 this share has declined. Today the dredged material from the Lower Ems consists almost completely of silt and clay. The volumes of the dredged material has increased significantly increased as well (Krebs and Weilbeer 2008). This indicates that the landward flux of fine sediments has increased over the last 40 years, which had resulted in higher sediment concentrations in the lower Ems river.

1.2 Problems in the Lower Ems

A number of observation station are present in the outer estuary, the navigation channel and the lower Ems river. Historical measurement from these stations show a clear increase in the tidal ranges in the region, especially in the upstream region in the Lower Ems river. The measurements of the tidal range over the last 70 years in given in figure 1.4.

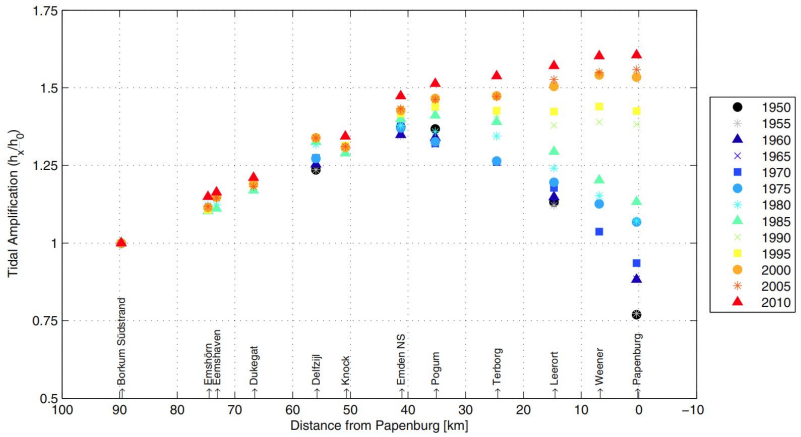

Figure 1.4: Observed tidal amplification h_x/h_0 in the Ems estuary and lower Ems river, defined as the tidal range relative to the tidal range at the most seaward station. Measurements from km 40 until km 0 represents are taken in the Lower Ems. From Maren, Winterwerp, and Vroom 2015

Sediment concentration measurements from various tidal station in the Lower Ems also show a dramatic increase in the sediment concentration in the Lower Ems. A contrast of measurements made in 1975 and 2005 is presented in figure 1.5. Measurements of the turbidity, which is related to suspended sediment concentrations, were made in 2005 using a vessel and echo equipment Talke, Swart, and De Jonge. The salinity and dissolved oxygen concentrations in the water column were measured at the same time. The results of these measurements are presented in figure 1.6. Note that the distance, is measured from the seaward end of the estuary in figure 1.5, rather than from the tidal weir near Herbrum, as is the case in figure 1.6.

The sediment concentrations in Lower Ems, presented in figure 1.6, are high enough to cause a collapse of the suspended sediments to the bed and the subsequent formation of fluid mud layers. Furthermore it is noted that the region with very low dissolved oxygen concentrations coincides with the region with very high sediment concentrations.

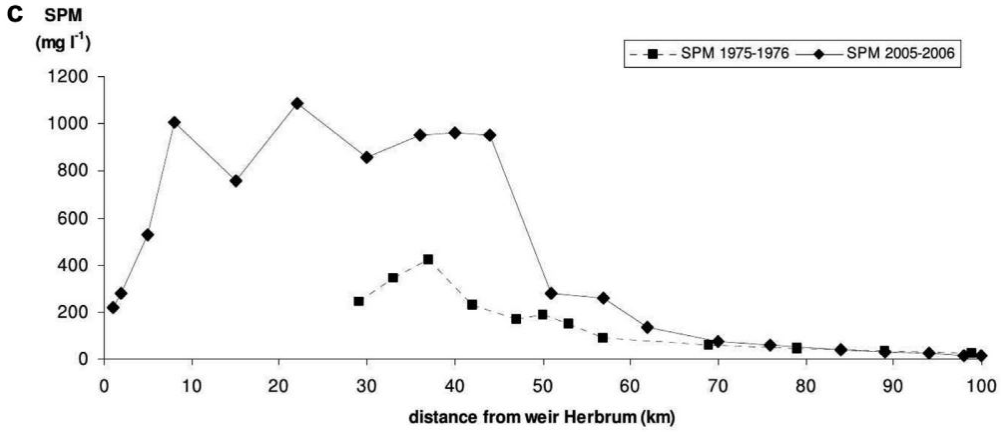

Figure 1.5: Change in the suspended sediment concentration between 1975 and 2005, from Talke, Swart, and De Jonge 2009

Measurements of other various characteristics of the water (for example temperature, salinity, dissolved oxygen concentration and turbidity) in the Ems estuary were also made at the various station in the region. An overview of these measurements is presented in figure 1.7.

From the measurements it is clear that the occurrence of very low dissolved oxygen concentrations has increased dramatically over the last 40 years. Furthermore, a clear negative correlation between turbidity and dissolved oxygen concentrations can be seen, especially when the water temperature is high.

Both the increase in tidal ranges, as well as the decline in water quality in the upstream part of the lower Ems river can be explained by the increased concentrations in this part of the river. The exact mechanisms that govern these phenomena will be explained in detail in the next chapter.

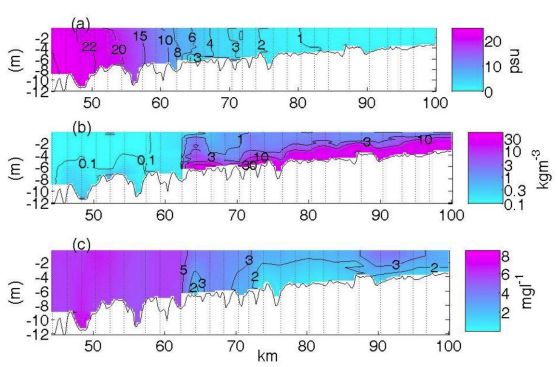

(a) The ebb tide of august 2, 2006

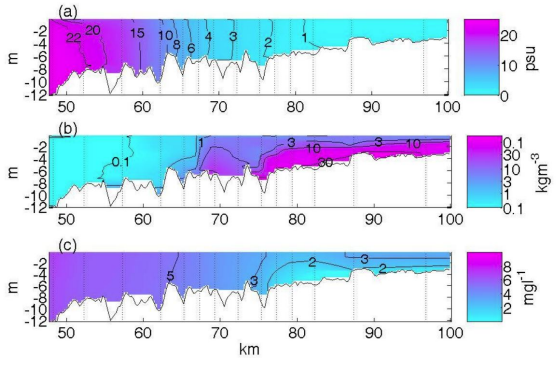

(b) The flood tide of august 2, 2006

Figure 1.6: Interpolated results of the salinity (top), SSC (middle) and dissolved oxygen concentration (bottom) along the longitudinal axis of the Ems estuary. The locations of the measurements are shown by the vertical dotted lines. From Talke, Swart, and De Jonge 2009

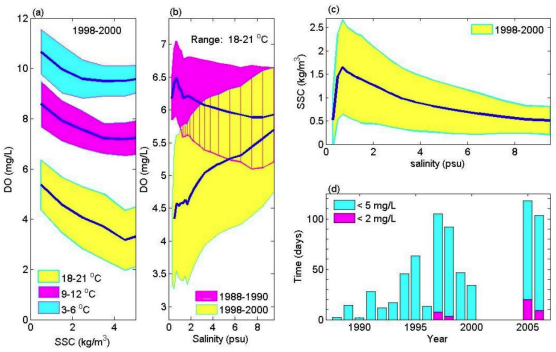

(a) Measurements of the station in Terborg

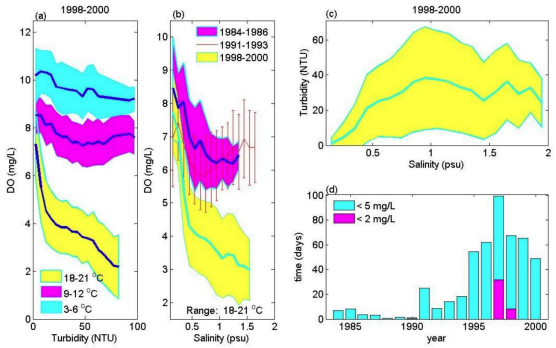

(b) Measurements of the Leer-Leda station

Figure 1.7: Measurements showing variations of the DO vs. SSC for 1998-2000, DO vs. salinity, SCC vs. salinity and the amount of days SSC was below $2mgl^{-1}$. The solid lines depict the bin-averaged data. For the first two plot the data was binned into separate temperature ranges. Measurements were collected 1.5m above the bed. From Talke, Swart, and De Jonge 2009

1.3 Masterplan Ems 2050

In an effort to counteract the decline of the water quality and the problems regarding groundwater levels, flood risks and freshwater intake, the national government of Germany, together with various local governments and conservation groups and local shipyards have have started the 'Masterplan Ems 2050' project at the start of 2015.

The agreement establishes a binding framework for the cooperation between the parties. The goal of the agreement is to restore the aquatic environment and achieve the long term development of the Ems estuary. The parties also intent to fulfill the tasks stipulated by a number of European regulations and directives. Examples of these are the Habitat Directive, the Birds Directive and the Water Framework Directive. Lowering the fine sediment concentrations in the Lower Ems was identified as the most important way to increase the water quality in the region. The agreement also proposes three distinct actions that were to be taken, in order to address the various problems in the region. These three measures were:

- The installation of a tidal weir at the Ems Barrier, with the goal of raising the low tide level of the Lower Ems
- The construction of tidal reservoirs on the Ems, in order to increase the seaward conveyance of sediment.
- Tidal control at the Ems barrier, which means temporarily constricting the cross section of the Ems at the barrier in such a way that the reduction in tidal asymmetry will reduce the conveyance of sediment.

At the time the agreement was signed, feasibility studies of some of these measures were already underway. In this report the focus will be on the tidal control at the Ems barrier.

1.4 Tidal barrier operation

The feasibility studies of the operation of the tidal barrier have since been completed. Comparisons of model results and a prototype test performed in 2012 showed that the driving hydrodynamic phenomena behind the upstream sediment transport were reproduced very well, although the comparison only involved a single barrier operation mode. For these studies an extensive state-of-the-art Delft3D model was used. The model resolved the hydrodynamics from the seaward end of the Ems estuary up to the tidal weir near Herbrum and showed that the operation of the tidal barrier had a clear impact on the tidal asymmetry (Oberrecht and Wurpts 2014).

Based on feasibility studies from 2016 (Oberrecht and Wurpts 2019b; Oberrecht and Wurpts 2020), two different control mode variants were distinguished. The first operation mode constricts the available cross section

near the barrier by approximately 66% at low tide, for a period of 2 to 6 hours. The goal of this mode is to shift the tidal asymmetry in order to create a more symmetric tide. This symmetric tide would decrease the upstream transport in the lower Ems. The ebb currents would not be affected so the export of sediment during the ebb would not be affected either.

The second operation mode completely closes the barrier for a period of time around low water. This would result in a decrease in tidal volume. The main goal of this operational mode is to hasten the sedimentation and consolidation of the sediment in the water column onto the bed. By facilitating the formation of fluid mud the occurrence of strongly stratified conditions would decrease. This would then result in less frequent occurrences of poor water quality (Oberrecht and Wurpts 2019b; Oberrecht and Wurpts 2019a).

The effect of these barrier operations was modelled using a similar model as used during the prototype test comparisons. In this case only a morphological model component was added to the model. The results of these simulations showed that both of these operation modes could contribute to the decrease in fluid mud formation in the Lower Ems.

A third mode consisting of a combination of the operation modes mentioned above was also shown to be able to contribute. This operation mode was formulated to represent a 'traffic-friendly' mode in the review. Due to shipping activities in the region the barrier cannot be operated during regular shipping times, which are currently set a-priori by the local shipping authority (Oberrecht and Wurpts 2019b).

1.5 Methodology

In the feasibility studies discussed previously only a few different operation modes were simulated. This is understandable, since the computational costs of these extensive and detailed models is very high. The desire to find optimal barrier operation was expressed when the comparison of the prototype test and numerical models was made (Oberrecht and Wurpts 2014).

The barrier operation is determined by a number of parameters. In order to find an optimum the effects of a large number of different operation modes must be modelled. However, the costs of modelling the effects of different operation modes using the complex models used in the feasibility studies are too high. One of the goals of this project is therefore to find a simplified formulation of the barrier operation modes and a model that can approximate the effects of the barrier operation mode, while also being computationally inexpensive.

The models used in the feasibility studies resolved both the hydrodynamics in three dimensions, as well as sediment transport. The computational costs of the model would be decreased significantly if the hydrodynamics could be approximated using a 2D or even 1D model. The computational costs can be reduced even further by estimating sediment transports based on the simplified hydrodynamics.

The sediment fluxes will be evaluated qualitatively based on the tidal asymmetry in the Lower Ems. Although sediment transport itself a complex process which involves on many different processes, the long term transport is largely determined by the tidal asymmetry (van Leussen, 1991). The way tidal asymmetry affects sediment transport will be discussed in greater detail in the literature review.

Other processes that are important in determining the sediment transport are the export of sediment as a result of high river discharges and dredging activities. The reduction of the sediment concentration in the lower Ems will be realized by reducing the import of sediment as a result of tidal asymmetry. This reduction of the sediment import will be the result of tidal barrier operation. The export as a result of high river discharges and dredging will not be affected and these processes will cause the sediment concentrations in the Lower Ems to decrease. The conceptual model on which this model study is based will be discussed in greater detail in chapter 3.

To recap, the overall goal of this project is to find an optimal barrier operation mode. In order to find this optimimum a number of different questions must be answered.

- Which simplifications must be made to obtain a model that can be used to optimize the barrier operation?
- Which parameters determine the tidal barrier operation?
- What are the limitations imposed on the tidal barrier operation?
- What are the characteristics of an 'optimal' barrier operation?
- What is the character of the asymmetry of the unaltered tide?
- What is the effect of the tidal barrier operation on the tidal asymmetry?
- What other characteristics of the tide are affected by the barrier operation and are these side-effects beneficial or not?
- How do the changes to the hydrodynamics which result from the barrier operation affect sediment transport and the issues that occur in the region?

The first three sub-questions will be answered in the chapters discussing the methodology. The remaining questions will be answered in the conclusion.

1.6 Report structure

In the chapter 2, past literature will be reviewed. First of all, the causes of the increase in sediment concentrations and the mechanisms that contributed to this shift to a hyper turbid regime will be discussed. After that the mechanisms by which the increase in sediment concentrations are connected to the problems occurring in the Ems are reviewed. Lastly, some mathematical descriptions of tidal asymmetry are reviewed and the mechanisms linking tidal asymmetry to sediment transport will be discussed in greater detail. In chapter 3 the methodology will be discussed. The model results will be presented in chapter 4 and finally the results will be discussed and conclusions will be presented in chapters 5 and 6.

Chapter 2

Literature review

In this chapter a detailed description is given of a number of processes that govern the hydrodynamics in the present-day Lower Ems. The process through which large parts of the Lower Ems became hyper-turbid will be treated. Additionally, the effect of the increased sediment concentrations on the dissolved oxygen dynamics and tidal propagation will be discussed. Lastly a summary will be made of a mathematical description of tidal asymmetry.

2.1 Shift to a hyper-turbid regime

The deepening and straightening of channels in the Ems estuary and Lower Ems river has affected the hydrodynamics of the region significantly. A study by Chernetsky, Schuttelaars, and Talke (2010), using an idealized 1DV point model, showed that as a result of the change in depth the asymmetry of the tide became more flood dominant. The tidal penetration and as a result the tidal amplitudes have also increased. The effect of these changes was especially evident in the Lower Ems. The change in tidal amplitude was attributed to a significant decrease of the vertical eddy viscosity and bottom stress parameters.

Although sediment transport is a complex process of erosion, transport and sedimentation and the properties of each process can vary enormously throughout an estuary, tidal asymmetry was identified as an important process in determining the long term sediment transport in an estuary (Leussen 1991). Simulations performed by Chernetsky, Schuttelaars, and Talke (2010) did show an upstream shift in the location of the estuarine turbidity zone as a result of channel deepening, but the order of magnitude of the sediment concentrations could not be reproduced. The model also did not manage to reproduce the shift of the estuarine turbidity zone up to the tidal weir at Herbrum. Model studies by Jonge et al. (2014) showed a similar result.

Studies investigating the role of suspended fine sediments in the water column (Winterwerp 2006; Winterwerp, Lely, and He 2009 and Winterwerp 2011) showed that even for low concentrations of suspended sediment, an appreciable modification of vertical velocity profiles, turbulent stresses and vertical eddy viscosity and diffusivity can be observed. Four processes through which this occurs could be identified. These are:

- Buoyancy destruction induced by vertical gradients in suspended sediment concentrations.
- Turbulence damping by fluid mud formation
- Reduction in bed forms, resulting in a reduction in form drag
- Thickening of the viscous sub-layer through viscous damping induced by mud flocs

An expression for the effect of the presence of sediment on the hydraulic drag was formulated and calibrated based on experimental data. This expression only includes the effects resulting from buoyancy destruction by applying a correction to the Chézy roughness factor, based on the Richardson and Rouse numbers (Winterwerp 2011).

Winterwerp and Wang (2013a, 2013b) combined the conclusions of earlier investigations that channel deepening caused an import of fine sediment and the known relations between sediments to form a conceptual model explaining the significant increase in sediment concentrations in the Lower Ems river. The conceptual model identifies a feedback loop of decreasing hydraulic drag, tidal deformation and increases in sediment import.

This feedback process is set in motion by increases in the channel depth. The increase in depth lowers the hydraulic drag in the channel. This can easily be understood by considering the White-Colebrook formula.

$$C = 18log\left(\frac{12h}{k_s}\right) \tag{2.1}$$

Deepening the channel increases the value for h and possibly decreases the value for k_s because bed forms are removed during the deepening process. If the depth h increases and k_s decreases, the value for C increases. As a result less friction is experienced by a tidal wave. The deepening of the channels significantly affects the tidal propagation of the tidal wave, which results in net sediment import. Incidentally, the deepening of the channel also decreases the flushing capacity of the river, further increasing the sediment import. The increased suspended sediment concentrations resulting from the import reduce the friction in the estuary further, for example when the higher concentrations allow the formation of fluid mud layers, creating a positive feedback loop. It was also noted that the narrowing of many rivers in the 19th century contributed to the deformation of the tidal wave (Winterwerp and Wang 2013).

Through this feedback cycle the significant increases in sediment concentrations could be explained. Furthermore it was argued that this hyper-turbid state is very stable and self-maintaining, since the presence of very high sediment concentrations is favourable from an energetics point of view. An illustration of this conceptual model can be found in figure 2.1.

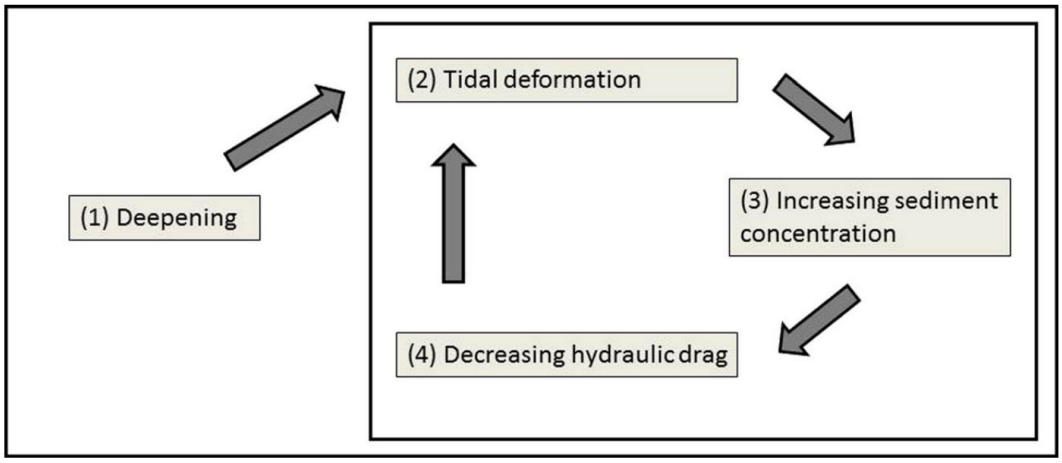

Figure 2.1: Estuarine response to channel deepening, which sets in motion a response of the tidal dynamics, which in turn increases sediment import. This reduction in hydraulic drag leads to progressively larger tidal deformation. From Winterwerp and Wang (2013)

A model study performed by Maren, Winterwerp, and Vroom (2015) yielded results that were expected based on the conceptual model formulated by Winterwerp and Wang (2013a, 2013b). The model used was a complex numerical Delft3D model, which included hydrodynamic and morphological components. The model used a detailed representation of the bathymetry and a simplified sediment transport model to reproduce the most important transport mechanisms. The results of the model suggested that the deepening of the channels is sufficient to import large quantities of suspended sediments. The import is caused by a amplification of the tide and a reduction of the flushing capacity of the river. The increase in sediment concentration reduced the hydraulic roughness, further amplifying the tidal wave. The reduction of the flushing capacity is not influenced by the decrease in hydraulic roughness. This confirmed the idea that the reduction in flushing capacity is not part of the feedback cycle. The model results also confirmed the notion about the stability of the hyper-turbid regime, since the suspended sediment concentrations remained high for low roughness conditions, even if dredging was halted.

Dijkstra, Schuttelaars, and Winterwerp (2018) and Dijkstra, Schuttelaars, Schramkowski, et al. (2019) provided further strong evidence for the feedback process hypothesis. Using the 1DV iFlow model, the shift in suspended sediment concentrations was reproduced using only a change in the channel depth. It was concluded that including hindered settling is the key in reproducing the concentration shift. Based on their model results, two conditions required for a shift towards a hyper-turbid system were formulated. The first condition is that the character of the erosion must be supply-limited rather than erosion-limited. This means that the hydrodynamic conditions must be such that all sediment available for erosion is suspended into the water column. The second condition simply includes that enough sediment must be available for erosion. De Jonge et al. (2014) noted also the importance of sediment availability in the sediment transport process and suggested that the removal of sturdy bed layers during the deepening process may have greatly increased the sediment availability in the Ems region.

2.2 Dissolved oxygen dynamics

Occurrences of low dissolved oxygen (DO) concentrations in the water column are often called hypoxic conditions or hypoxia. Various thresholds for hypoxic (or anoxic) conditions exist. Hypoxia in general results from an imbalance of the ”production” and consumption of oxygen. Oxygen is introduced into the water column as a result of photosynthesis and air/water exchange processes. The consumption is mostly a result of breakdown of organic matter in the water column, but respiration processes can also temporarily consume oxygen. Short episodes of hypoxia caused by respiration of organisms often occurs in the summer (Pena et al. 2010). Since the location of the production of oxygen is often the top of the water column and the location of the consumption is often near the bed, processes that hinder vertical exchange can also cause hypoxia. One such a process is stratification as a result of high sediment concentrations (Lin et al. 2006).

Investigations by Lin et al. (2006) using an idealized model consisting of DO concentration models and hydrodynamics model found that the DO behavior is particularly sensitive to the relative strength of the classic two layer estuarine circulation and the relative strength of the consumption near the bed and vertical mixing strength. It also found that if the strength of the estuarine circulation is low, the oxygen profile becomes more sensitive to the relative vertical mixing strength. In the lower Ems river, the conditions are such that the strength of the estuarine circulation is low and that the oxygen profile is highly dependent of the vertical mixing strength.

Another study by Talke, Swart, and De Jonge (2009) applied a similar idealized model to the Ems estuary. This time, in addition to hydrodynamic and DO concentration model, the model also included a morphodynamic component. Talke, Swart, and De Jonge (2009) concluded that for turbid estuaries like the Ems, suspended sediment dynamics controlled DO concentrations rather than water residence times or nutrient inputs, which are other common causes of hypoxic and anoxic conditions.

2.3 Tidal wave deformation

The distortion of the semi-diurnal tide as it propagates from the open ocean into estuaries can be represented as the non-linear growth of harmonic constituents with periods that are a fraction of the main M_2 tidal component. The tidal distortion is a compromise between the distortion caused by friction in channels and the distortion caused by intertidal areas and marshes. During low water the effect of friction is greater than during high water. As a result the propagation of low water is slowed, shortening the flood duration.

Extensive intertidal storage slow the propagation of high water. This is also due to friction, as the relative friction experienced on intertidal areas is greater compared to the friction experienced in the channels. The intertidal area is submerged only during high water, resulting in a slower high water propagation speed. The most important distorting harmonic constituents beside the M_2 tidal component is the M_4 tidal component. The sea surface can be modelled as a superposition of the distinct harmonic components. For example the

surface elevation and flow velocity can be reproduced, to a relatively detailed degree, using only the M_2 and M_4 components (Friedrichs and Aubrey 1988). In reality there are many more tidal components.

$$\zeta = a_{M_2} cos(\omega t - \theta_{M_2}) + a_{M_4} cos(2\omega t - \theta_{M_4}) \tag{2.2}$$

$$u = v_{M_2} cos(\omega t - \phi_{M_2}) + v_{M_4} cos(2\omega t - \phi_{M_4}) \tag{2.3}$$

The sea surface phase of the M_4 relative to the M_2 is defined as:

$$2M_2 - M_4 = 2\theta_{M_2} - \theta_{M_4} \tag{2.4}$$

A direct measure of the sea surface distortion is:

$$\frac{M_4}{M_2} = \frac{a_{M_4}}{a_{M_2}} \tag{2.5}$$

Likewise the distortion of the velocity signal can be expressed as:

$$2M_2 - M_4 = 2\phi_{M_2} - \phi_{M_4} \tag{2.6}$$

$$\frac{M_4}{M_2} = \frac{v_{M_4}}{v_{M_2}} \tag{2.7}$$

The the relative phase between the M_4 and M_2 has a value between 0°and 180°, the distorted tide has a higher flood velocity and is therefore flood dominant. Likewise if the relative phase is a value between 180°and 360°, the ebb velocities are higher and the tide is ebb dominant.

2.4 Tidal pumping

As was mentioned earlier in this chapter, the long term transport of fine sediments is the result of a number of processes that take place within a tidal cycle. The long term transport is the result of differences between sediment import and export. These sediment fluxes are dependant on a wide number of factors, which in turn can vary throughout an area in both longitudinal direction and along the cross-section. In general the transport of fine sediments is proportional to the flow velocities.

For long term sediment transport, asymmetric flow velocities play an important role (Leussen, 1991). If the tide is flood-dominant the upstream transport of sediment is larger than the downstream transport, since the flood velocities are higher than the ebb velocities. Over many tidal cycles this results in a net upstream transport of sediment. A schematisation of this process is given in figure 2.2.

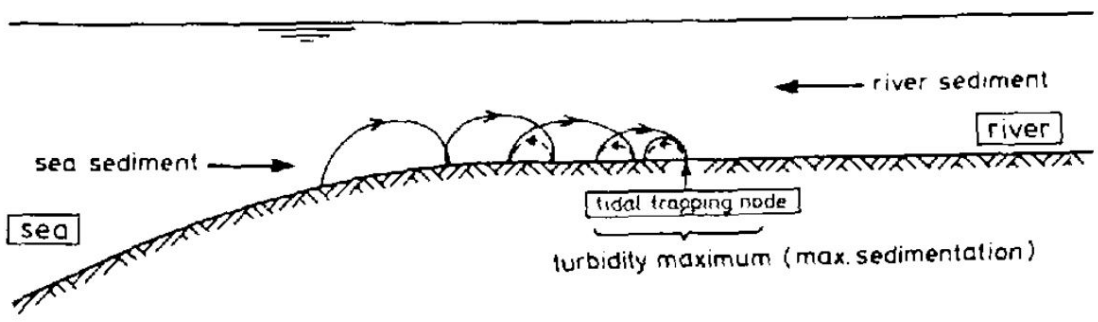

Figure 2.2: Schematisation of the transport of sediment resulting from tidal asymmetry. From van Leussen (1991)

Chapter 3

Methodology

In order to answer the research questions a numerical model will be constructed to simulate tidal waves affected by various barrier control modes. The make-up of the numerical model and the method for evaluating the effects of the barrier control modes is based on a conceptual understanding of the processes that determine the hydrodynamics in the region. This conceptual model will be discussed in the following sections. Afterwards the numerical representation of the Lower Ems and the tidal barrier will be discussed. The different operation mode variants will be discussed last.

In order to evaluate the ability of the model to reproduce the tidal characteristics, comparisons will be made with data from the tidal station in the Lower Ems. The measurement data is provided by the Niedersächsischer Landesbertieb für Wasserwirtschaft, Küsten- un Naturschutz.

3.1 Conceptual model

The conceptual model is based on a understanding of the processes that are largely govern the sediment import into the Lower Ems. In order to keep the computational costs low a number of processes have to be omitted or simplified. The processes that are considered in this report and the ways different variables and processes interact with each other can be found in figure 3.1. A brief overview of the conceptual model will be given below.

One of the main goals of the Masterplan Ems is to reduce the sediment concentration in the Lower Ems. Although the modelling of the sediment fluxes itself is not part of this project, the literature suggests that tidal distortion is the primary factor that causes increased sediment imports over the long term. One way to decrease the sediment import is to reduce the tidal amplification that currently occurs. This was one of the conclusion of Maren, Winterwerp, and Vroom (2015). However, one of the clear goals formulated in the Masterplan Ems contract states that the current tidal volume must be maintained as much as possible. This method is therefore not an acceptable method for reducing the sediment import.

Another option, that is the subject of this report is to deform the tidal wave in such a way that the tide comes symmetrical. This would also result in a reduced sediment import. The resulting stop of sediment import would lead to reduced sediment concentrations when the remaining sediment is either removed by dredging or flushed out during episodes of high river discharge.

The model will focus on modelling the hydrodynamics, especially the tidal asymmetries. The asymmetry will be evaluated by analysing the relation of the primary overtide M4 and the main M2 constituent. using the amplitude ratio and the relative phase angle. An approximation of the tidal prism will be made to review the impact of the barrier operation on tidal volumes. A simplified model of the hydrodynamics in the Lower Ems will be formulated based on 1D depth and width averaged shallow water equations.

The operation of the barrier will be determined by three variables: closing durations, closure percentage, river discharge and opening time. An optimisation of the first two variables will be made, while the influence of the last two variables will be described, but no optimisation will be performed. Lastly the effect of restriction on the barrier operation will be quantified using criteria based on shipping interests and ecological considerations. A detailed review of the schematisation of the tidal barrier will follow later in this chapter.

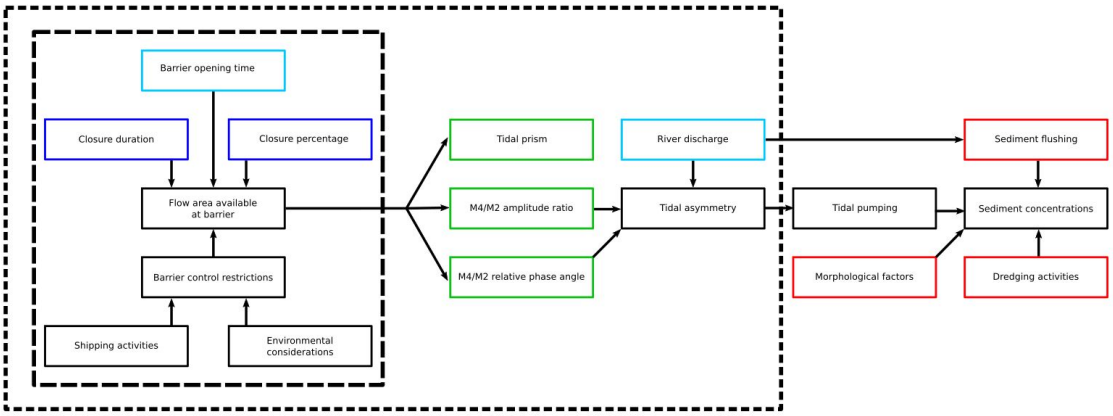

Figure 3.1: An overview of the different factors that determine the operation of the tidal barrier (grouped within the smaller box) and the hydrodynamic processes and characteristics that are considered in this project. The latter is grouped in the larger box. The relation to of the modelled hydrodynamics to the sediment transport are illustrated too, but are not part of the model.

3.2 Numerical model

Previous research into the causes of the regime shift in the Ems estuary and Lower Ems were performed using either simple, idealized models that allowed the modeller to isolate individual processes or state-of-the-art numerical models. State-of-the-art models allow a very detailed description of the bathymetry and geometry to be included, but are very computationally expensive and require extensive calibration and model input.

The model that will be used in this project is similar to the idealized models in that the bathymetry and geometry of the domain will be described using very simple formulations. Since this research is more focused on the hydrodynamics in the system because of their role in the sediment import, a simple formulation of the hydrodynamics is used. In the past research, processes like baroclinic forcing (resulting from both salinity and sediment concentration gradients) is often included and there is overwhelming evidence that baroclinic forces play an important role. However, due to limitations to the project duration and available numerical expertise, these shortcomings are accepted. It is also expected that the operation of the tidal barrier will affect the hydrodynamics much more than it will affect baroclinic processes. The results from the model will be used as a first estimate of the optimal operating regime of such a barrier. More detailed studies, perhaps using state-of-the-art models could provide a more detailed picture.

3.2.1 Model domain

This project focuses on the deformation of a tidal wave when it is impeded by a tidal barrier. Therefore the only section of the Ems river that is of interest is the part of the river that is influenced by tide waves. The influence of the tide in the Ems river only reaches until the tidal weir at Herbrum. The presence of this tidal weir is fortunate from a modelling standpoint, since it provides a static upstream boundary with a very simple accompanying boundary condition. The seaward boundary is set at the end of the training dam near Knock. Within this chosen domain, the flow can be considered one-dimensional, because the longitudinal length scale of the domain ($\approx$60km) is much larger than the transversal and vertical length scales ($\approx$500m and $\approx$10m, respectively). This allows the equations that describe hydrodynamics to be greatly simplified.

3.2.2 Model equations

The water motion in the model domain can be described by the one-dimensional De Saint – Venant equations, which are presented below (equations 3.1 and 3.2).

$$\frac{\partial \zeta}{\partial t} + h\frac{\partial u}{\partial x} = 0 \tag{3.1}$$

$$\frac{\partial u}{\partial t} + \frac{\partial u^2}{\partial x} + g\frac{\partial \zeta}{\partial x} + g\frac{u|u|}{C^2 R} = 0 \tag{3.2}$$

Equation 3.1 represents a continuity equation. Equation 3.2 represents a momentum balance equation. The first term represents the local inertia, the second term represents advection, the third term represents the pressure gradient and the last term represents friction.

Most of the data available for the Ems river is provided in terms of discharge, so it is more convenient to rewrite these equations in terms of discharge instead of flow velocity. Using $u(x,t) = \frac{Q(x,t)}{A(x,t)}$ the following equations are derived. These equations are shown below (equations 3.3 and 3.4)

$$\frac{\partial \zeta}{\partial t} + \frac{1}{W(\zeta)}\frac{\partial Q}{\partial x} = 0 \tag{3.3}$$

$$\frac{\partial Q}{\partial t} + \frac{\partial}{\partial x}\frac{Q^2}{A(\zeta)} + gA(\zeta)\frac{\partial \zeta}{\partial x} + g\frac{Q|Q|}{C^2 A(\zeta) R} = 0 \tag{3.4}$$

As was mentioned before, the model does not include any baroclinic forcing. Additionally, the model assumes hydrostatic pressure throughout the model. This assumption is valid if the length of modelled waves is much larger than the vertical length scale (channel depth) of the domain. As a result of this simplification, short waves cannot be modelled. The non-linear term representing advection and a non-linear formulation of the friction term are included in the equations, since those two processes play an important role determining tidal deformation. Another important influence in determining tidal wave deformation is the influence of intertidal area. In general, intertidal areas cause a tidal wave to become more ebb-dominant because the friction experienced by the wave during high water is increased. This is because during high water the friction experienced by the wave is much higher over the very shallow intertidal areas.

3.2.3 Channel geometry

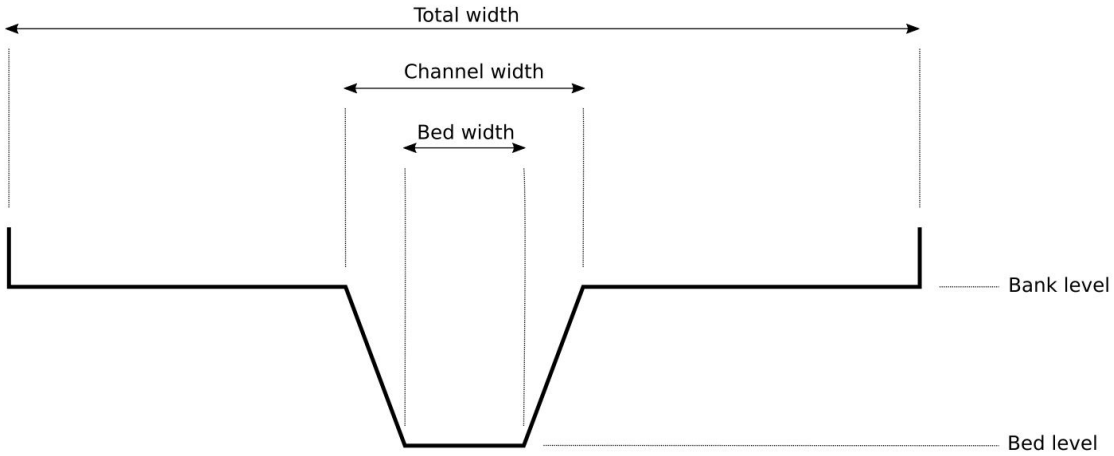

Figure 3.2: An overview of the schematisation applied to the bathymetry of the domain. The bottom graphs show the difference between the estimated dimensions and the converging functions used to approximate them.

In order to capture the influence of the intertidal areas while maintaining the simplicity of the model, a parametrised channel geometry is used. The assummed general shape of the channel, along with the parameters that describe it can be found in figure 3.2. The bed level, channel top level, bed width and channel top width were determined by evaluating bathymetry data from Maren, Winterwerp, and Vroom (2015), which is presented in figure 3.3. Based on this data 3D figures of the channel bathymetry were produced based on a interpolation technique. The general shape of the channel, as well as the parameters used to describe the geometry were estimated based on these figures. The 3D bathymetry figures can be found in the appendix, in figure 7.1.

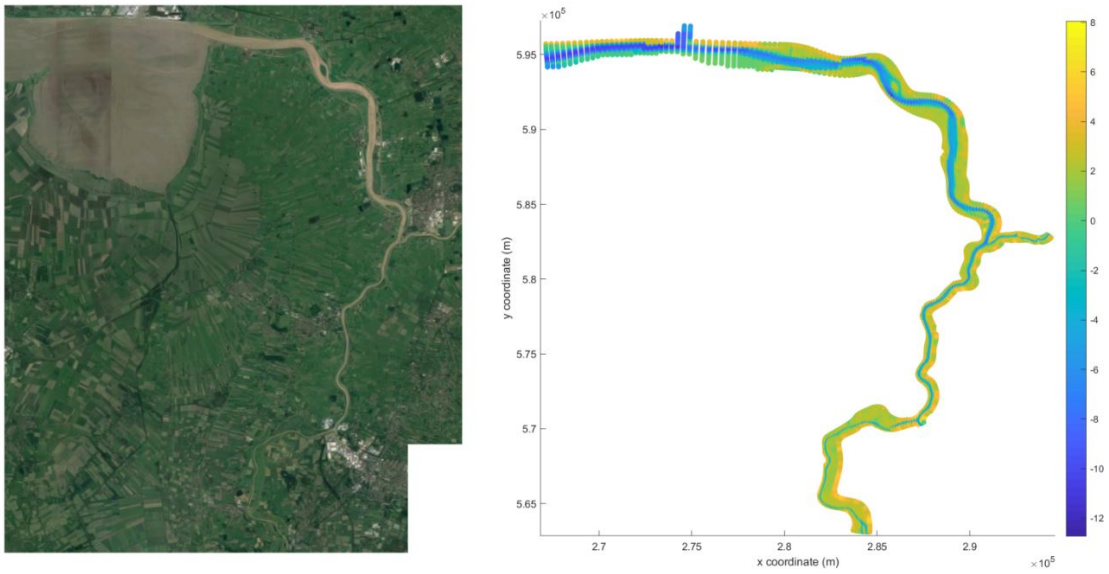

Figure 3.3: A satellite picture of the lower Ems River (left) along with a plot of the detailed bathymetry data used to determine a simple channel geometry.

An exponentially decreasing function was fitted to these estimations. The convergence length of these functions was set to 30 km, which is a value that has been used in other idealized models in the past (Chernetsky, Schuttelaars, and Talke 2010), (Winterwerp and Wang 2013). In figure 3.4 the estimates of the channel parameters, as well as the best fite line and the line used in the model are presented. Some parameters were adjusted slightly during the calibration process in order to improve the models ability to reproduce the tidal asymmetry. The calibration of the model will be discussed in the next chapter.

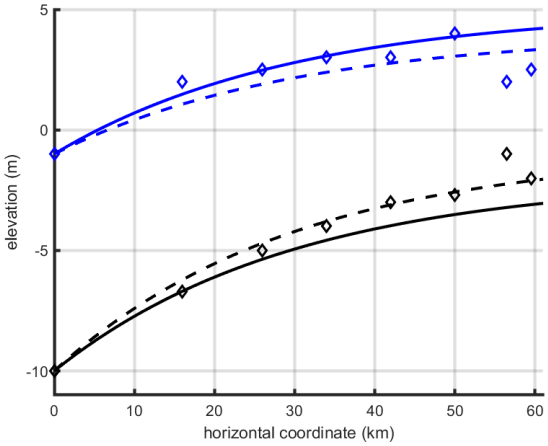

(a) An overview of the estimated values and best fit lines of the bed level (black lines and diamonds) and bank level (blue lines and diamonds). The dashed lines denote the best fit line, while the solid lines present the values actually used in the model.

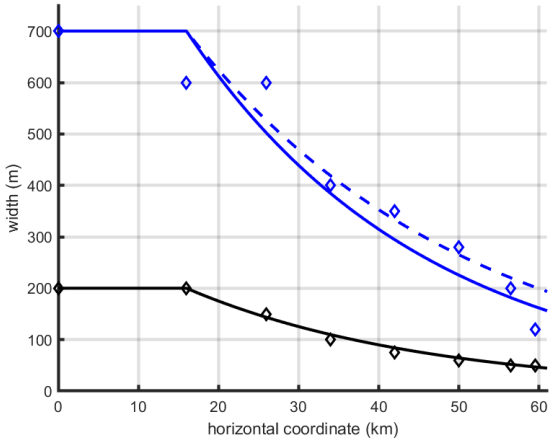

(b) An overview of the estimated values and best fit lines of the bed width (black lines and diamonds) and channel width (blue lines and diamonds). The dashed lines denote the best fit line, while the solid lines present the values actually used in the model.

Figure 3.4: Overview of geometric parameter estimates and model expressions

The total width of the channel, which denotes the width between the levies on either side of the channel is estimated using Google Earth images. It has to be noted that the total width varies greatly along the lower Ems river. In general it decreases almost linearly but in the middle reaches of the channel (km 20-40) the width is much smaller than in the other reaches. In order to maintain a simple expression of the channel geometry, the total width was assumed to be constant over the entire domain. At the seaward boundary, a weakly-reflective condition was applied. The initial water level in the model was set to the mean sea level, which was estimated as the average value between high and low water.

3.3 Boundary conditions

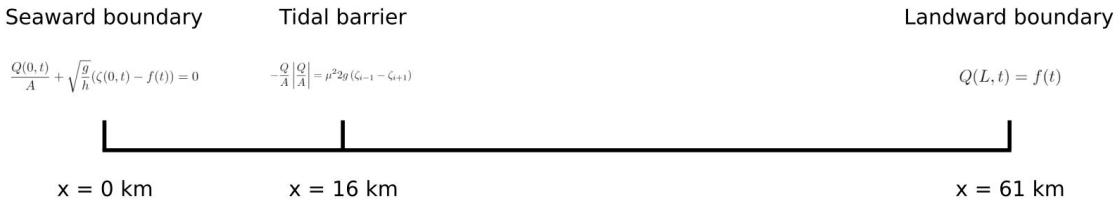

Figure 3.5: An overview of the domain, its boundaries and boundary conditions and the locations of the tidal barrier. The flow equation at the location of the tidal barrier is also presented.

At the seaward boundary the following weakly-reflective boundary condition is specified.

$$\frac{Q(0,t)}{A} + \sqrt{\frac{g}{h}}(\zeta(0,t) - f(t)) = 0 \tag{3.5}$$

The boundary condition near the tidal weir at Herbrum is specified as a discharge condition. This discharge condition represents the Ems river discharge. Because of the nature of the tidal weir, it does not matter that such a discharge condition does reflect waves that propagate against it. The value of the specified discharge is set to be equal to the average discharge over the simulation period.

$$Q(L,t) = f(t) \tag{3.6}$$

3.4 Discretized equations

The model will be solved numerically. The model domain is transformed to a equidistant, colocated numerical grid, with M grid points. The location of each grid point is defined by $x_m = \Delta x m$, with m = 0, 1, ..., M. At every time step n, the surface elevation and discharge are defined. These are denoted by ζ_m^n and Q_m^n. Geometric parameters like channel width at the surface, channel area and hydraulic radius are also defined at every grid point (A_m^n, W_m^n, R_m^n). A BTCS scheme (similar to Van der Zee, 2017) is applied to equations 3.3 and 3.4, which results in the following discretized equations.

$$\frac{\zeta_m^{n+1} - \zeta_m^n}{\Delta t} + \frac{1}{W_m^n} \frac{Q_{m+1}^{n+1} - Q_{m-1}^{n+1}}{2\Delta x} = 0 \tag{3.7}$$

$$\frac{Q_m^{n+1} - Q_m^n}{\Delta t} + \frac{Q_{m+1}^n \frac{Q_{m+1}^{n+1}}{A_{m+1}^n} - Q_{m-1}^n \frac{Q_{m-1}^{n+1}}{A_{m-1}^n}}{2\Delta x} + g A_m^n \frac{\zeta_{m+1}^{n+1} - \zeta_{m-1}^{n+1}}{2\Delta x} + g \frac{Q_m^{n+1} |Q_m^n|}{C^2 A_m^n R_m^n} = 0 \tag{3.8}$$

Two variables (ζ and Q) are defined at each grid point. Therefore both the continuity and momentum equations are solved at each grid point. At the landward boundary, the continuity equation is replaced by the discharge boundary condition and at the seaward boundary the momentum equation is replaced by the non-reflective boundary condition.

3.5 Schematisation of the tidal barrier

The tidal barrier in the Lower Ems primarily functions as a flood defence structure. It was constructed between 1998 and 2002 and is located near Gandersum, 45 km downstream from the tidal weir at Herbrum and at km 16 of the model domain. The barrier consists of a number of gates and rotating segments, divided over 7 segments. Two of the segments also function as a shipping passages and feature rotating segments. The rest of the segments feature only gates. The total width of the barrier is 476m. The elevation of the sill varies between -9m and -5m. Roughly 18% of the cross section of the channel is blocked by the pillars. An illustration of the cross section of the tidal barrier can be found in figure 3.6.

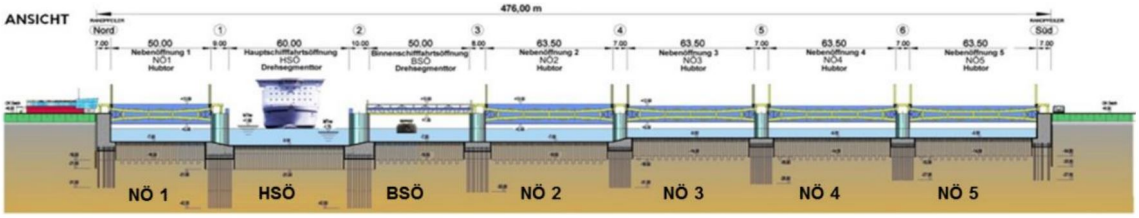

Figure 3.6: A crossection of the tidal barrier, highlighting the different section and closing mechanisms. from Oberrecht and Wurpts (2019)

The real barrier, with a number of different segments and ways to close each segment will be represented in the model as a single segment with a controllable gate. A schematisation of the Ems barrier can be seen in figure 3.7. The area available for water to flow through is denoted by D. The water level on the seaward side and landward side of the barrier is denoted by ζ_{i-1} and ζ_{i+1}, respectively.

The equations which links these variables together is derived from a simple 1D energy balance. Here it is assumed that no energy is dissipated when the water flows through the barrier. Furthermore, the kinetic energy of the water on the upstream side of the flow is neglected. The parameter μ is a flow form parameter which for this simple model is set to 1.

$$-\frac{Q}{D}\left|\frac{Q}{D}\right| = \mu^2 2g\left(\zeta_{i+1} - \zeta_{i-1}\right)$$

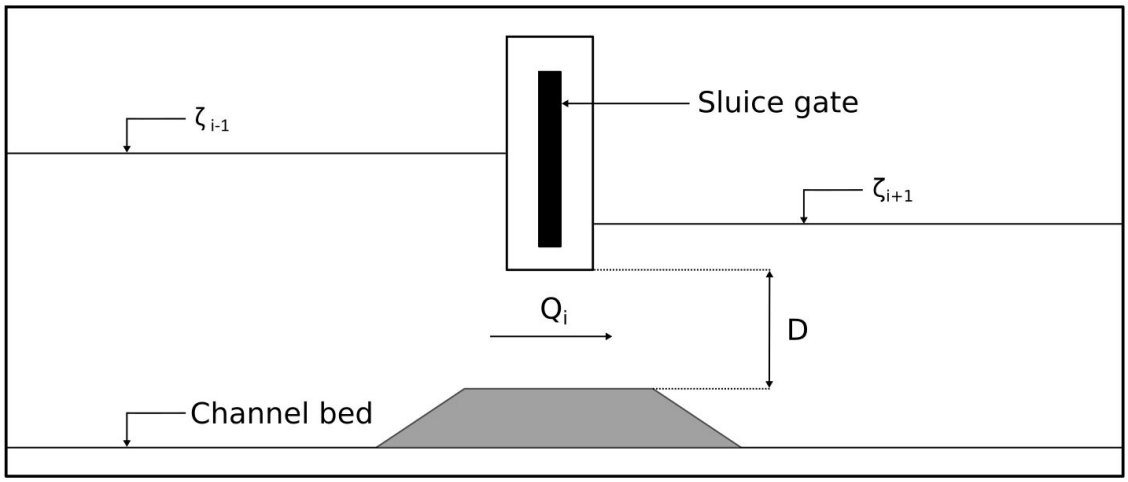

Figure 3.7: A schematisation of the tidal barrier. The barrier is operated by lowering the sluice gate, thus decreasing the flow area D. ζ_{i-1} and ζ_{i+1} denote the water level on the seaward and landward side of the barrier, respectively.

Equation 3.5 is discretised in the following way. The non-linear term that includes Q^2 is linearised by letting one part of the equation lag one time step behind. By using an implicit formulation the following equation is derived.

$$\frac{Q_i^{n+1}}{D^{n+1}} \left| \frac{Q_i^n}{D^{n+1}} \right| + 2g\mu^2\zeta_{i+1}^{n+1} - 2g\mu^2\zeta_{i-1}^{n+1} = 0$$

Here the 'i' denotes the location of the barrier. 'i-1' denotes the landward side of the barrier and 'i+1' denotes the seaward side of the barrier. Lastly, since the there is no water level defined at the location of the barrier, the continuity equation is not solved. The momentum equation at the location of the barrier is replaced by this 'barrier condition'. The momentum equation on the grid points on either side of the barrier are adjusted slightly because no water level is defined at the location of the barrier.

3.6 Operation mode variants

The main principle on which this tidal barrier operation is modelled is that the flood wave has to be impeded in order to slow the flood wave down. This in turn lengthens the time between low water and high water therefore reduces tidal asymmetry. At low water the barrier will close by reducing its normal 'open' flow area by a certain percentage. This parameter is called the closure percentage and is defined as:

$$\text{closure percentage} = \left(1 - \frac{D_{closed}}{D_{open}}\right) * 100\%$$

The barrier is closed over a period of 20 minutes. The second parameter that affects the operation of the barrier is the 'closure duration' which simply is the amount of minutes that the barrier remains closed. After the duration of the closure has passed the barrier is opened again. This process is set to take 45 minutes. The moment of closure of the barrier, as well as the assumed opening and closing times are based on schematisations from Oberrecht and Wurpts (2019).

A schematisation of a number of different operation modes can be found in figure 3.8. The barrier operation modes that will be simulated are very similar to one kind of operation mode modelled (in greater detail) in earlier studies by the NLKMS. This modelling study differs from those performed previously by the Oberrecht and Wurpts (2019, 2020) because a larger variation of closure durations will be evaluated. Additionally, the closure percentage, which was fixed in earlier studies, will be varied as well. The duration of the closure is varied between 120 and 480 minutes. The closure percentage was varied between 50% and 96%.

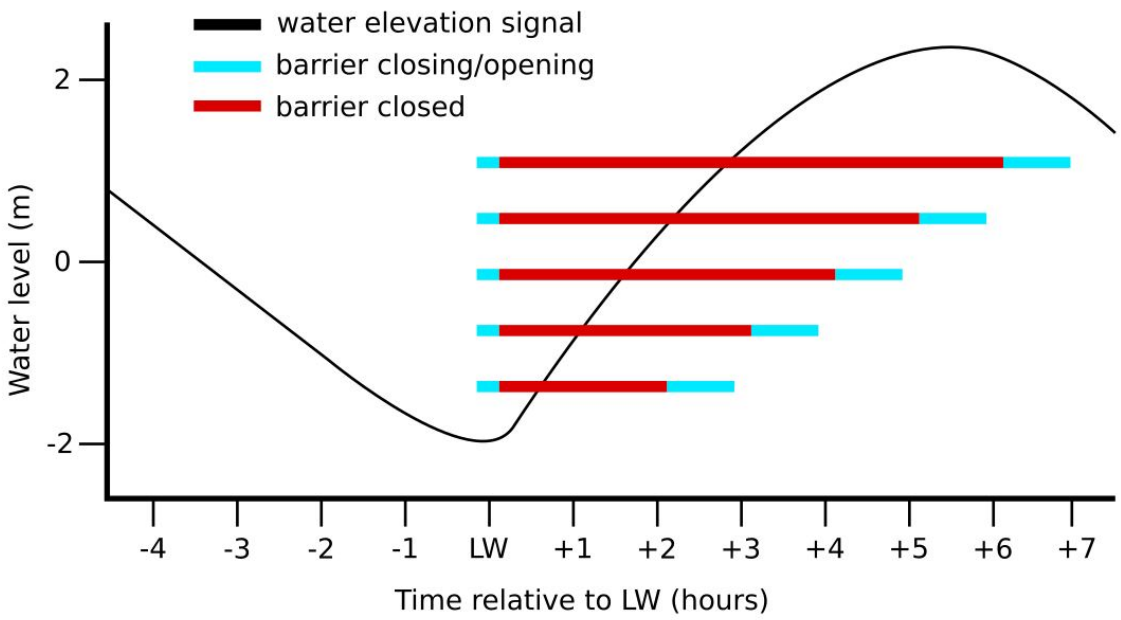

Figure 3.8: A number of different operating modes is illustrated here, along with a sample of a water level signal near the tidal barrier. The time during which the barrier is closed is varied. The opening and closing time are 45 minutes and 15 minutes, respectively.

In this study a further distinction will be made based on when the barrier operation described above will be performed. It is not feasible to perform a barrier operation every tidal wave, as this would impede shipping in the region. In order to quantify the effects of the operation restriction on the results a number of different variants will be simulated.

Variants	Description
Variant 1	Barrier operation every tidal cycle
Variant 2	Barrier operation every other tidal cycle
Variant 3	Barrier operation only when allowed

The first two variants represent theoretical cases in which every tidal wave is affected or barrier operations are performed at a set interval. The third variant represents a simulation in which rudimentary restriction based on shipping activities are imposed. The restrictions that influence barrier operations for variant 3 are based on the most lenient restriction applied in earlier studies (Oberrecht and Wurpts 2019b). These restrictions prevent barrier operation between 6 AM and 6 PM.

3.7 Evaluation criteria

First a simulation is performed in which the model remains fully open. The water level signal at the location of the barrier is then used to determine the exact moment of low water. This moment, together with the closure duration and the closure percentage is used to generate an input signal. This signal represents the flow area of the barrier at every time step the model resolves. When this input signal is constructed, it is assumed that the effects of the operation of the barrier on a tidal wave do not influence the next tidal wave.

3.7.1 Tidal prism

As was mentioned previously in section 3.6, the tidal prism of the Ems river cannot be reduced too much. It is clear that heightening or lowering the water levels in the Ems river affects the habitat of bird, among other species. The tidal prism is the volume of water that passes through a certain cross-section in a river between low water and high water. The tidal prism is calculated as follows:

$$P = \int_{t_{LW}}^{t_{HW}} Q dt \approx \sum_{t=t_{LW}}^{t_{HW}} Q_t \Delta t$$

Due to the large time step in the simulation (10 minutes) the calculations of the tidal prism are relative inaccurate. In order to reduce this inaccuracy, the average of the tidal prism of every flood wave is calculated instead.

3.7.2 Relative phase change

As was mentioned in chapter 2, the tidal asymmetry is primarily characterised using the relative phase difference between the M2 and M4 tidal components. A direct measure for this phase difference is:

$$2M_2 - M_4 = 2\theta_{M_2} - \theta_{M_4} \tag{3.9}$$

If the relative phase difference has a value between 0° and 180°, the tidal wave is flood dominant. If the relative phase difference has a value between 180°and 360°, the tidal wave is ebb-dominant.

3.7.3 Amplitude ratio change

The ratio of the amplitude of the M2 and M4 components is another way of evaluating the severity of the asymmetry of the tide. The ratio is defined as:

$$\frac{M_4}{M_2} = \frac{a_{M_4}}{a_{M_2}} \tag{3.10}$$

Determining the amplitude ratio of the M2 and M4 components does not say anything about ebb or flood dominant. The criteria will be applied only to verify that the M4 component has not been damped out by the barrier operation. The calculations of the phase angles for tidal components is less accurate for components with small amplitudes.

3.7.4 Secondary considerations

Other criteria which will be used to evaluate the barrier operation are related to controllability of the flow. A clear distinction can be made between operation regimes which impede the propagation of the wave and operation regime which more or less stop the propagation of the wave and then release a large volume of water over a short period of time. Lastly, the time-water level signal will be evaluated. The intended approach of the model is to determine the asymmetry by analysing the components of the tidal signal. A crucial assumption of the approach is that the signal consists of harmonic components. If the barrier operation regime results in a water level series where this assumption is violated, the results become very difficult to evaluate properly.

Chapter 4

Results

The calibration and validation of the model is performed using data from the tidal stations in the Lower Ems. The model is calibrated for river discharge conditions which are typical during summer months. The model is then validated for typical summer discharge conditions as well as discharge conditions that are typical for winter months. The exact periods over which calibration and validation is performed are shown in table 4.1.

Action	Start date	End date
Calibration	01-05-2005	01-06-2005
Validation summer	01-06-2005	02-07-2005
Validation winter	01-02-2005	04-03-2005

Table 4.1: Overview of the periods over which the model is calibrated and validated.

4.1 Model calibration

The model was calibrated, using a trial and error method, to reproduce the key characteristics of the tidal asymmetry as well as possible. The Chézy friction factor was the primary calibration parameter, which was constrained between 90 and 100 $m^{0.5}/s$. These are typical values for very smooth beds. In order to further improve the models ability to reproduce the characteristics, the expression that define the tidal asymmetry were adjust slightly as well. An overview of the expressions of the parameters that are used to determine the channel geometry can be seen in figure 3.4.

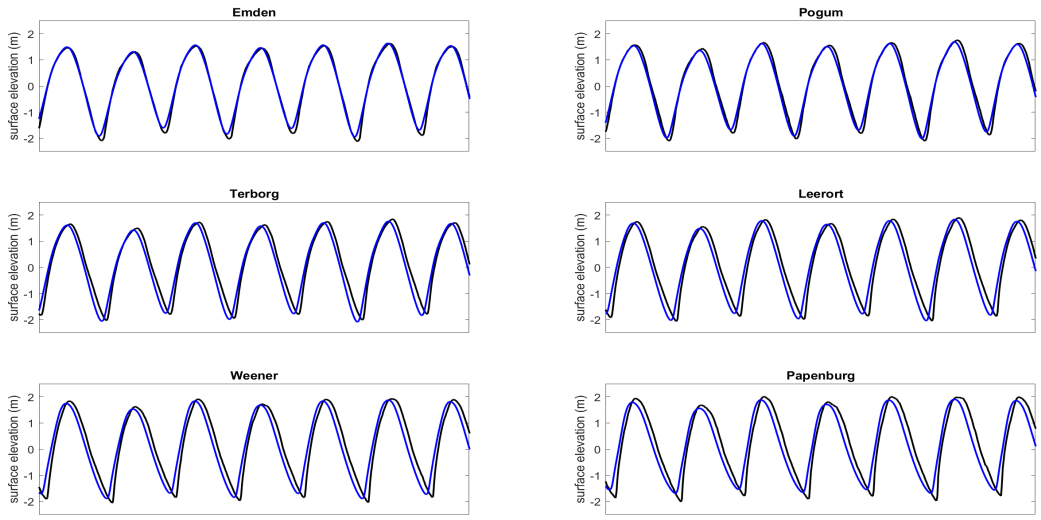

Figure 4.1: A comparison of water level measurements (black lines) and model results (blue lines) for data from a number of tidal stations in the lower Ems over part of the summer calibration period.

In figure 4.1 a comparison of the simulated water levels and the measured water levels is presented. The figures are ordered in distance from the seaward boundary. From the figure it is clear that the propagation speed of the tidal wave is too high in the region between Pogum and Terborg, as well as the region between Weener and Papenburg. As a result of the higher propagation speed the measurements lag behind the modelled values. This error should not substantially impact the results of the tidal asymmetry since this involves the shape of the wave, rather than the propagation speed.

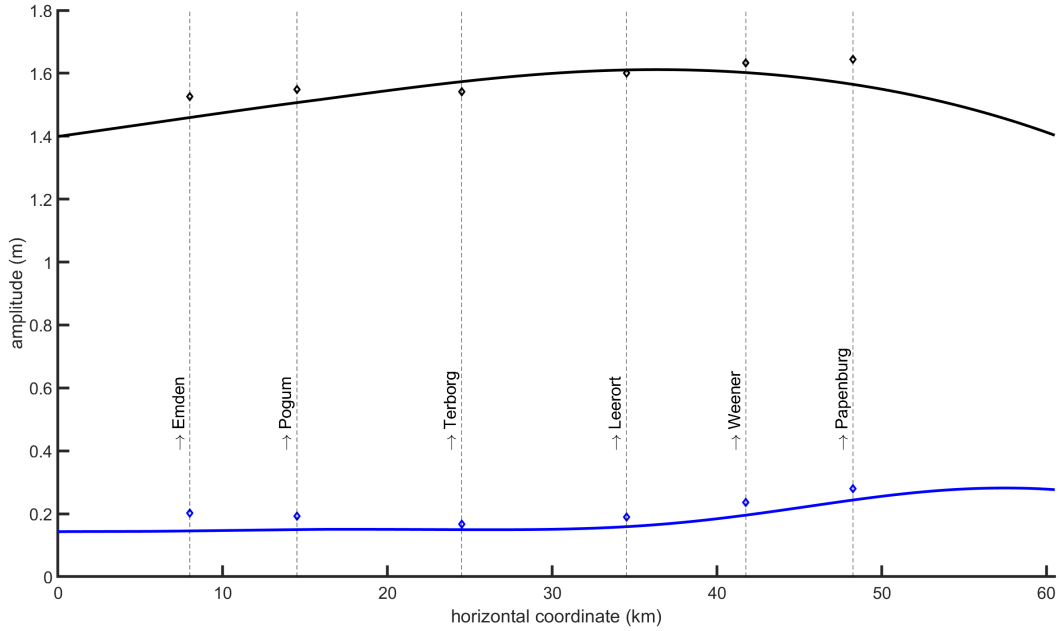

Figure 4.2: Comparison of the M2 amplitude measurements (black diamonds), modelled M2 amplitudes (black line), M4 amplitude measurements (blue diamonds) and modelled M4 amplitudes (blue line) for the results obtained during the calibration period.

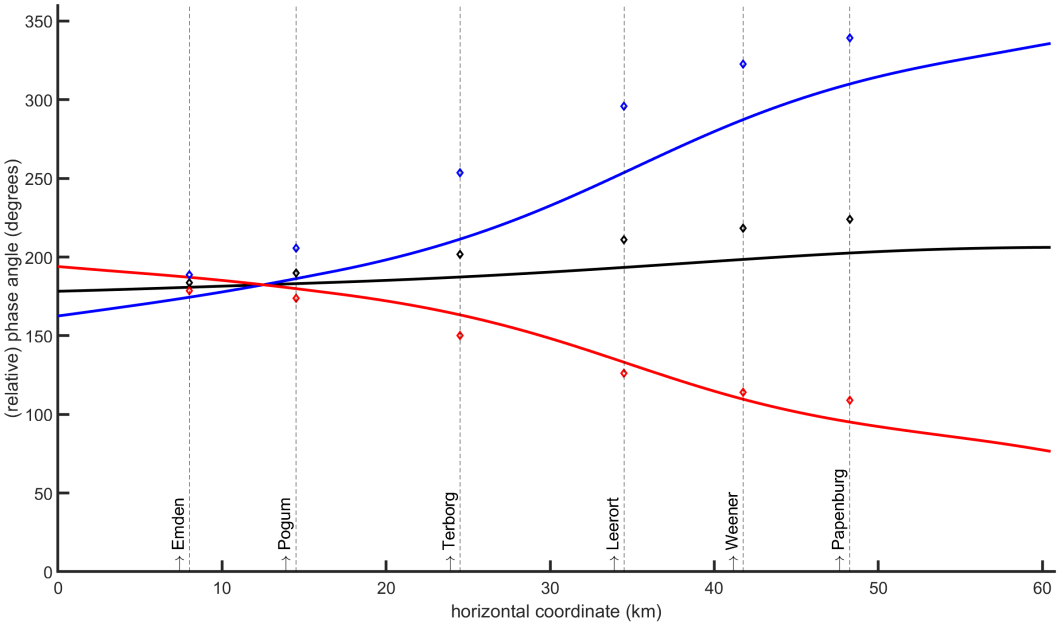

Figure 4.3: Comparison of the M2 phase measurements (black diamonds), modelled M2 phases (black line), M4 phase measurements (blue diamonds) and modelled M4 phases (blue line). The same data is presented in the form of a relative phase angle (red diamonds and line) for the results obtained during the calibration period.

In figures 4.2 and 4.3 a comparison of modelled and measured amplitudes for the M2 and M4 tidal components is presented, as well as a comparison of the phase lags and relative phase angle. The amplitude of the M2 component is slightly overestimated near the seaward side of the model and between Weener and Papenburg. In the stretch of the Lower Ems between Terborg and Leerort the M2 amplitude is underestimated slightly. The amplitude of the M4 component is overestimated slightly throughout the model. The internal amplification of the M4 component is reproduced well by the model.

An overview of the phase angles of the M2 and M4 components is presented in figure 4.3. The phase lags of the M2 and M4 components individually is overestimated. This is the result of the higher propagation speed of the tidal wave in the model. The relative phase angle between the M2 and M4 components is reproduced much better. It is overestimated slightly from the seaward end of the model up to Weener. From Weener on the relative phase angle is overestimated slightly. The difference between measured and modelled values appears to be smaller than 20°.

The fit of the relative phase angle is much better due to the way the it is calculated. Since two overestimated phase angles are subtracted the effect of overestimating both phase angles is diminished. A comparison of the component amplitudes and phase angles for conditions typical during winter can be found in the appendix, figure 7.2 and 7.3.

4.2 Model validation

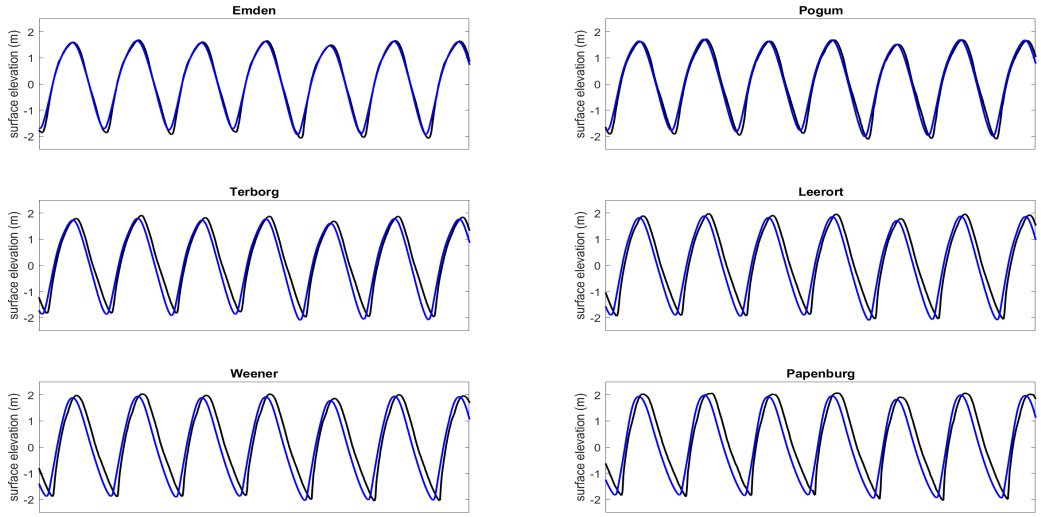

Figure 4.4: A comparison of water level measurements (black lines) and model results (blue lines) for data from a number of tidal stations in the lower Ems, over part of the summer validation period.

The validation of the model, performed for both discharge conditions that are typical during summer and winter months, shows similar characteristics to the calibrated model. The propagation velocity of the tidal wave is still too high. This results in a similar comparison of the phase angles as in figure 4.3. The calculated relative phase angles compare to the measured values in a similar way as well. The comparison of measurements and model results for the winter validation period yielded similar results. An overview of those results can be found in the appendix (figure 7.2 and 7.3).

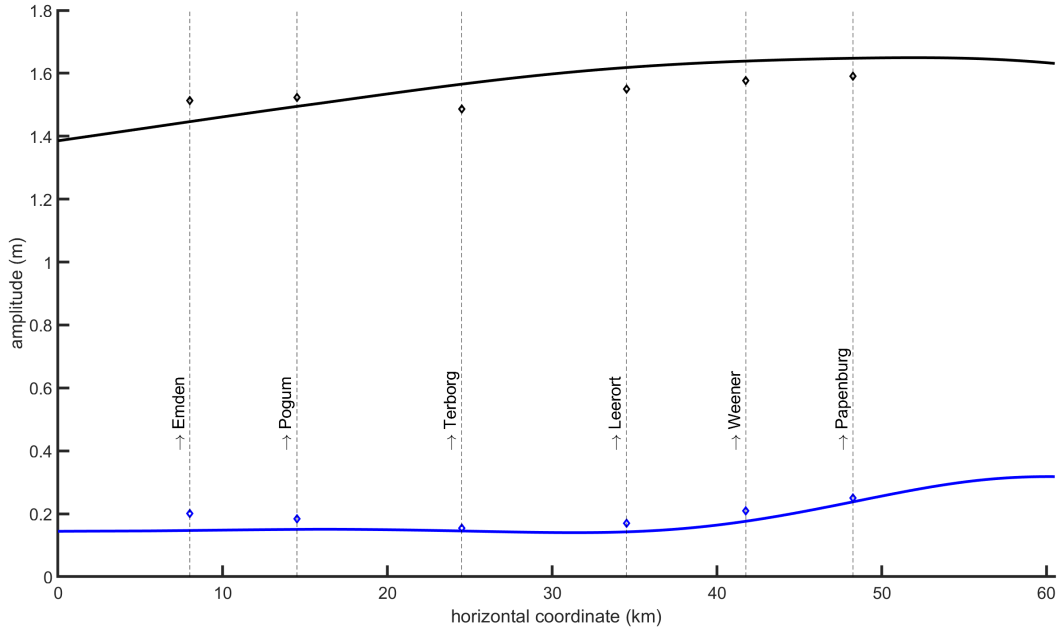

Figure 4.5: Comparison of the M2 amplitude measurements (black diamonds), modelled M2 amplitudes (black line), M4 amplitude measurements (blue diamonds) and modelled M4 amplitudes (blue line) for the results obtained during the summer validation period.

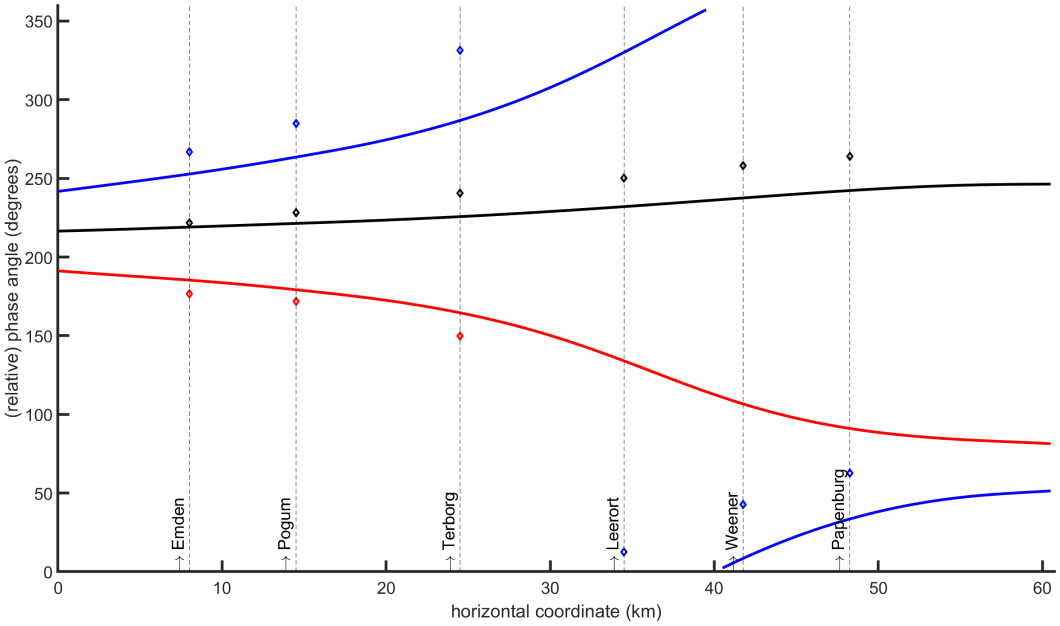

Figure 4.6: Comparison of the M2 phase measurements (black diamonds), modelled M2 phases (black line), M4 phase measurements (blue diamonds) and modelled M4 phases (blue line). The same data is presented in the form of a relative phase angle (red diamonds and line) for the results obtained during the summer validation period.

4.3 Simulation results

4.3.1 Behaviour of the unaltered tidal wave

A tidal wave propagating through the Lower Ems, unimpeded by any barrier operation, will deform considerably before reaching the tidal weir at Herbrum. The amplitude of the tidal wave increases and the duration of the flood will shorten. This change is also obvious from the results of the calibration and validation. As can be seen in figures 4.2 and 4.5, the amplitude of the M2 component increases steadily until reaching a maximum near Papenburg. The M4 amplitude remains roughly constant until Leerort, after which it starts to increase as well.

The change in asymmetry is illustrated well by figures 4.3 and 4.6. The phase angle of the M2 component increases slightly throughout the model domain while phase angle of the M4 component increases sharply. The resulting relative phase angle indicates that the tidal waves from a slightly ebb-dominant character seaward of Pogum, to a very flood-dominant character near Papenburg.

4.3.2 Flow behaviour near the barrier

The operation of the tidal barrier accomplishes the goal of shifting the asymmetry of the tidal wave by impeding the tidal wave. Due to the restriction of the flow area at the barrier a water level difference must first build up before the discharge through the barrier can increase. When the barrier is subsequently opened the water levels on either side of the barrier slowly approach the water level of the unimpeded wave again. This behaviour is reproduced by the model. Figures 4.7 and 4.8 show that the magnitude of the water level difference is proportional to the closure percentage, although there appears to be a exponential relation between the two. It is also clear from figure 4.8 that the high water moment is delayed by up to around 40 minutes as a result of the operation.

The influence of the closure duration is presented in figures 4.9 and 4.10. From the moments the water levels start approaching the 'normal' water level again the different closure durations can easily be distinguished. The effect of the closure duration of the delay of the high water moment is not as clear as it was for the closure percentage. There is a clear difference in the high water times if the closure duration is longer than 240 minutes. However, for closure durations shorten than 240 minutes the effect appears to be minimal.

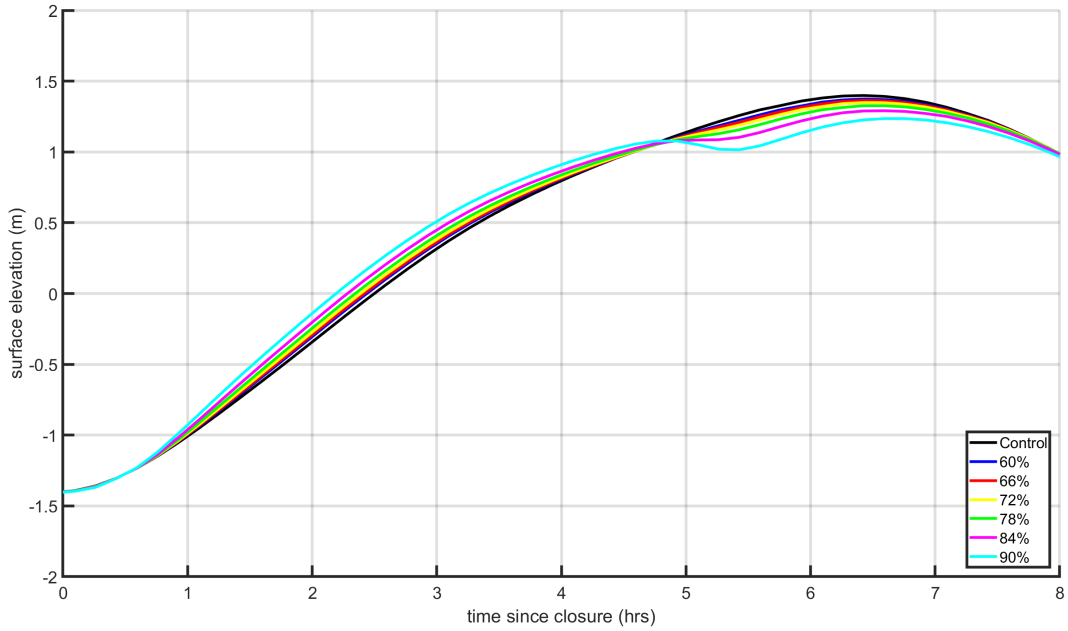

Figure 4.7: A comparison of parts of water level signals on the seaward side of the tidal barrier for a number of different barrier operation modes with changing closure percentages. Horizontal coordinate x = 15.5 km.

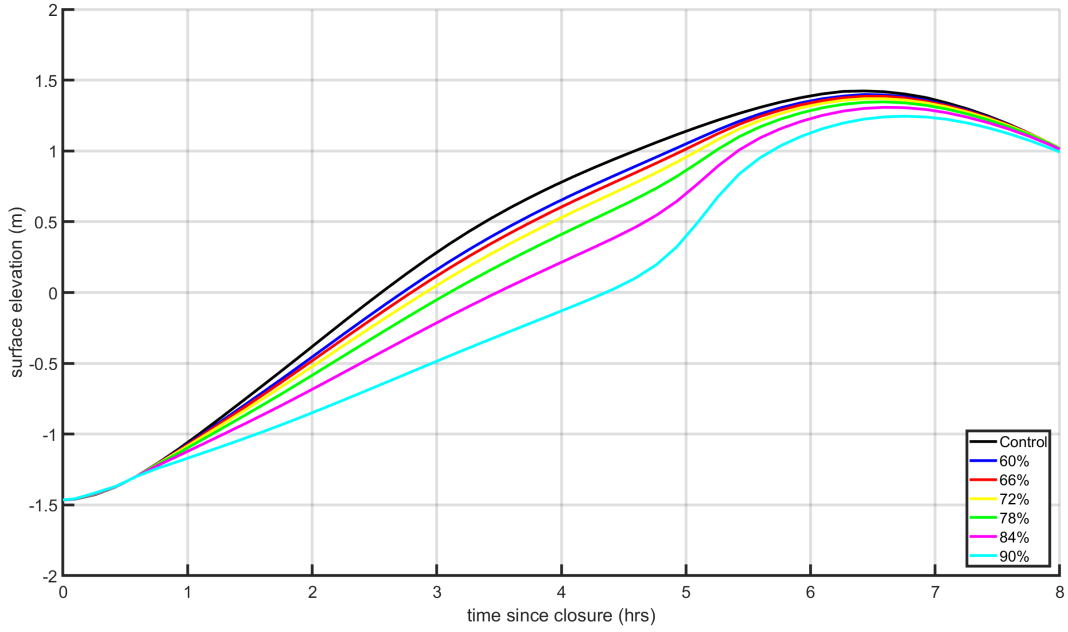

Figure 4.8: A comparison of parts of water level signals on the landward side of the tidal barrier for a number of different barrier operation modes with changing closure percentages. Horizontal coordinate x = 16.5 km.

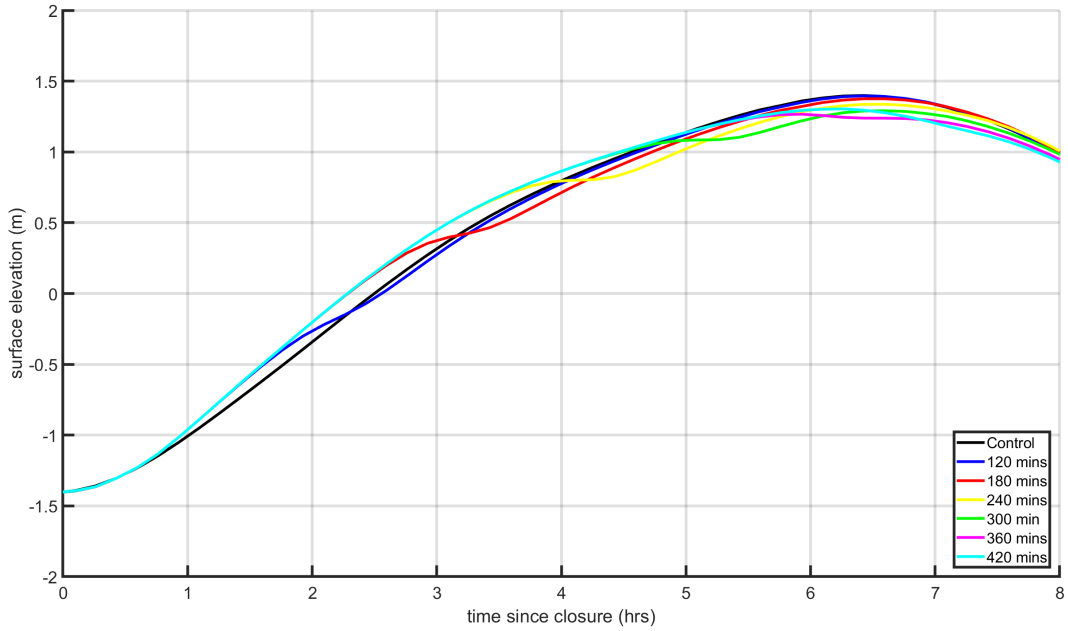

Figure 4.9: A comparison of parts of water level signals on the seaward side of the tidal barrier for a number of different barrier operation modes with changing closure durations. Horizontal coordinate x = 15.5 km.

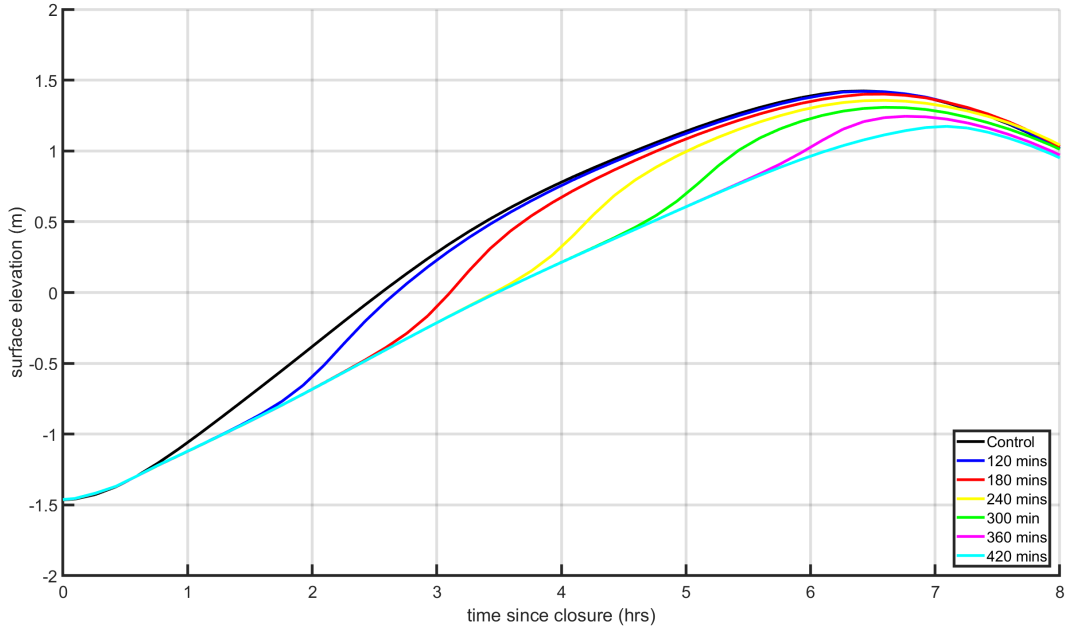

Figure 4.10: A comparison of parts of water level signals on the landward side of the tidal barrier for a number of different barrier operation modes with changing closure durations. Horizontal coordinate x = 16.5 km.

4.3.3 Effect of the opening time

For barrier operation modes that involve a closure durations less than 360 minutes, the release of water occurs before the high water moment (figure 4.10). In cases with a significant build-up of water in front of the barrier a sudden and quite violent release of water can occur. This can have negative effects on the stability of the structure and bed protection. In figures 4.11 and 4.12 the influence of the opening time in prevention this sudden release of water is illustrated. For all other simulations the opening time of the barrier is set to 45 minutes. A sudden release of water occurs for opening times of 15 and 30 minutes. In order to release the build up water more gradually, the opening time can be extended to 60 minutes, but increasing the opening time further has negligible results.

4.3.4 Influence of the river discharge

In order to determine the effect increased river discharge has on the effectiveness of the barrier operation, a simulation was also made of the tidal waves in a winter month. The river discharge was set increased to match the average discharge over the entire simulation period. The effectiveness of the barrier operation is very similar to that barrier operations performed under typical summer conditions. Only the decrease of the tidal prism increased. An overview of the results of the simulation is available in the appendix (figures 7.4, 7.5, 7.6 and 7.7).

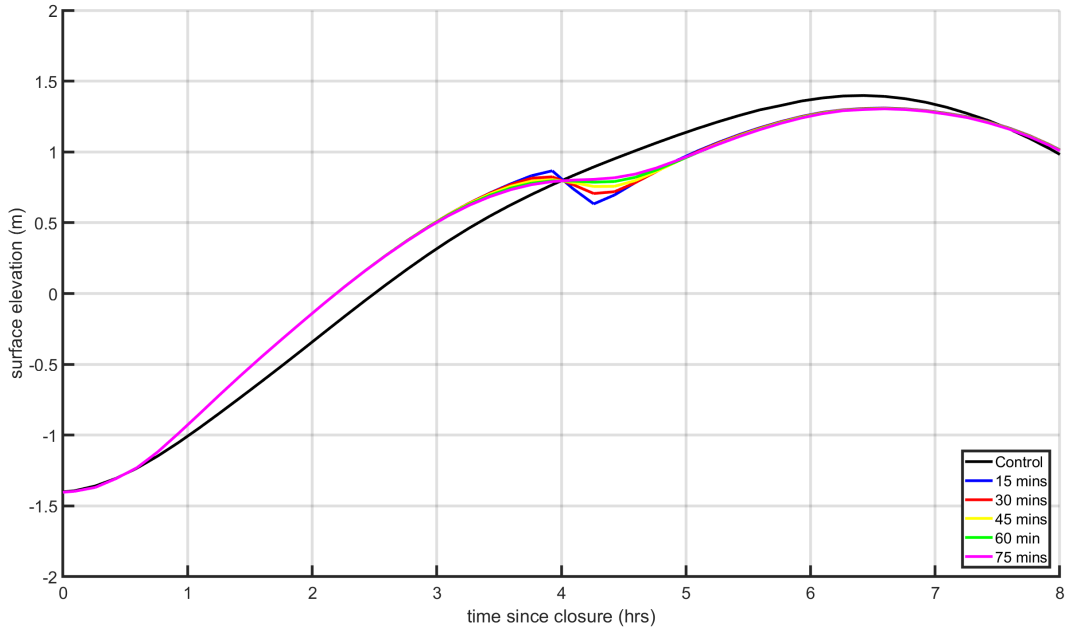

Figure 4.11: Comparison of parts of water level signals near the tidal barrier. The closure percentage and closure duration is kept constant. Only the opening time of the barrier operation mode is varied. Horizontal coordinate x = 15.5 km

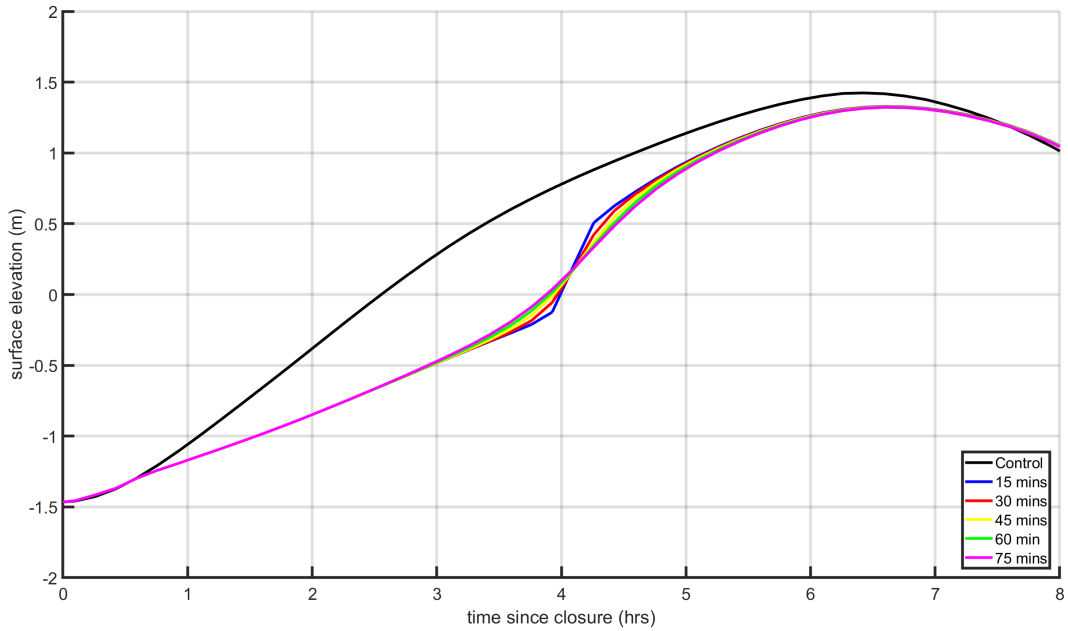

Figure 4.12: Comparison of parts of water level signals near the tidal barrier. The closure percentage and closure duration is kept constant. Only the opening time of the barrier operation mode is varied. Horizontal coordinate x = 16.5 km

4.3.5 Variant 1

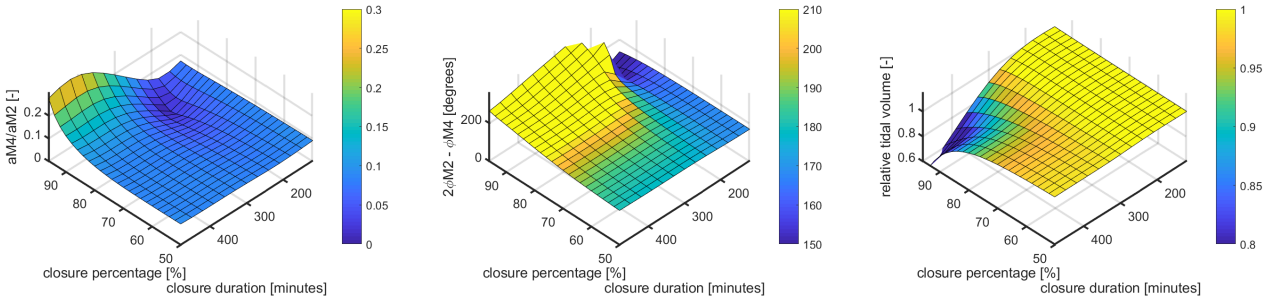

(a) M4/M2 amplitude ratio. (b) M4/M2 relative phase angle. (c) Relative tidal prism.

Figure 4.13: An overview of the evaluation criteria for a range of different closure percentage and closure durations.

An overview of the evaluation criteria for a wide array of combinations of closure percentages and closure durations is presented in figure 4.13. The results in figure 4.13 represent the characteristics near Terborg. Similar figures are also available for other locations. These can be found in the appendix (figure 7.8, 7.9 and 7.10).

The closure duration has a distinctly binary effect on the deformation if the closure percentage of the operation mode is less than 75%. This behavior is evident in figures 4.13b and 4.13c. In figure 4.13b the effect of the barrier operation is negligible for closure durations shorter than approximately 240 minutes. Once this threshold is passed, the barrier operation results in an increase in the relative phase angle, but further increases of the closure duration do not lead to a substantial further increase. For closure percentages higher than 75%, increases in closure duration generally result in increased tidal amplitudes, decreased upward shift in the relative phase angle and a increased reduction of the tidal prism.

The binary character of the effect of increased closure duration persists through the entire model domain. The values of the evaluation criteria are plotted for a number of different closure durations in figures 4.15, 4.17. In these figures it is also clear that the effectiveness of the barrier operation is similar for closure durations of 120 and 180 minutes. The effect of the barrier operation for closure durations of 300, 360 and 420 minutes is also similar. The evaluation criteria for closure durations between 180 and 300 minutes have a value that is in between these two bands. The threshold value of the closure duration appears to be slightly higher than 240 minutes if the reduction of the tidal prism is considered (figure 4.19).

The changes to the amplitudes and phases of the M2 and M4 component as a result of the barrier operation tend to be very similar, provided that the closure duration exceeds the threshold value of around 240 minutes. The amplitude of the M2 component is decreased uniformly on the landward side of the barrier. On the seaward side of the barrier the M2 amplitude decreases slightly. The amplitude of the M4 component increases on the seaward side of the barrier and decreases on the landward side of the barrier. The decrease more pronounced from km 30 onward.

The phase of the M2 component is increased slightly on the landward side of the barrier. The change in relative phase angle is mostly governed by the change in phase of the M4 component, which decreases significantly on the landward side of the barrier. The deviation of the M4 of an unaltered wave is damped out before the tidal wave reaches the tidal weir at Herbrum. The relative phase angle of an altered and unaltered wave become similar again around km 50.

Increasing the closure percentage simply seems to amplify the changes described above, but it does not change the general trends (figure 4.14 and 4.17). The only exception is to the amplitude of the M4 component. The component of an unaltered wave reaches a minimum around km 35. Increasing the closure percentage

also pushes the location of the minimum amplitude further upstream. This effect is clearly visible in figure 4.14.

As a result of the barrier operation the tidal volume in decreased uniformly throughout the domain. Increased closure percentages result in further decreases in the tidal volume. This tendency is illustrated in figure 4.18. The reduction in tidal volume, expressed as a percentage is approximately constant throughout the domain. Near the landward boundary, the reduction in tidal volume increases sharply. It is unclear whether this is caused by the tidal barrier operation or due to inaccuracies in the calculation of the tidal volume stemming from the relatively large time step and relatively small tidal volume.

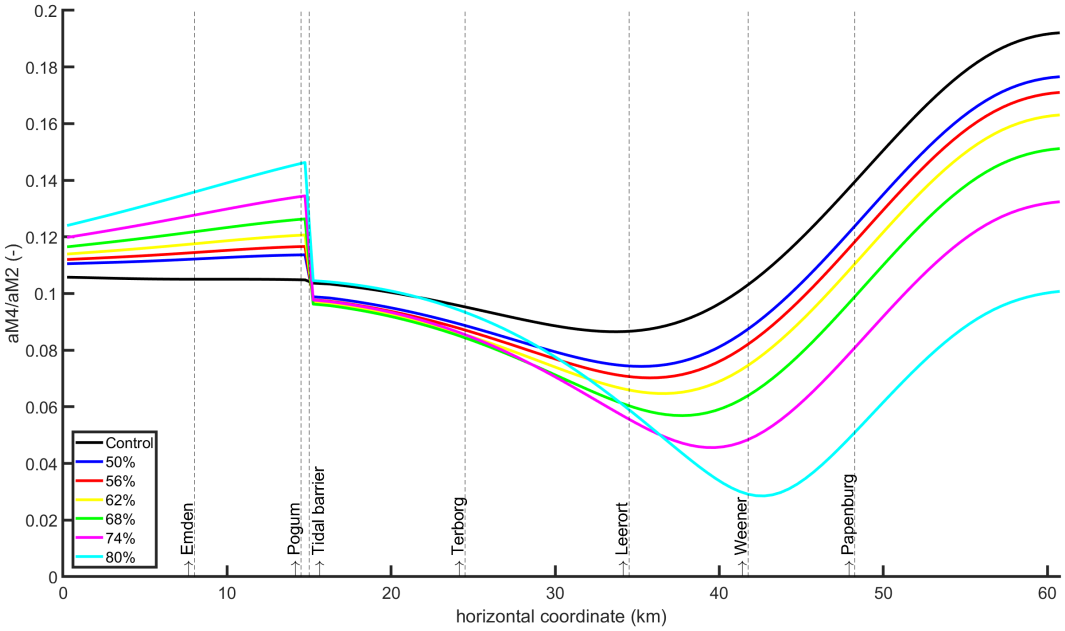

Figure 4.14: The effect of variations in closure percentage on the tidal amplitude ratio throughout the model domain. Closure duration = 300 min, closure percentages vary.

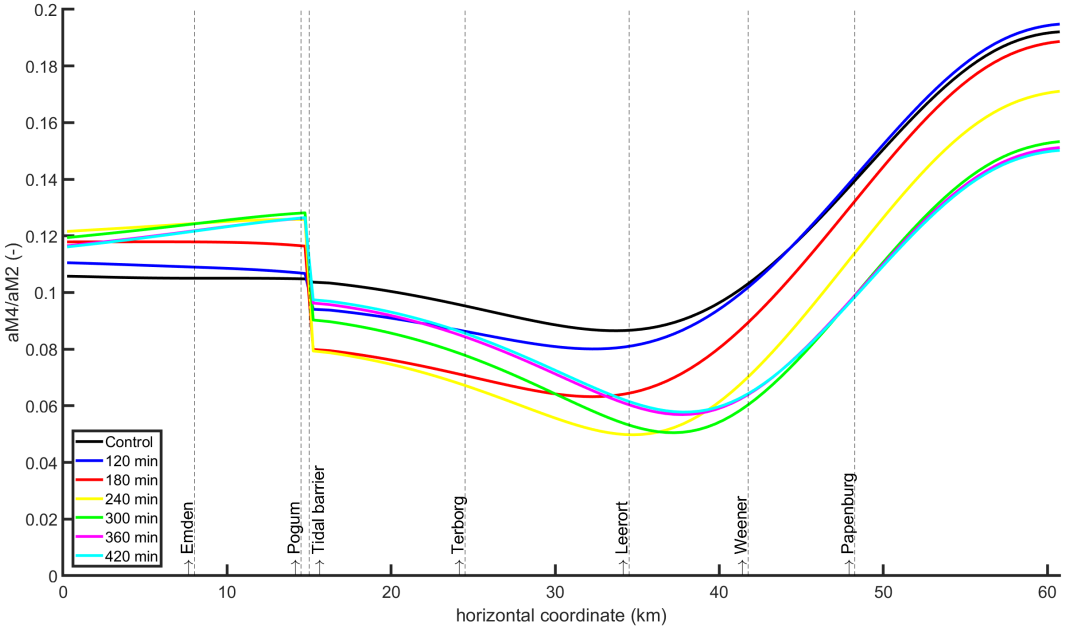

Figure 4.15: The effect of variations in closure duration on the tidal amplitude ratio throughout the model domain. Closure percentage: 68%, closure durations vary.

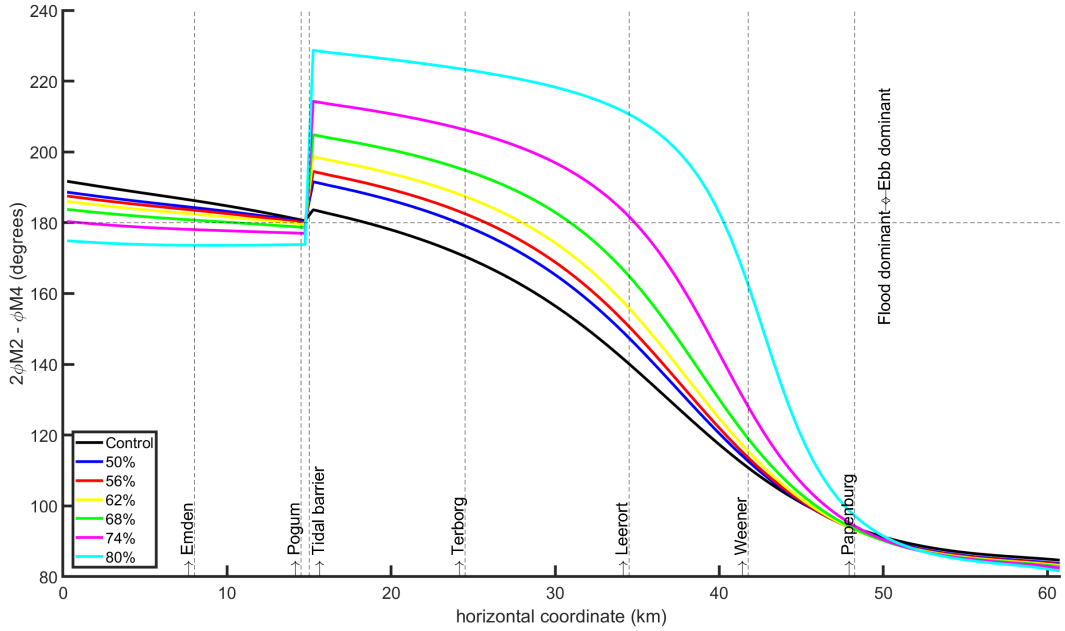

Figure 4.16: The effect of variations in closure percentage on the relative phase angle throughout the model domain. Closure duration = 300 min, closure percentages vary.

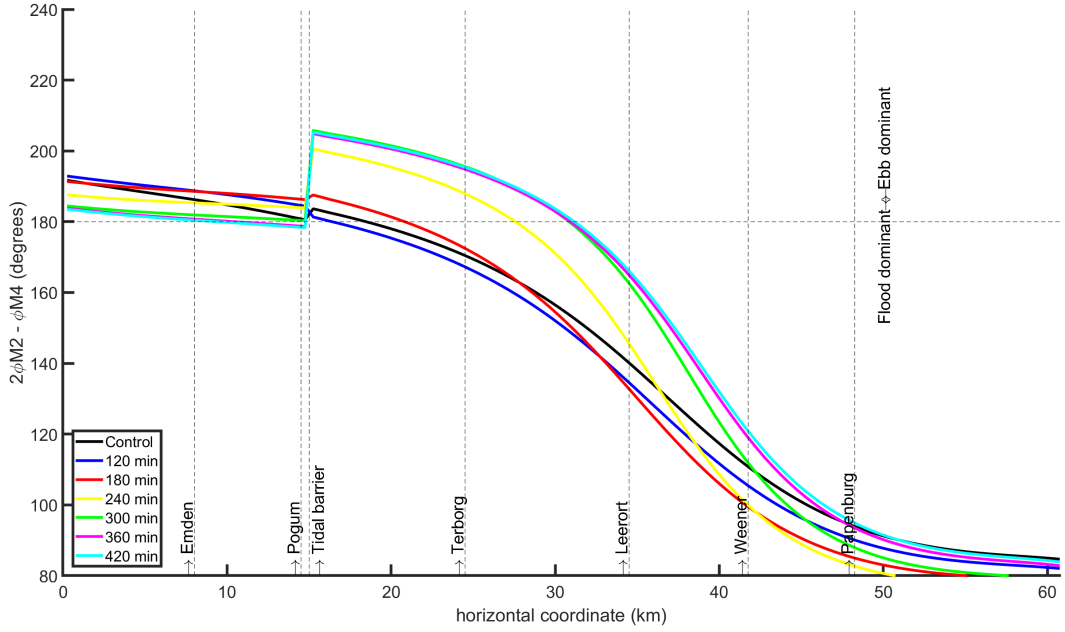

Figure 4.17: The effect of variations in closure duration on the relative phase angle throughout the model domain. Closure percentage: 68%, closure durations vary.

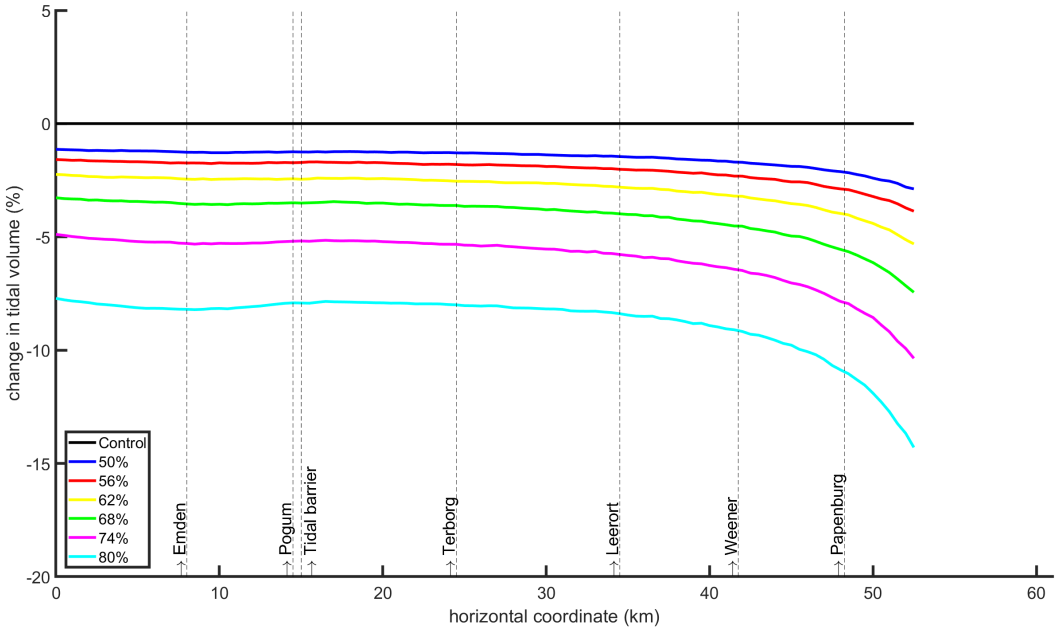

Figure 4.18: The effect of variations in closure percentage on the relative tidal prism throughout the model domain. Closure duration = 300 min, closure percentages vary.

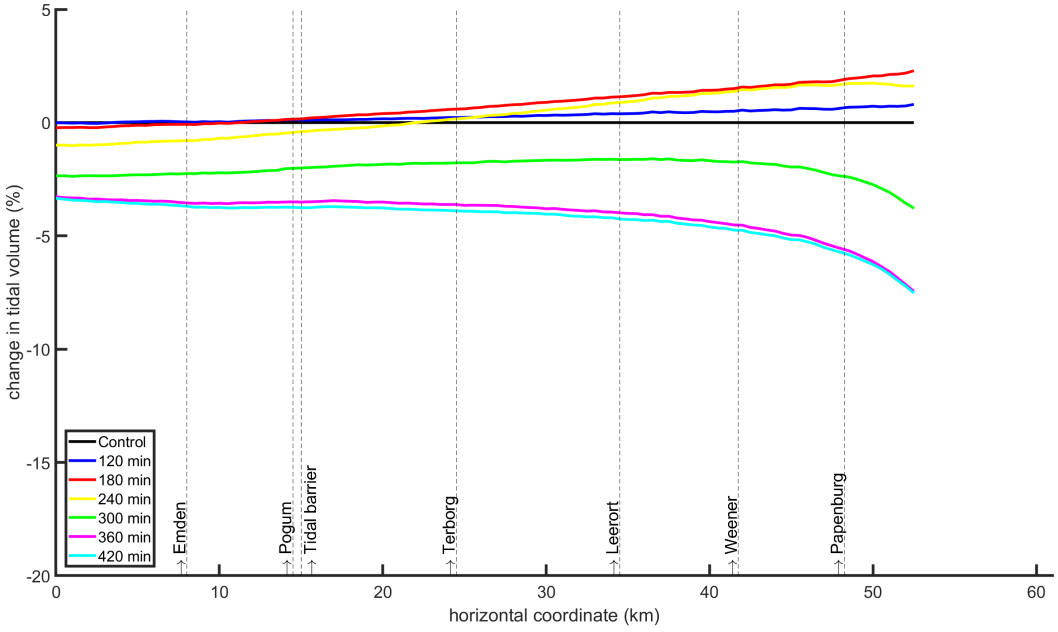

Figure 4.19: The effect of variations in closure duration on the relative tidal prism throughout the model domain. Closure percentage: 68%, closure durations vary.

4.3.6 Variant 2

In figure 4.20 the results of simulations of variant 2 are shown. From this figure it is clear that the effects of a barrier operation do not affect tidal waves on which the operation was not performed. This means that a water level signal resulting from operation variant 2, can be interpreted as a combination of altered and unaltered tidal waves. Barrier operation variant 2 involves performing a barrier operation every other tidal period. Since only half of the tidal waves is deformed by a barrier operation the overall effects of the barrier operation will be reduced by 50% as well.

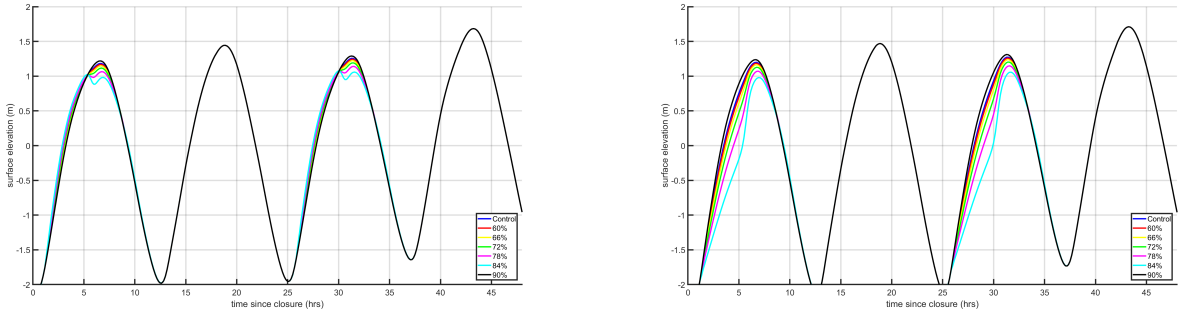

(a) Horizontal coordinate x = 15.5 km

(b) Horizontal coordinate x = 16.5 km

Figure 4.20: A typical water level signal resulting from a controlled barrier operation every other tide.

The overall character of the results is similar to the results of variant 1. For example, the binary nature of the influence of the closure duration is still evident from the values of the amplitude ratio (figure 4.23), relative phase angle (figure 4.21b and 4.25) and relative tidal prism (figures 4.21c and 4.19). The changes in amplitude ratio and relative tidal prism for different closure percentages (figure 4.14, 4.16 and 4.18) are similar to those of variant 1, but are smaller in magnitude. The decrease appears to be roughly proportional to the reduction in the number of tidal waves that are adjusted.

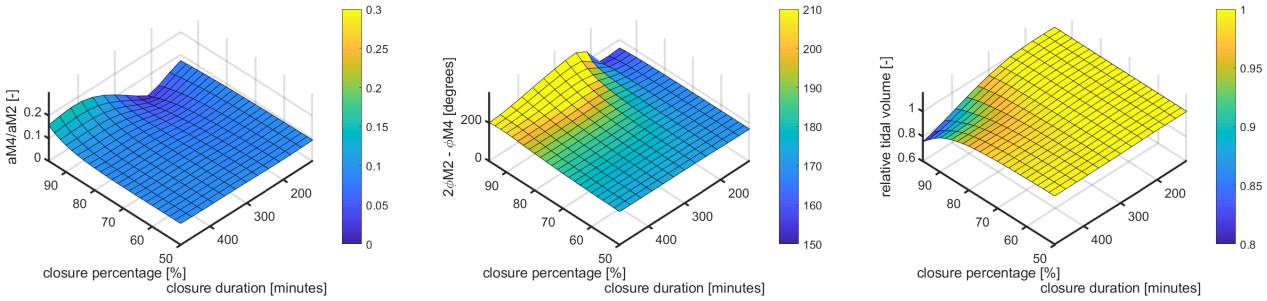

(a) M4/M2 amplitude ratio

(b) M4/M2 relative phase angle

(c) Relative tidal prism

Figure 4.21: An overview of the evaluation criteria for a range of different closure percentage and closure durations.

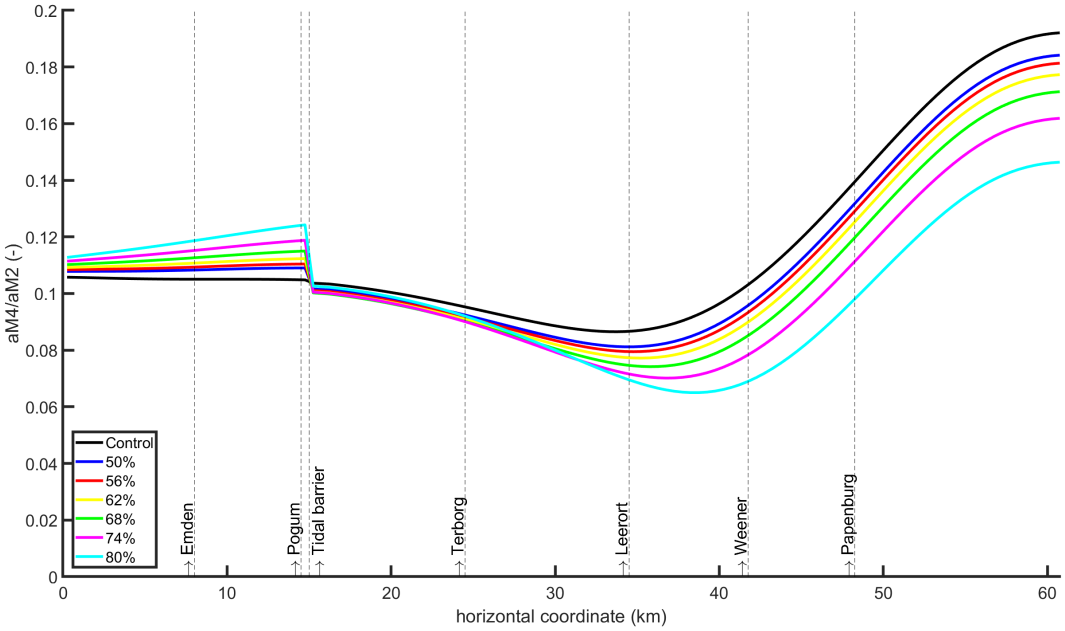

Figure 4.22: The effect of variations in closure percentage on the tidal amplitude ratio throughout the model domain. Closure duration = 300 min, closure percentages vary.

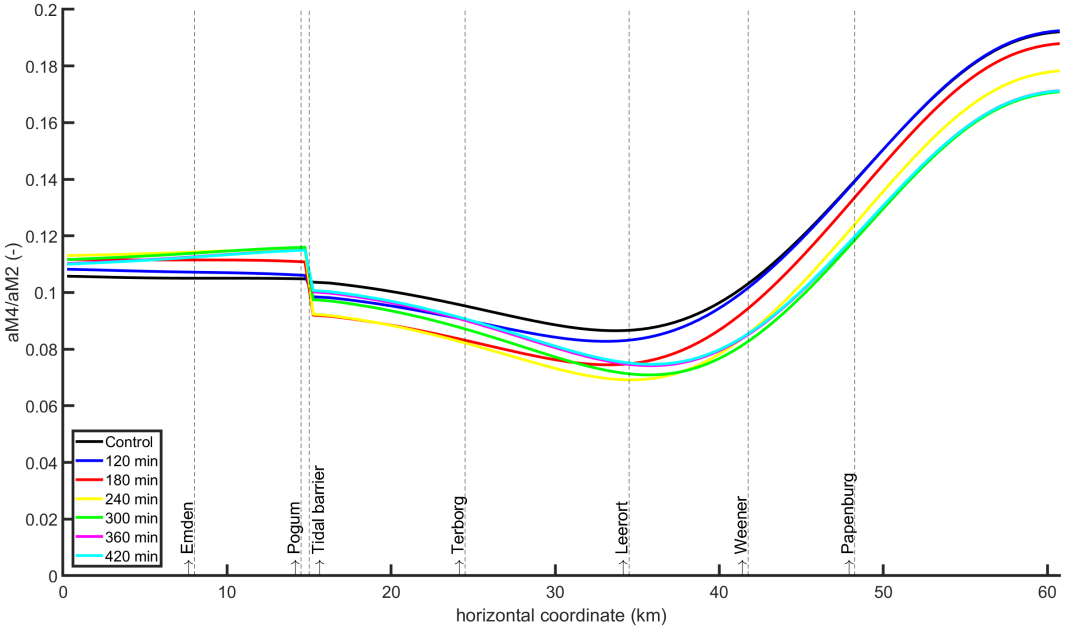

Figure 4.23: The effect of variations in closure duration on the tidal amplitude ratio throughout the model domain. Closure percentage: 68%, closure durations vary.

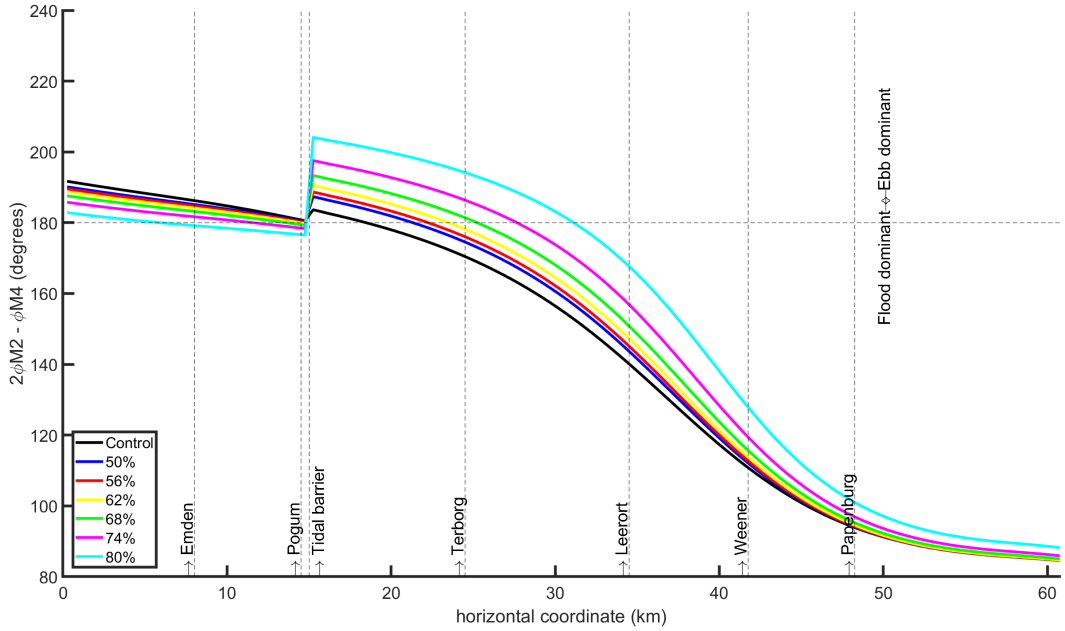

Figure 4.24: The effect of variations in closure percentage on the relative phase angle throughout the model domain. Closure duration = 300 min, closure percentages vary.

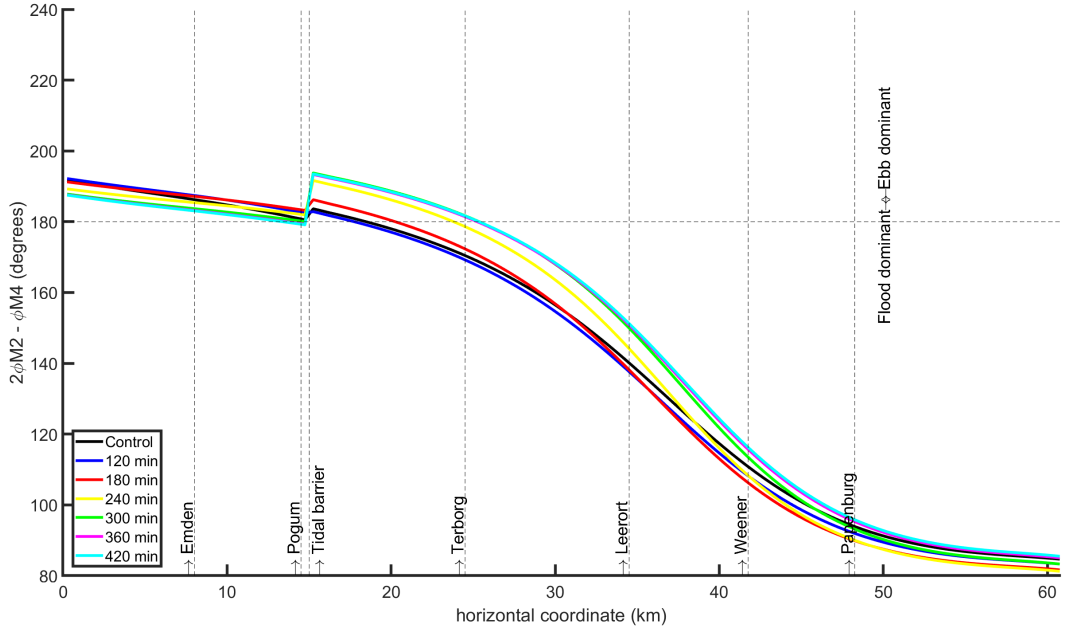

Figure 4.25: The effect of variations in closure duration on the relative phase angle throughout the model domain. Closure percentage: 68%, closure durations vary.

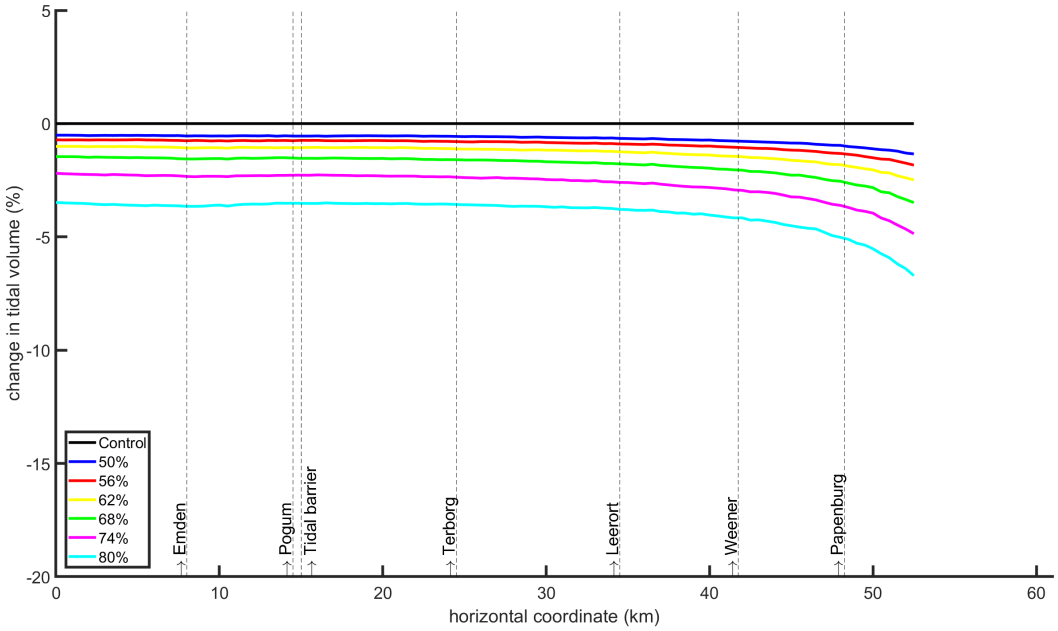

Figure 4.26: The effect of variations in closure percentage on the relative tidal prism throughout the model domain. Closure duration = 300 min, closure percentages vary.

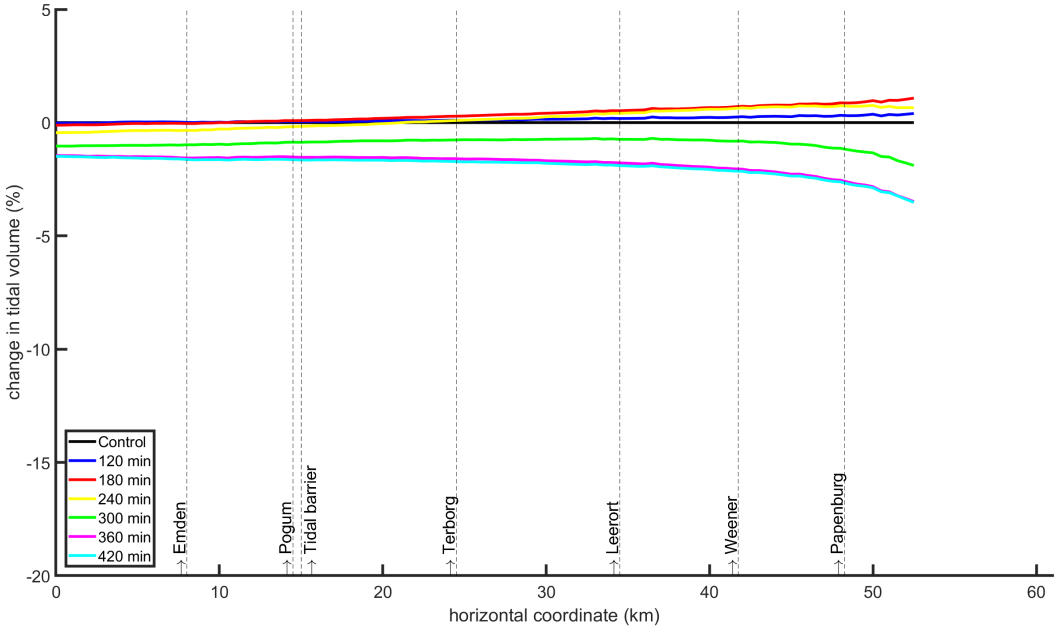

Figure 4.27: The effect of variations in closure duration on the relative tidal prism throughout the model domain. Closure percentage: 68%, closure durations vary.

4.3.7 Variant 3

Variant 3 involves only performing a barrier operation outside of regular shipping hours. This means that barrier operations are only performed if the entire operation can take place between 6PM and 6AM. Naturally the likelihood of an entire barrier operation fitting inside these hours is greater if the closure duration is shorter. This trend backed up by the simulation results, presented in figure 4.28. As a result of the restrictions, the number of tidal waves that is adjusted is reduced by between 61% and 75%, depending on the closure duration.

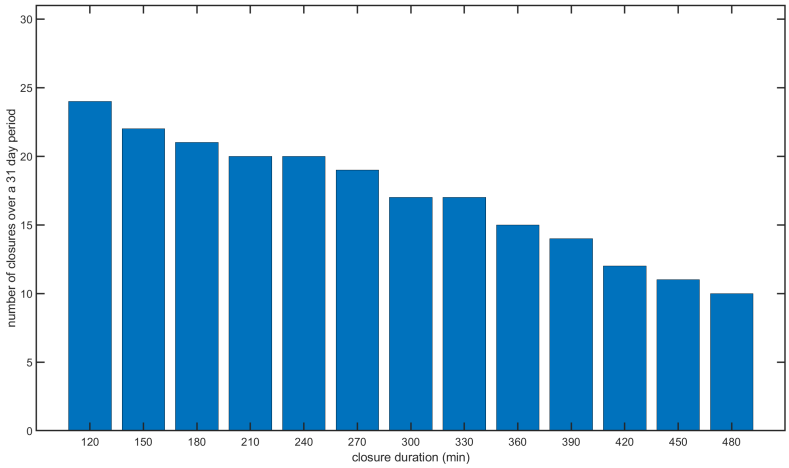

Figure 4.28: An overview of the number of barrier operations that were performed during the 31 day simulation period, for different closure durations.

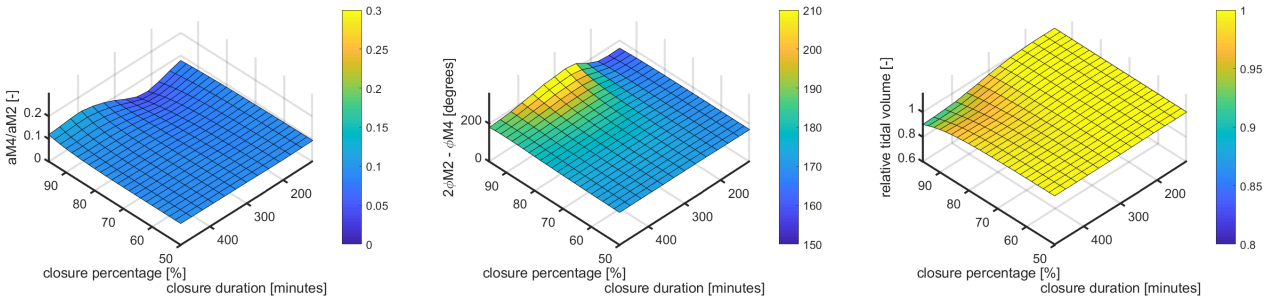

(a) M4/M2 amplitude ratio (b) M4/M2 relative phase angle (c) Relative tidal prism

Figure 4.29: An overview of the evaluation criteria for a range of different closure percentage and closure durations.

The greater likelihood of a barrier operation 'fitting' inside the permitted operation window is also observable in the results. Since even fewer tidal waves are adjusted in this case, the overall effect of the barrier operation is even smaller. However, in figure 4.29b the effect in the region of closure durations longer than 360 minutes is reduced even more than the decrease in effect in general. The previously binary effect of the closure duration is in this case replaced by an effect that is greatest for closure durations of around 240 minutes. The effect then decreases again for increased closure durations. The effect of the closure percentages is also similar to the behavior for variants 1 and 2.

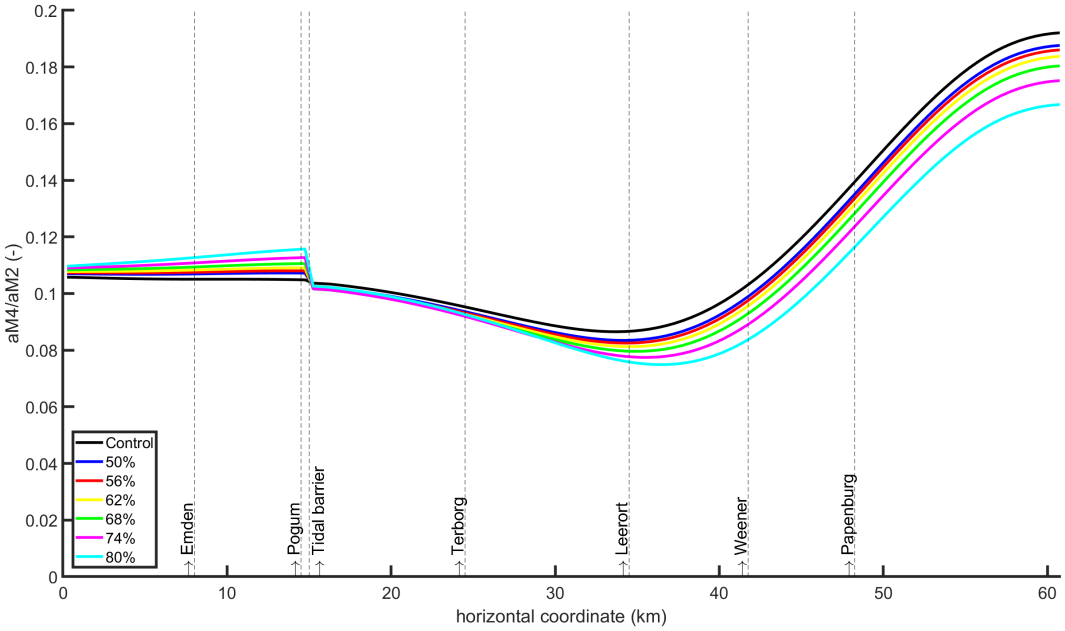

Figure 4.30: The effect of variations in closure percentage on the tidal amplitude ratio throughout the model domain. Closure duration = 300 min, closure percentages vary.

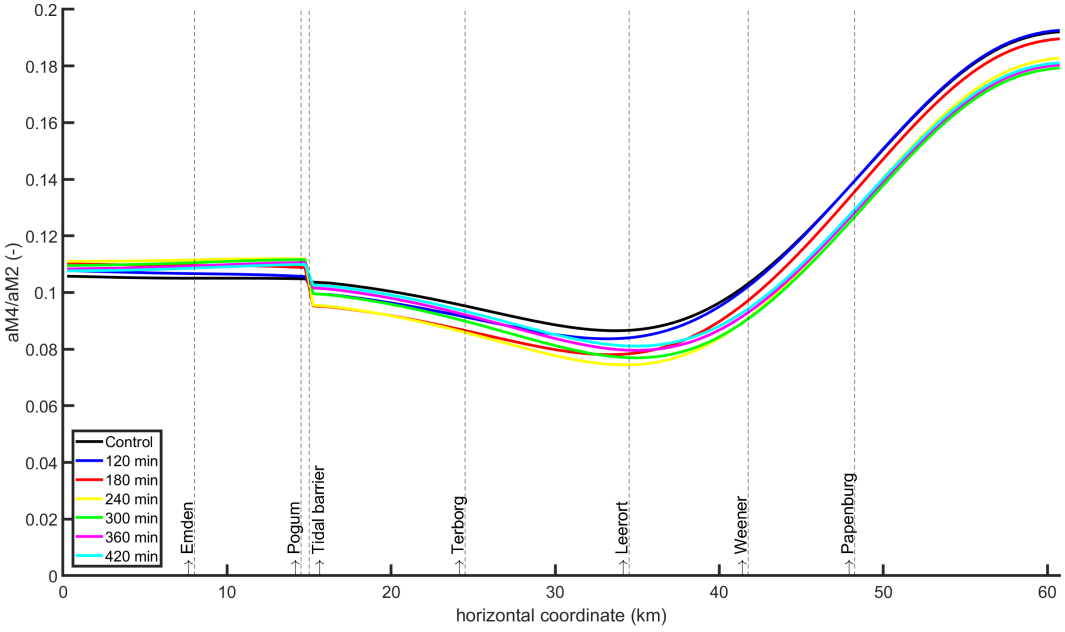

Figure 4.31: The effect of variations in closure duration on the tidal amplitude ratio throughout the model domain. Closure percentage: 68%, closure durations vary.

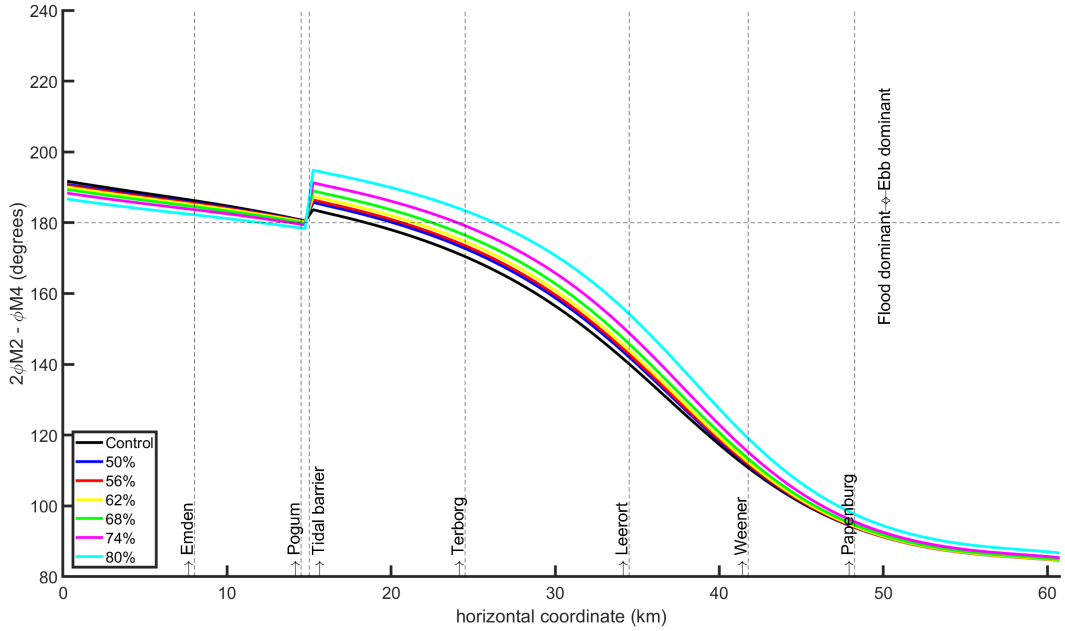

Figure 4.32: The effect of variations in closure percentage on the relative phase angle throughout the model domain. Closure duration = 300 min, closure percentages vary.

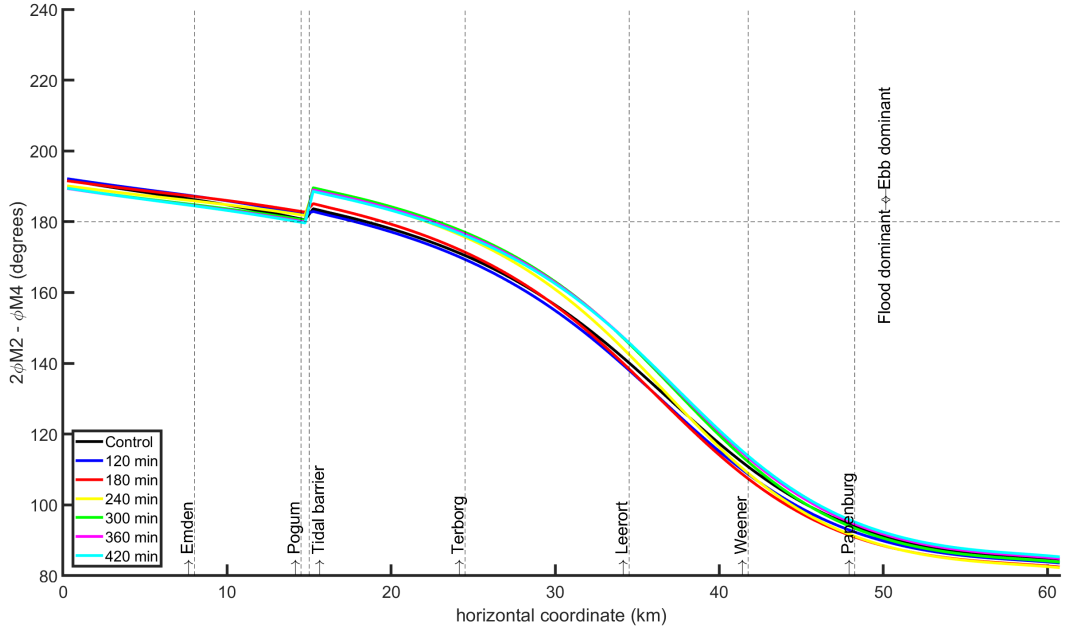

Figure 4.33: The effect of variations in closure duration on the relative phase angle throughout the model domain. Closure percentage: 68%, closure durations vary.

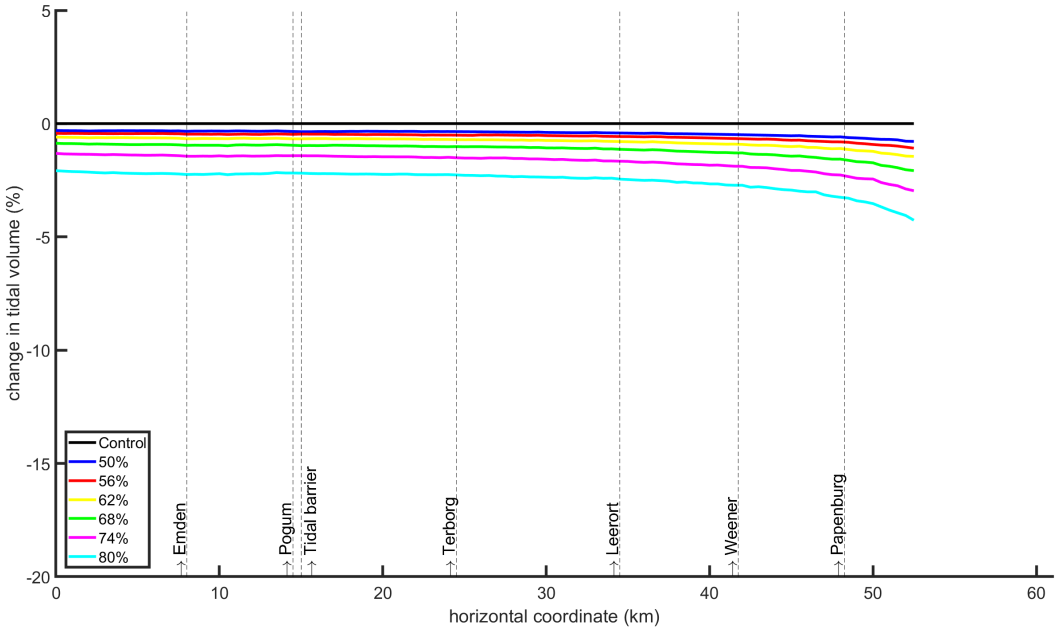

Figure 4.34: The effect of variations in closure percentage on the relative tidal prism throughout the model domain. Closure duration = 300 min, closure percentages vary.

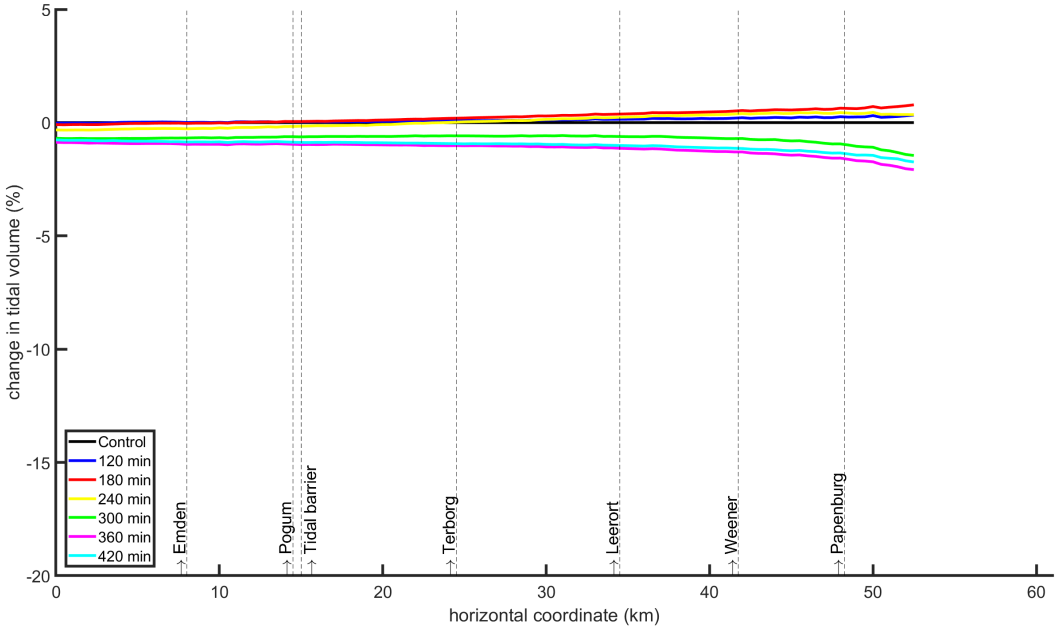

Figure 4.35: The effect of variations in closure duration on the relative tidal prism throughout the model domain. Closure percentage: 68%, closure durations vary.

4.3.8 Influence of the model boundary

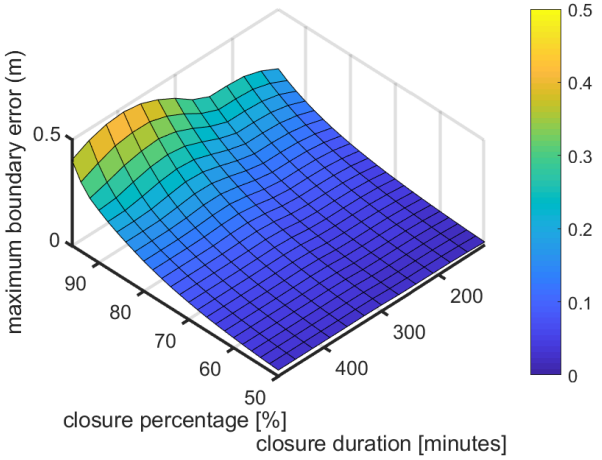

Figure 4.36: An overview of the maximum error near the seaward model boundary that occurred over the 31 day simulation period.

If the tidal barrier is open, a tidal wave will be damped out by the time it can reflect of the weir near Herbrum and travel back to the seaward boundary. In this case there is no interference between reflected tidal waves and the seaward boundary. When the tidal barrier is closed the build-up of water in front of the barrier extends to the seaward boundary. As a result of this build-up the water level at the boundary is higher than prescribed. An overview of the magnitude of this error is illustrated in figure 4.36. The error near the boundary is largest for barrier operations involving a high closure percentage. The resulting simulations are not as reliable as those involving a lower closure percentage. In other situations it would be standard practice to move the seaward boundary away from the barrier. In this case that is not possible since the assumptions on which this model is founded do not hold beyond the current model boundary.

4.4 Result conclusions

From results a number of conclusions have been made. These will be summarised briefly below.
The closure duration has a binary effect on the impact of the tidal barrier operation. If the closure duration is shorter than approximately 240 minutes the effects of the tidal barrier operation are negligible. If the closure duration is longer than approximately 240 minutes, the operation impacts the hydrodynamics in the system but further increases in closure duration will not lead to a further increase in effect.

As a result of the tidal barrier operation the relative phase angle on the landward side of the tidal barrier is increased. This is the result of a decrease in the phase angle of the M4 component, the phase M2 component is increased slightly. Increasing the closure percentage increases the upward shift of the relative phase angle on the landward side of the barrier. This effect does not persist up to the tidal weir near Herbrum. The relative phase angle of the altered tidal wave coincides with the phase angle of the unaltered wave near Papenburg, regardless of the closure percentage. As a result of the tidal barrier operation the amplitude ratio of the M2 and M4 component is decreased. Increasing the closure percentage leads to a further decrease in the amplitude ratio. The minimum of the amplitude ratio is also shifted further upstream. The tidal prism in the Lower Ems is reduced as a result of the barrier operation. The relative decrease in tidal prism is constant throughout the Lower Ems. Increased closure percentage lead to further decrease of the tidal prism. The river discharge has very little influence on the effectiveness of the barrier operation. Only the reduction of the tidal prism appears to be slightly larger in situation with higher river discharge.

When the barrier operation is performed a water level difference on either side of the tidal barrier is generated, which is expected. When the barrier is subsequently opened, there is a possibility of a sudden large discharge

of water into the Lower Ems if the opening time is too short. The opening time of 45 minutes, which is applied in most calculation prevents this sufficiently long to prevent this. The opening time can be increased to 60 minutes facilitate a more gentle release but increases beyond this point have very little effect.

When the tidal signal is considered of operation variants where a barrier operation is not performed every tide, the effect of the operation is diminished. This decrease appears to be linearly proportional to the decrease in the number of openings. When the restriction on the barrier operation, imposed by shipping, are considered the percentage of the tidal waves that can be adjusted varies between 39% and 25%. Barrier operations with a longer closure duration have a smaller change of complying with the shipping restriction and therefore result in a lower percentage of the tidal waves that are adjusted.

Chapter 5

Discussion

5.1 Modelling approach

In this project a simple, computationally inexpensive hydrodynamic model has been formulated. This model can be used to investigate the effects of a wide variety of barrier operation modes on the propagation of tidal waves in the Lower Ems. The hydrodynamics that are simulated are greatly simplified. This is the result of simplifications regarding the processes that are included in the model, as well as the formulation of the channel geometry.Although the baroclinic forces play a role in the morphology and hydrodynamics in the region, the operation of the tidal barrier primarily impacts the barotropic dynamics. For this reason it is acceptable to ignore the baroclinic processes.

The bathymetry of the Ems estuary has been described using a general assumed channel shape and a number of geometric parameters, determined from observations of detailed bathymetry measurements. A converging, funnel shaped estuary is common in nature. Despite this there are significant differences between the assumed channel geometry and the actual channel bathymetry. This is especially true for the channel depth. As a result it is not possible to completely reproduce all characteristics of the tidal wave. In this study, it was acknowledged that a substantial difference exists in the propagation speed of the modelled and real tidal wave.

Based on the geometry of the lower Ems river, the model equations were simplified to a 1D formulation. This 1D representation of the flow is acceptable because the along channel dimensions are much greater than the transverse and vertical dimensions of the domain. This formulation is very inexpensive computationally but it is limiting the size of the model domain. The ratio of the dimensions that makes a 1D model applicable are valid up until the end of the Geisedamm, near the port of Emden. Beyond this point the dimensions of the Ems estuary can no longer be assumed to be one-dimensional.

Due to the relatively short distance between the model boundary and the tidal barrier, the conditions applied at the seaward boundary interferes with the influence of the tidal barrier operation. One way to solve this problem is to move the model boundary further away from the tidal barrier. This is however not possible due to the reasons mentioned above. Furthermore, In the 1D formulation of the model it is actually assumed that the transverse boundary represented by the Geisedamm is impermeable. In reality, this dam is not impermeable and there are even some indications that it plays an important role in the transport of sediment into the Ems river.

In this study the tidal barrier is schematized as a single structure that controls the area available for water to flow through. In reality this tidal barrier consists of several different sections, connected by pillars. As mentioned in chapter 4, two different methods are used to close the barrier. In the main channel a rotating segment is used, while in the other sections of the barrier a gate in lowered into the channel.

In the very simple schematisation of the tidal barrier only a form variable (μ) was used to correct for the shape of the flow around the barrier. The available area for the water to flow through (in case the barrier is open) was also assumed to be constant, rather than dependent on the local water level. The equation relating the discharge through the barrier to the water levels on either side of the barrier assumed no energy losses. In more complex models the energy loss caused by the barrier are taken into account (Oberrecht and Wurpts 2014). In a more detailed study, the schematisation of the tidal barrier should be more detailed. The flow around the tidal barrier, including potential effects on the bed protection and loads on the structures. This

detailed study should be part of the final stages of the design cycle.

5.2 Evaluation of research questions

Controlled tidal barrier operation was identified as possible method for decreasing the suspended sediment concentrations in the Lower Ems river. The reduction of sediment should result from a reduction of sediment import, brought about by the tidal barrier operation, while the export of sediment by episodes of high river discharges would not be affected.

The present-day, unaltered tidal wave imports sediment due to amplified tidal ranges in the upstream regions of the Lower Ems and flood-dominant asymmetry of the tidal wave. Over the long term, the reduction of the sediment import could be achieved by shifting the asymmetry of the tidal wave to a more symmetrical or slightly ebb-dominant character.

5.2.1 Properties of an optimal barrier operation

The characteristics of an optimal tidal barrier operation can be divided into two categories. The first is related to the impact of the barrier operation on the hydrodynamics. One obvious requirement is that the adjusted tidal wave should be symmetrical or slightly ebb-dominant. Furthermore, the reduction of the tidal volume should be as low as possible. This requirement is explicitly mentioned in the contract of the Masterplan Ems 2050. An optimal operation regime results in the smallest reduction of the tidal volume, while still satisfying the primary requirement of shifting the asymmetry of the tidal wave.

The second characteristic of the optimal barrier operation stems from the restrictions imposed by the shipping activities in the region. As a result of these restrictions, controlled barrier operations are only allowed to take place outside of regular shipping hours. The likelihood of an entire controlled barrier operation fitting inside this window increases if the closure duration shorter. If more controlled barrier operations are able to be performed, the effectiveness of the barrier operations as a whole increase. The reduction of the effectiveness of the tidal barrier operation was found to be roughly proportional to the reduction in the number of tidal waves on which a barrier operation was performed. In the context of this project, an optimal controlled barrier regime has the shortest possible closure duration, while still satisfying the primary requirement of shifting the asymmetry of the tidal wave.

5.2.2 Impact of controlled barrier operation on the tidal wave

Operation of the tidal barrier, deforms the tide to become more symmetrical or ebb-dominant in the region on the landward side of the tidal barrier. The M4/M2 amplitude ratio is decreased in the region between the tidal barrier and weir at Herbrum. The tidal volume is decreased throughout the model domain. These overall tendencies are amplified by higher closure percentages. If the duration of the closure does not exceed an apparent threshold of 240 minutes, the effects of the barrier operation are negligible. The extent of the area in which the tidal wave maintains a symmetric or ebb-dominant character is dependent on the magnitude of the increase in the relative phase angle caused by the tidal barrier. Regardless of closure percentage, no modelled barrier operation was able to sufficiently shift the asymmetry in the entire estuary.

It is assumed that if the tidal asymmetry in a long enough stretch of the Lower Ems river becomes symmetrical or slightly ebb-dominant, the upstream sediment transport in the lower Ems should be reduced. Since the sediment fluxes are not computed directly it is difficult to determine how long this stretch of river should be. If it is assumed that a stretch of around 10 to 12 km is sufficient to accomplish this, a closure percentage of 60% to 65% will suffice. The closure duration should be long enough to pass the apparent threshold value of around 240 minutes.

5.2.3 Expected impact of the barrier operation

The mechanisms through which the suspended sediment concentrations in the Lower Ems should decrease are visualised in figure 3.1. If a suitable barrier operation is found that significantly reduce the import of sediment, the suspended sediment concentration in the upstream reaches of the Lower Ems will reduce as a result of either high discharge events or dredging activities. This decrease in sediment concentrations will reduce the stratification of the water column, especially during low discharge conditions. The reduction of the stratification likely decrease the occurrence of low D.O. conditions.

If the decrease in suspended sediments is enough to remove a large part of the fine sediment in the Lower Ems, it may be possible for the bed to transition back to sandy bed. This transitions, which likely also involves the reappearance of bed forms would result in a significant increase of the hydraulic drag and decrease the tidal amplification in the upstream part of the Lower Ems, thus increasing flood safety.

5.3 Further research

This study is only an indicative study into the effect of controlled barrier operation on the tidal asymmetry. The model that is described in this report is a very simple model and is used to assess the effect of a wide range of control regimes. While more detailed models are able to reproduce the hydrodynamics in greater detail, the computational costs of such an modelling such a broad spectrum would be very demanding. These detailed models should be used in a later stage of the design process, to determine the effects with greater certainty. In an even more advanced state the safety and structural integrity of the barrier and estuary and river. Special attention should be paid as well to the effects of the controlled barrier operation on the ecology and environmental quality, since these should influence the restrictions for the operation significantly. The more detailed model that is used to verify the result of this modelling effort should correct a number of shortcoming of the model used in this study. These shortcomings have been discussed at the start of this chapter.

In this project, the evaluation criteria of the relative phase angle between the M4 and M2 tidal components is used as a proxy for tidal asymmetry. Tidal asymmetry has been found to play a contributing role to long term sediment transport so this a useful way to make conclusions about the sediment transport without actually computing the sediment transport. However, the evaluation criteria used in this project (relative phase angle) requires a frequency analysis of a water level signal. This makes evaluating simulations where the controlled barrier operation is only performed during specific times. In this case the water level signal consists of two distinct and independent signals. Using a single expression to evaluate such a mixed signal is troublesome. In further modelling efforts this should not be a significant issue since the transport of the sediment can be computed directly.

Chapter 6

Conclusions and recommendations

6.1 Role in a broader context

This project is part of an effort to mitigate the negative consequences of the increased levels of suspended sediment concentration in the Ems river and estuary. The concept of altering the characteristics of a tidal wave by opening and closing a tidal barrier at appropriate moments has been shown to work in recent years. Until now very little effort has gone into investigating for which parameters of the barrier operation this operation would be the most effective. That is the knowledge gap this thesis attempts to fill.

In the process of answering that question, first a simple, computationally cheap model is generally formulated and applied to a broad spectrum of parameters. More detailed and reliable, but also computationally more expensive and complicated models should be applied in a later stage to determine the effects of a barrier operation with greater certainty.

6.2 Answers to the remaining research questions

What is the character of the asymmetry of the unaltered tide?

The tidal wave is slightly ebb-dominant near the seaward model boundary. As the tidal wave propagates through the Lower Ems is becomes increasingly flood dominant. The amplitude of the M4 component decreases from the seaward model boundary until the middle reaches of the domain and then increases again towards the landward end of the model.

What is the effect of the barrier operation on the tidal asymmetry?

In general the tidal barrier operation results in an increase of the relative phase angle on the landward side of the tidal barrier. This increase in the relative phase angle increases as the closure percentage increases but the shift resulting from the barrier operation does not persist until the landward model boundary. Regardless of closure percentage, the relative phase angle of the altered tide approaches that of the unaltered tide around Papenburg. According to these model results it is not possible to create a symmetrical or ebb-dominant tide in the entire Lower Ems. On the seaward side of the barrier the relative phase angle decreases slightly.

As was mentioned previously, the closure percentage increases the shift in relative phase angle on the landward side of the barrier. The closure duration appears to have a clear binary effect. If the closure duration of the barrier operation exceeds a threshold value (around 240 minutes) the barrier operation is effective, resulting in the increase in relative phase angle mentioned. If the closure duration is shorter than this threshold value the barrier operation appears to be not effective. Increasing the closure duration beyond this threshold value does not result in a further increase in the relative phase angle. When the restrictions based on shipping activities are included, barrier operations with a high closure duration become less effective, since the likelihood the barrier 'fits' within the permitted window is reduced.

What other characteristics of the tide are affected by the barrier operation and are these side-effects beneficial?

The tidal volume on the landward side is reduced by the barrier operation. If the closure percentage increases, the tidal volume decreases. The amplitude of the M4 component is reduced by the barrier operation. Increasing

the closure duration further decreases the amplitude of the M4 component. The location of the minimum amplitude is shifted further upstream as well.

What are the characteristics of an optimal barrier operation?

The optimal barrier operation mode reduces the import into the Lower Ems by shifting the tide towards a symmetric or slightly ebb-dominant tide. It is not possible to create a symmetric tide in the entire Lower Ems. The sediment transport can still be interrupted if a large enough stretch of the Lower Ems has a symmetric tide. As a first estimate of this required length the tidal intrusion length is taken, which is around 12 km for the Lower Ems.

The closure percentage of the optimal barrier operation mode should be as low as possible to maintain the tidal volume as much a possible. The closure duration should be as short as possible so that the likelihood of a barrier operation occurring is as high as possible, taking into account restrictions resulting from shipping activities.

What is the optimal tidal barrier operation?

Based on the criteria mentioned above, the optimal barrier operation mode consists of a closure duration of 300 minutes and a closure percentage of approximately 60%.

How do the changes to the hydrodynamics resulting from barrier operation affect sediment transport and the issues that occur in the region?

The operation of the tidal barrier should reduce the import of sediment into the Lower Ems. The sediment concentration in the Lower Ems are subsequently reduced by dredging activities and episodes of high river discharge.

The decreased sediment concentration in the Lower Ems result reduce the stratification of the water column induced by density gradients. This should increase the vertical transport of dissolved oxygen in the water column, especially during episodes of low river discharge. This should decrease the occurrence of anoxic or hypoxic episodes. The decrease in sediment concentration should also prevent fluid mud layers from forming. This increases the hydraulic drag experienced by tidal waves, resulting in less tidal amplification and a decrease of the tidal ranges.

6.3 Recommendations

The next step in the process should be modelling a number of operating regimes that have according to the results of this study a favourable effect on the asymmetry in the Lower Ems. The result of this study can be verified by a more complex model that is able to capture the details of the channel bathymetry fully. Applying 2D or 3D model also allows the model boundaries to be moved. This way the effect of the interference of the boundary in this study can be removed.

After the effect of the tidal barrier operation on the hydrodynamics are verified, the sediment transport in the Lower Ems should be modelled directly in order to determine the effects of the barrier operation on the sediment concentrations with more confidence. Another interesting factor to consider is the effect of irregular barrier operations on the distribution on sediment in the Lower Ems.

Bibliography

[1] Alexander S Chernetsky, Henk M Schuttelaars, and Stefan A Talke. "The effect of tidal asymmetry and temporal settling lag on sediment trapping in tidal estuaries". In: *Ocean Dynamics* 60.5 (2010), pp. 1219–1241.

[2] Yoeri M Dijkstra, Henk M Schuttelaars, George P Schramkowski, et al. "Modeling the transition to high sediment concentrations as a response to channel deepening in the Ems River Estuary". In: *Journal of Geophysical Research: Oceans* 124.3 (2019), pp. 1578–1594.

[3] Yoeri M Dijkstra, Henk M Schuttelaars, and Johan C Winterwerp. "The hyperturbid state of the water column in estuaries and rivers: the importance of hindered settling". In: *Ocean Dynamics* 68.3 (2018), pp. 377–389.

[4] Carl T Friedrichs and David G Aubrey. "Non-linear tidal distortion in shallow well-mixed estuaries: a synthesis". In: *Estuarine, Coastal and Shelf Science* 27.5 (1988), pp. 521–545.

[5] Victor N de Jonge et al. "The influence of channel deepening on estuarine turbidity levels and dynamics, as exemplified by the Ems estuary". In: *Estuarine, Coastal and Shelf Science* 139 (2014), pp. 46–59.

[6] Martin Krebs and Holger Weilbeer. "Ems-dollart estuary". In: *Die Küste, 74 ICCE* 74 (2008), pp. 252–262.

[7] Wim van Leussen. "Fine sediment transport under tidal action". In: *Geo-marine letters* 11.3 (1991), pp. 119–126.

[8] Jing Lin et al. "Dissolved oxygen stratification in two micro-tidal partially-mixed estuaries". In: *Estuarine, Coastal and Shelf Science* 70.3 (2006), pp. 423–437.

[9] Dirk S van Maren, Johan C Winterwerp, and Julia Vroom. "Fine sediment transport into the hyper-turbid lower Ems River: the role of channel deepening and sediment-induced drag reduction". In: *Ocean Dynamics* 65.4 (2015), pp. 589–605.

[10] Dennis Oberrecht and Andreas Wurpts. "Auswirkungen des geplanten technischen Testbetriebs zur Wirkung der flexiblen Tidesteuerung". In: (2019).

[11] Dennis Oberrecht and Andreas Wurpts. "Hydro- und morphodynamische Auswirkungen de 4h-Flutstromsteuerung im Rahmen des geplanten technischen Testbetriebs zur Wirkung der flexiblen Tidesteuerung". In: (2020).

[12] Dennis Oberrecht and Andreas Wurpts. "Impact of controlled tidal barrier operation on tidal dynamics in the Ems estuary". In: *Die Küste, 81 Modelling* 81 (2014), pp. 427–433.

[13] Dennis Oberrecht and Andreas Wurpts. "Wirkung der flexiblen Tidesteurung auf die Reduzierung des Schwebstofftransportes und Bildung von Flüssigschlick in der Unterems". In: (2019).

[14] MA Pena et al. "Modeling dissolved oxygen dynamics and hypoxia". In: *Biogeosciences* 7.3 (2010), pp. 933–957. ISSN: 1726-4170.

[15] Stefan A Talke, Huib E de Swart, and VN De Jonge. "An idealized model and systematic process study of oxygen depletion in highly turbid estuaries". In: *Estuaries and coasts* 32.4 (2009), pp. 602–620.

[16] Wessel Van der Zee. "Flushing Basins: a study of the effect of geometric parameters of the performance of a flushing basin system". In: *TU Delft MSc Thesis* (2017).

[17] DS Van Maren et al. "The effect of land reclamations and sediment extraction on the suspended sediment concentration in the Ems Estuary". In: *Marine Geology* 376 (2016), pp. 147–157.

[18] Johan C Winterwerp. "Fine sediment transport by tidal asymmetry in the high-concentrated Ems River: indications for a regime shift in response to channel deepening". In: *Ocean Dynamics* 61.2 (2011), pp. 203–215.

[19] Johan C Winterwerp. "Stratification effects by fine suspended sediment at low, medium, and very high concentrations". In: *Journal of Geophysical Research: Oceans* 111.C5 (2006).

[20] Johan C Winterwerp, Marieke Lely, and Qing He. “Sediment-induced buoyancy destruction and drag reduction in estuaries”. In: *Ocean Dynamics* 59.5 (2009), pp. 781–791.

[21] Johan C Winterwerp and Zheng Bing Wang. “Man-induced regime shifts in small estuaries—I: theory”. In: *Ocean Dynamics* 63.11-12 (2013), pp. 1279–1292.

[22] Johan C Winterwerp, Zheng Bing Wang, et al. “Man-induced regime shifts in small estuaries—II: a comparison of rivers”. In: *Ocean Dynamics* 63.11 (2013), pp. 1293–1306.

Chapter 7

Appendix

7.1 Interpolated bathymetry figures

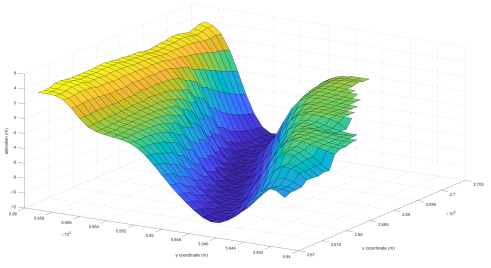

(a) x = 0 km

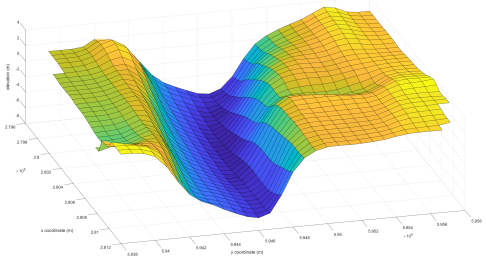

(b) x = 16 km

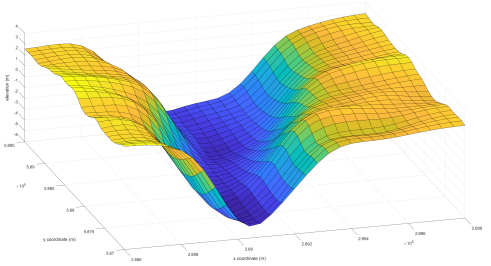

(c) x = 26 km

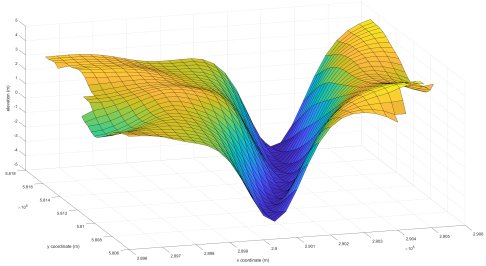

(d) x = 34 km

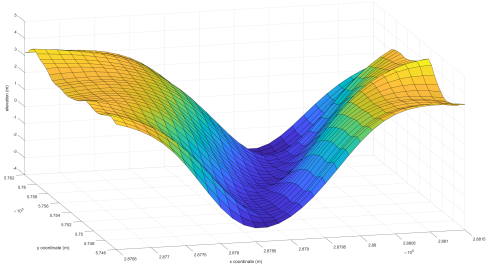

(e) x = 42 km

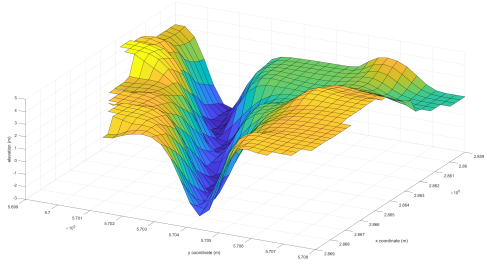

(f) x = 50 km

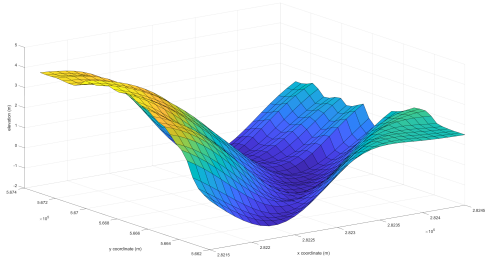

(g) x = 56.5 km

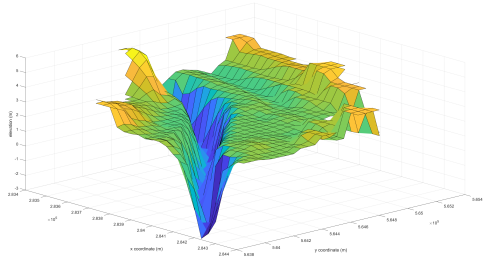

(h) x = 59.5 km

Figure 7.1: Interpolated channel bathymetry in a number of locations along the lower Ems river. The distance from the seaward boundary is given for each figure.

7.2 Model validation: winter month

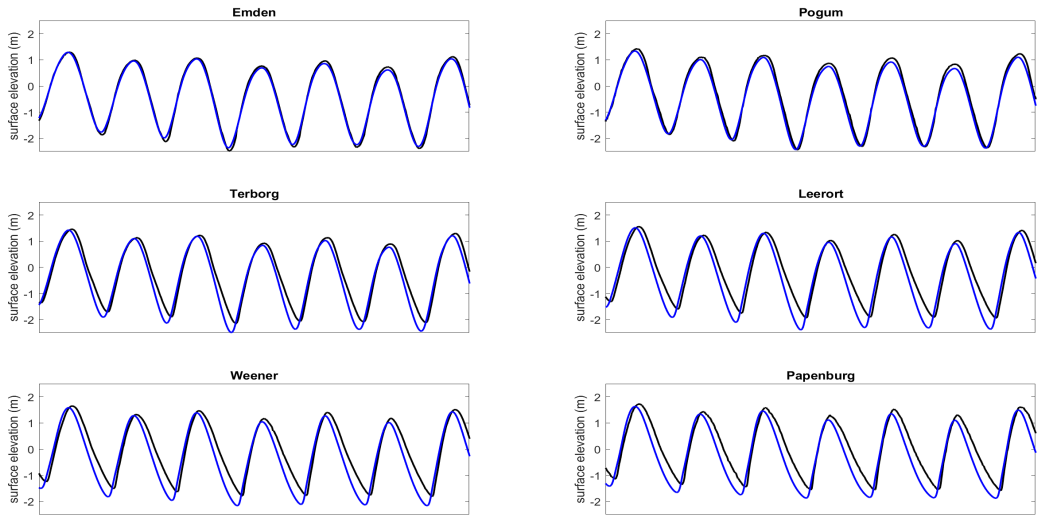

Figure 7.2: A comparison of water level measurements (black lines) and model results (blue lines) for data from a number of tidal stations in the lower Ems over part of the winter validation period.

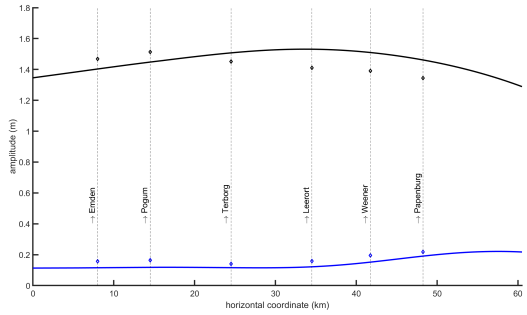

(a) Comparison of the M2 amplitude measurements (black diamonds), modelled M2 amplitudes (black line), M4 amplitude measurements (blue diamonds) and modelled M4 amplitudes (blue line).

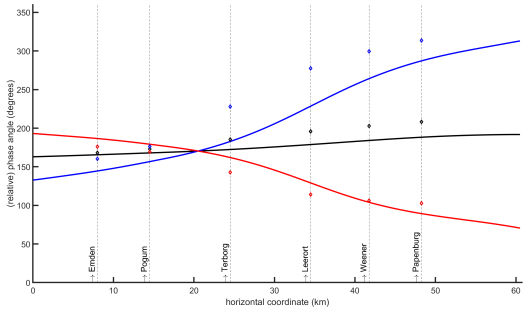

(b) Comparison of the M2 phase measurements (black diamonds), modelled M2 phases (black line), M4 phase measurements (blue diamonds) and modelled M4 phases (blue line). The same data is presented in the form of a relative phase angle (red diamonds and line).

Figure 7.3: Comparison of measured and modelled tidal characteristics for the calibration period.

7.3 Effect of river discharge

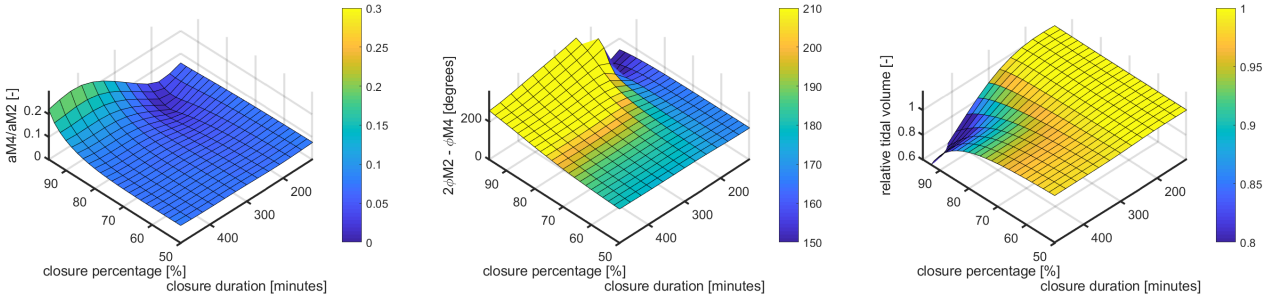

(a) M4/M2 amplitude ratio. (b) M4/M2 relative phase angle. (c) Relative tidal prism.

Figure 7.4: An overview of the evaluation criteria for a range of different closure percentage and closure durations.

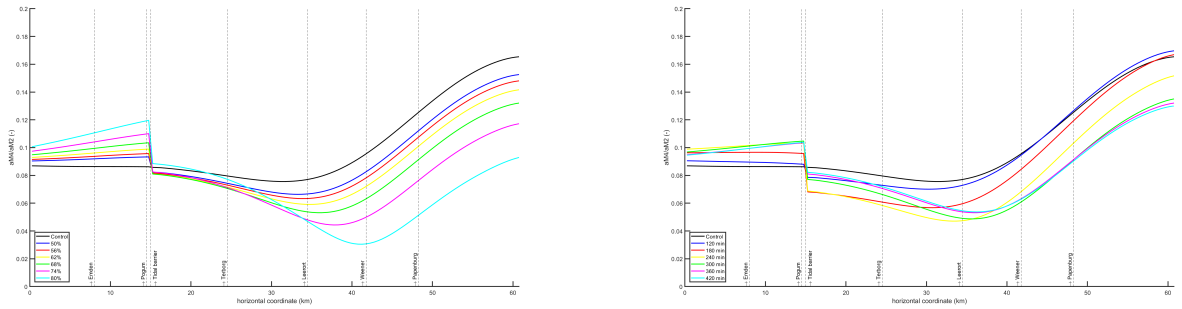

(a) Closure duration = 300 min, closure percentages vary. (b) Closure percentage: 68%, closure durations vary.

Figure 7.5: The effect of variations in closure duration and closure percentage on the tidal amplitude ratio throughout the model domain.

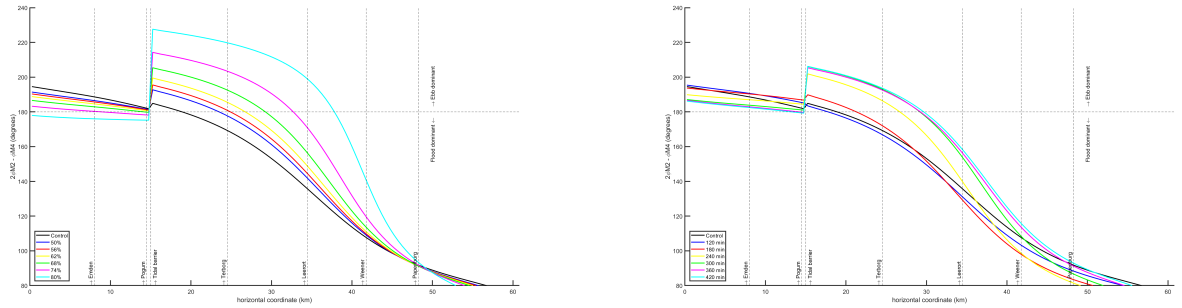

(a) Closure duration = 300 min, closure percentages vary. (b) Closure percentage: 68%, closure durations vary.

Figure 7.6: The effect of variations in closure duration and closure percentage on the relative phase angle throughout the model domain.

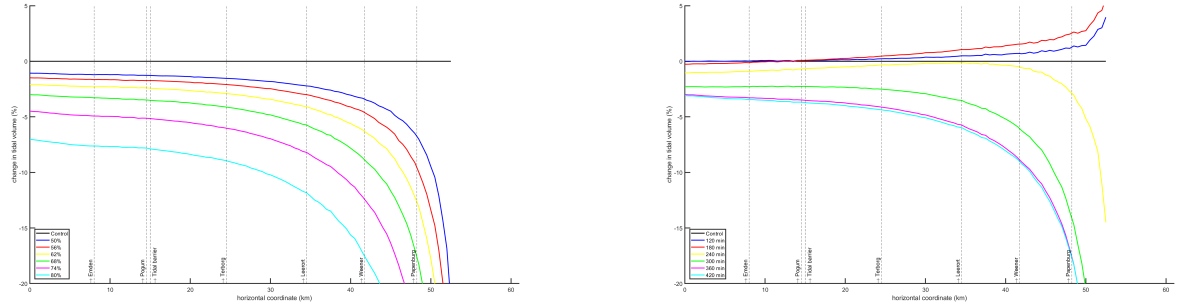

(a) Closure duration = 300 min, closure percentages vary. (b) Closure percentage: 68%, closure durations vary.

Figure 7.7: The effect of variations in closure duration and closure percentage on the relative tidal prism throughout the model domain.

7.4 Aggregate figures

7.4.1 Variant 1

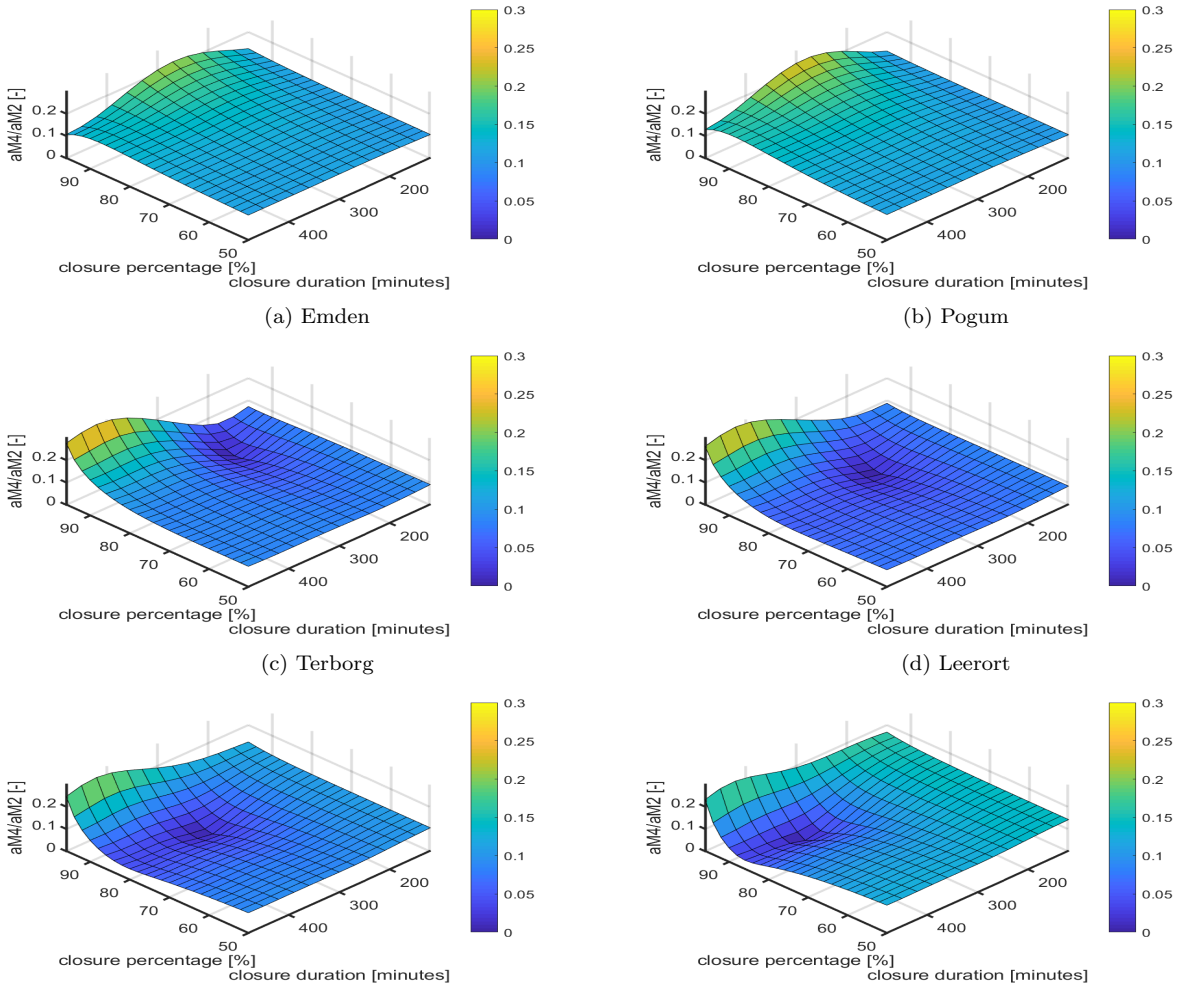

(a) Emden

(b) Pogum

(c) Terborg

(d) Leerort

(e) Weener

(f) Papenburg

Figure 7.8: An overview of the amplitudes of the M2 and M4 tidal components for a range of different combinations of closure percentage and closure durations.

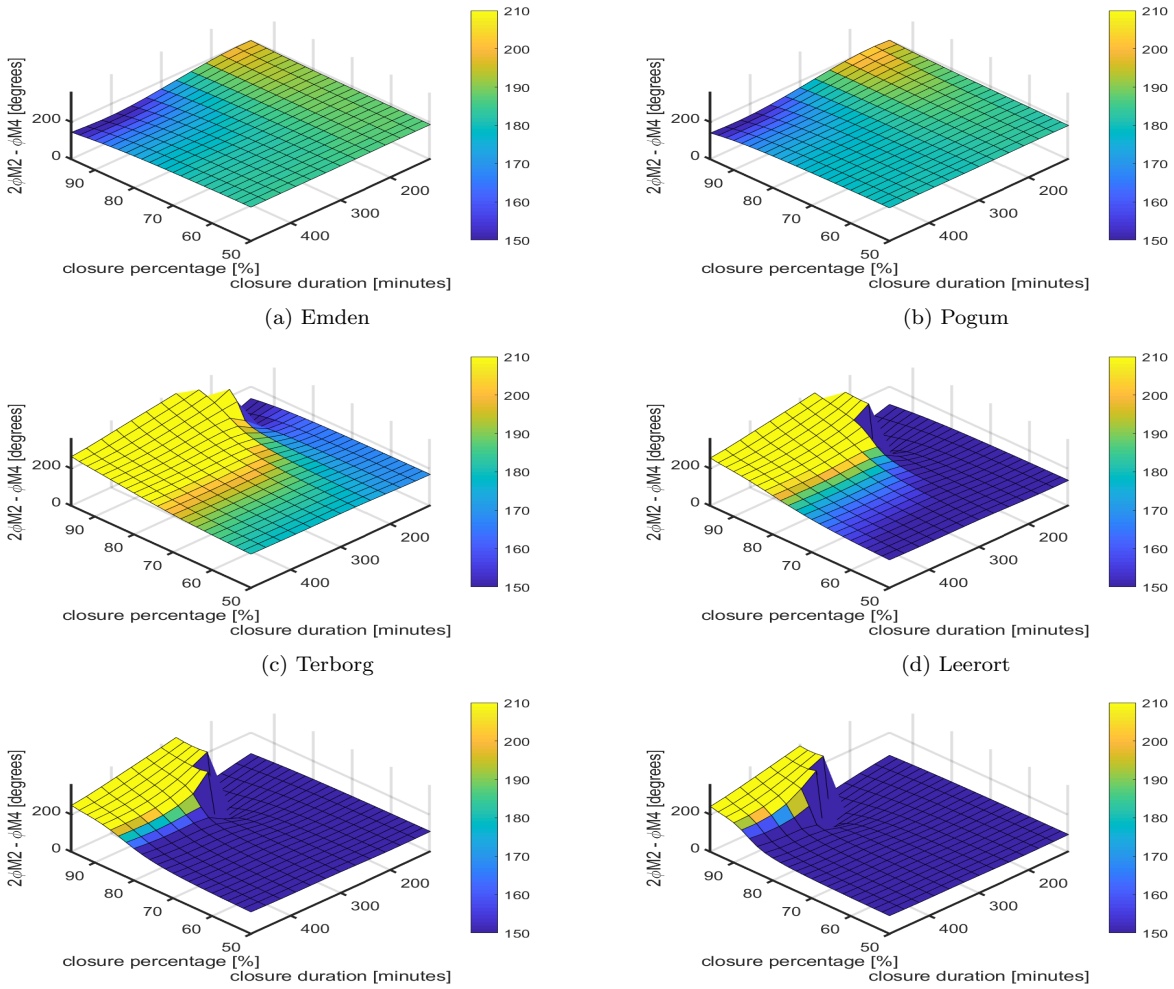

(a) Emden

(b) Pogum

(c) Terborg

(d) Leerort

(e) Weener

(f) Papenburg

Figure 7.9: An overview of the relative phase angle between the M2 and M4 tidal components for a range of different combinations of closure percentage and closure durations. A tidal wave is flood dominant if this angle has a value between 0 °and 180 °, and ebb dominant if it has a value between 180 °and 360 °

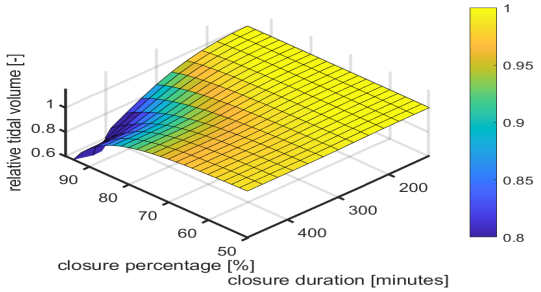

(a) Emden

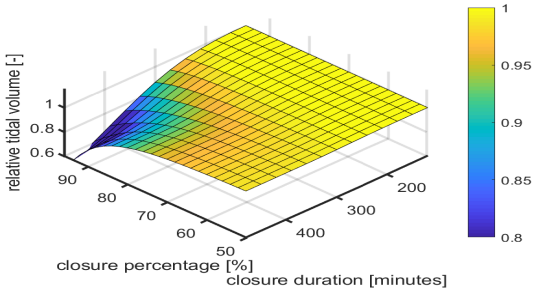

(b) Pogum

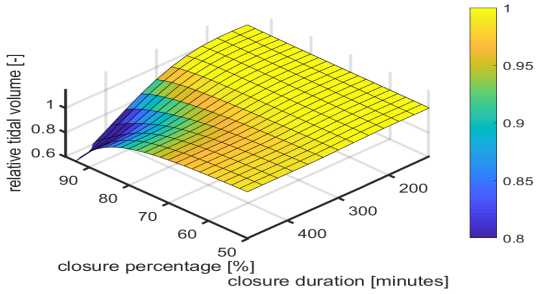

(c) Terborg

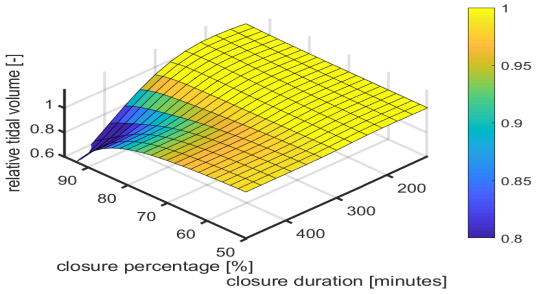

(d) Leerort

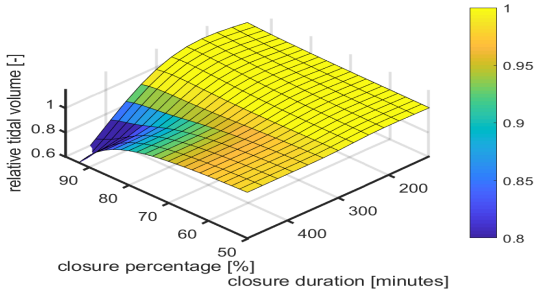

(e) Weener

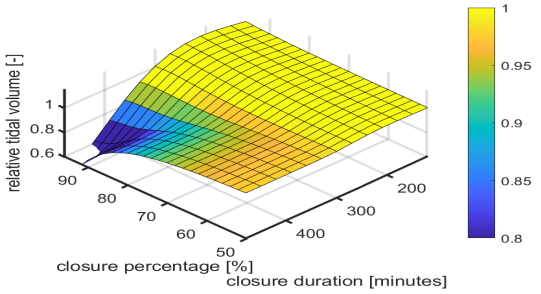

(f) Papenburg

Figure 7.10: An overview of the change relative tidal prism for a range of different combinations of closure percentage and closure durations.

7.4.2 Variant 2

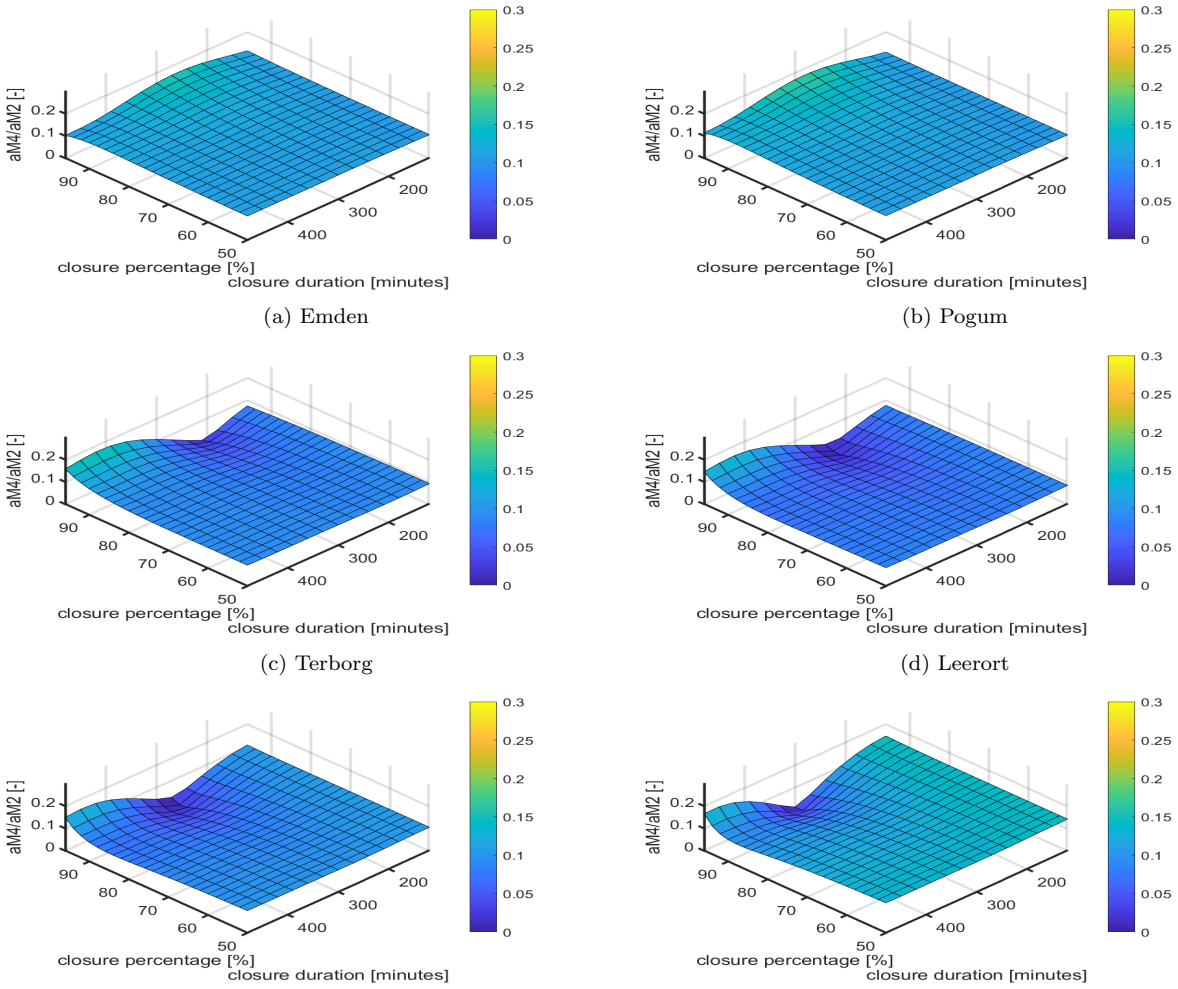

(a) Emden

(b) Pogum

(c) Terborg

(d) Leerort

(e) Weener

(f) Papenburg

Figure 7.11: An overview of the amplitudes of the M2 and M4 tidal components for a range of different combinations of closure percentage and closure durations.

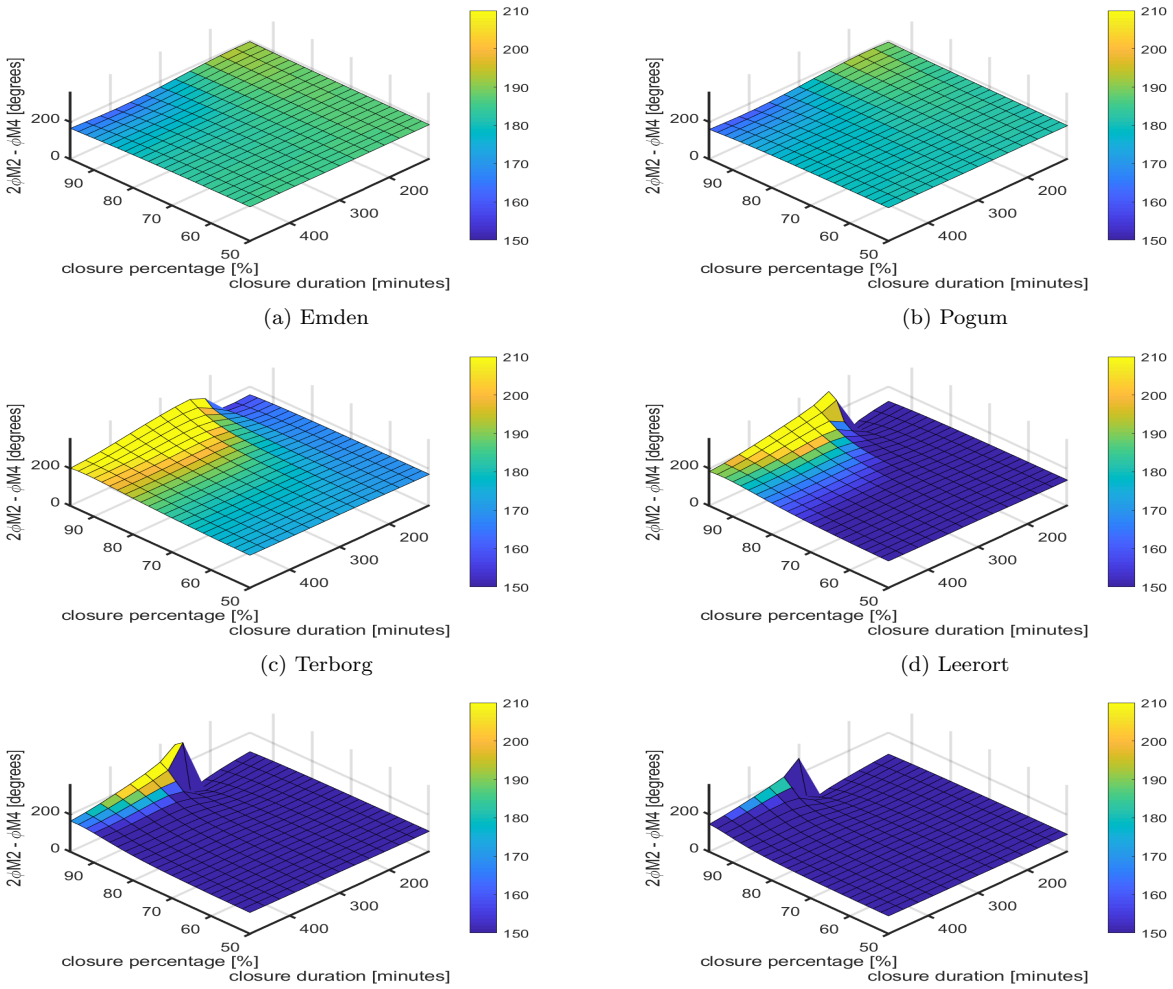

(a) Emden

(b) Pogum

(c) Terborg

(d) Leerort

(e) Weener

(f) Papenburg

Figure 7.12: An overview of the relative phase angle between the M2 and M4 tidal components for a range of different combinations of closure percentage and closure durations. A tidal wave is flood dominant if this angle has a value between 0 °and 180 °, and ebb dominant if it has a value between 180 °and 360 °

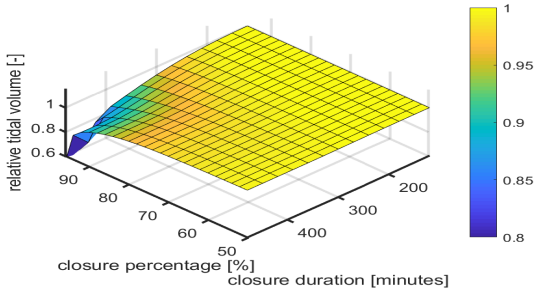

(a) Emden

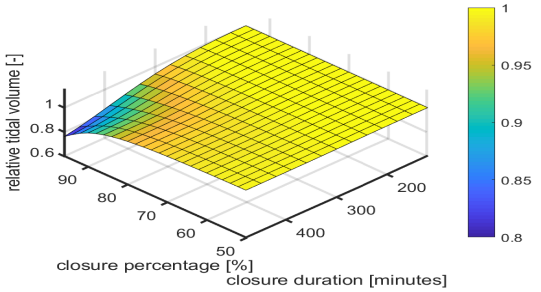

(b) Pogum

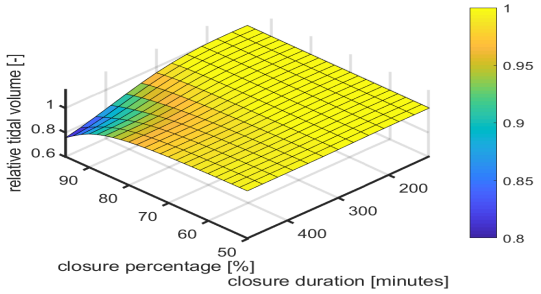

(c) Terborg

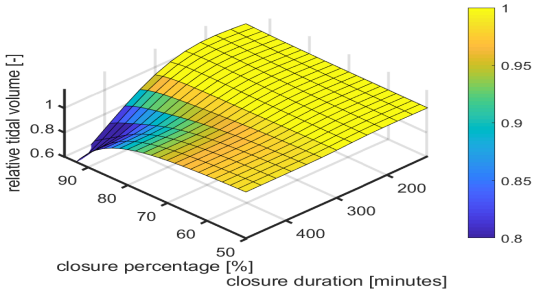

(d) Leerort

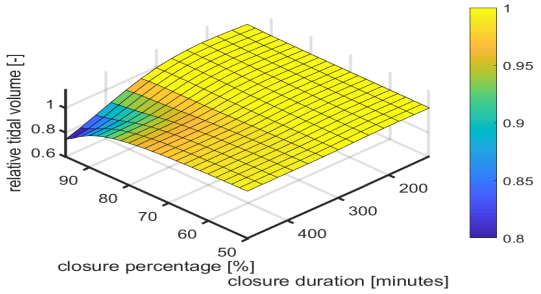

(e) Weener

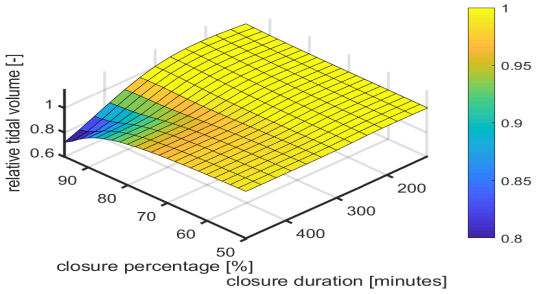

(f) Papenburg

Figure 7.13: An overview of the amplitudes of the M2 and M4 tidal components for a range of different combinations of closure percentage and closure durations.

7.4.3 Variant 3

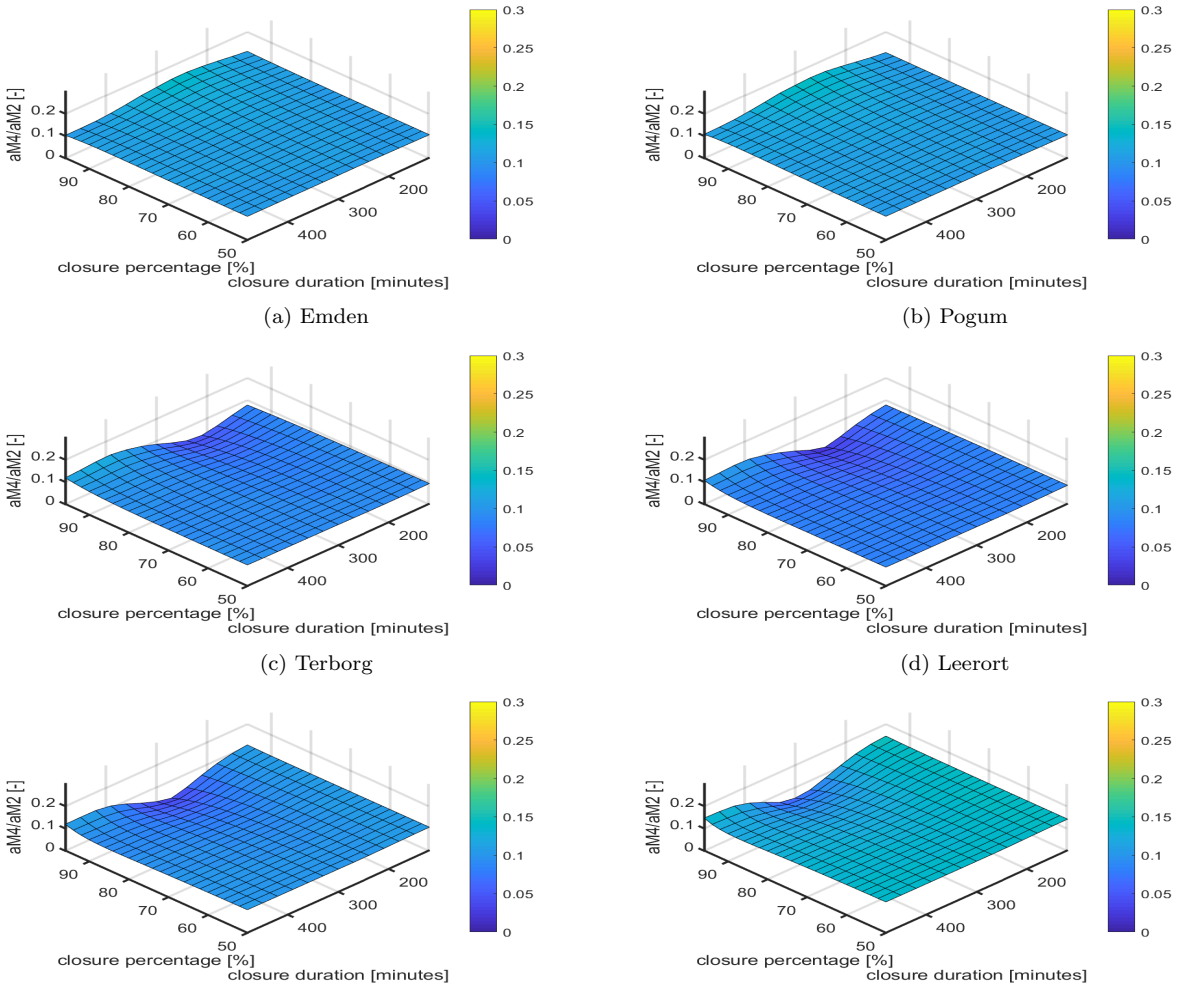

(a) Emden

(b) Pogum

(c) Terborg

(d) Leerort

(e) Weener

(f) Papenburg

Figure 7.14: An overview of the amplitudes of the M2 and M4 tidal components for a range of different combinations of closure percentage and closure durations.

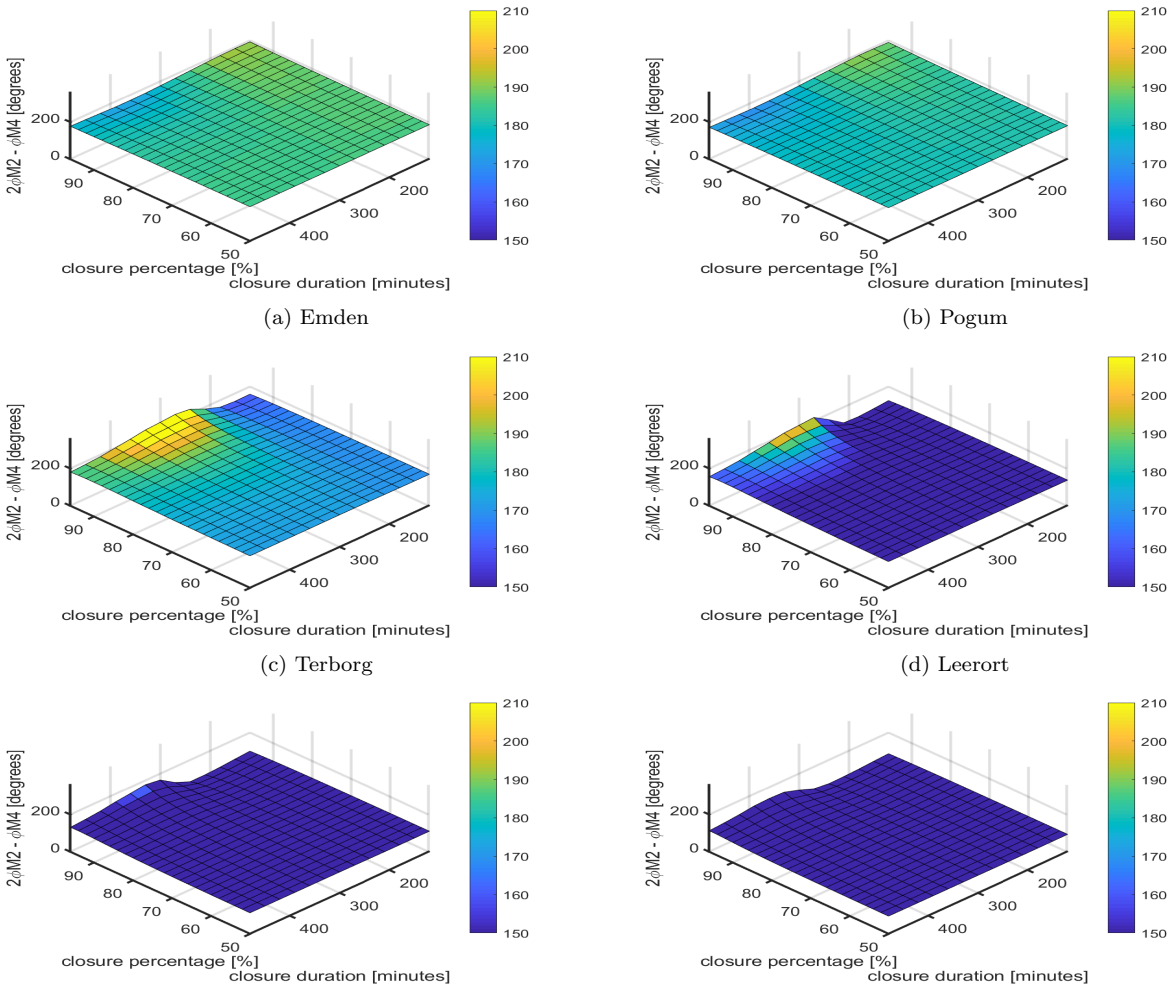

(a) Emden

(b) Pogum

(c) Terborg

(d) Leerort

(e) Weener

(f) Papenburg

Figure 7.15: An overview of the relative phase angle between the M2 and M4 tidal components for a range of different combinations of closure percentage and closure durations. A tidal wave is flood dominant if this angle has a value between 0 °and 180 °, and ebb dominant if it has a value between 180 °and 360 °

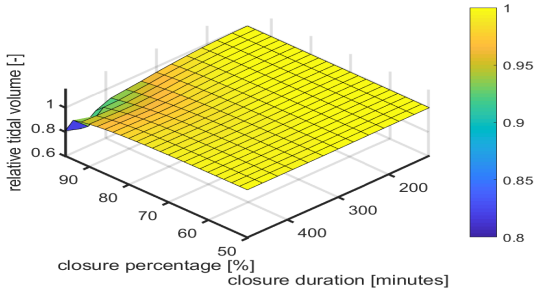

(a) Emden

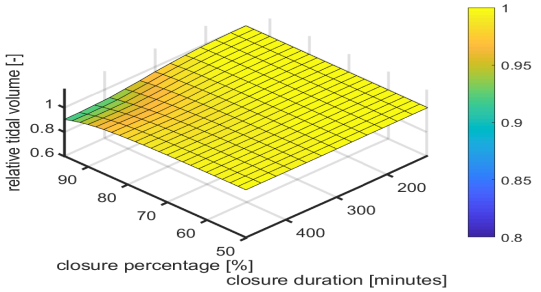

(b) Pogum

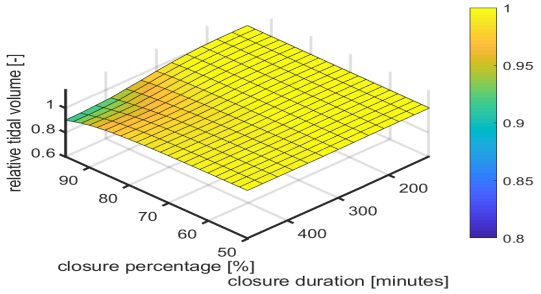

(c) Terborg

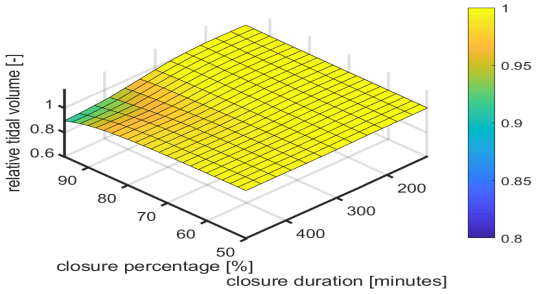

(d) Leerort

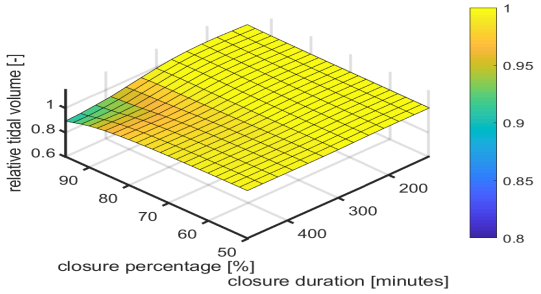

(e) Weener

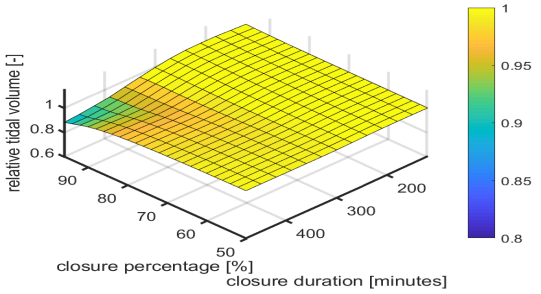

(f) Papenburg

Figure 7.16: An overview of the amplitudes of the M2 and M4 tidal components for a range of different combinations of closure percentage and closure durations.